Aus dem
Institute of Lung Biology and Disease (iLBD)/
Comprehensive Pneumology Center (CPC)
in Kooperation mit
dem Helmholtz-Zentrum München,
der Ludwig-Maximilians-Universität München und
den Asklepios Fachkliniken München-Gauting.

The role of the chromatin remodeling protein HMGN5 in COPD pathogenesis

Dissertation
zum Erwerb des Doktorgrades der Medizin
an der medizinischen Fakultät
der Ludwig-Maximilians-Universität zu München

vorgelegt von
Julian Dorer

geboren am
21.04.1993

in
Titisee-Neustadt

Jahr
2022

Mit Genehmigung der Medizinischen Fakultät
der Ludwig-Maximilians-Universität München

Berichterstatter:	Prof. Dr. med. Jürgen Behr
Mitberichterstatter:	PD Dr. Sandra Frank
	Prof. Dr. Hanno Leuchte
Mitbetreuung durch:	Dr. Ali Önder Yildirim
Dekan:	Prof. Dr. med. Thomas Gudermann
Tag der mündlichen Prüfung:	19.05.2022

Eidesstattliche Versicherung

Dorer, Julian

Name, Vorname

Ich erkläre hiermit an Eides statt,
dass ich die vorliegende Dissertation mit dem Titel

„The role of the chromatin remodeling protein HMGN5 in COPD pathogenesis"

selbständig verfasst, mich außer der angegebenen keiner weiteren Hilfsmittel bedient und alle Erkenntnisse, die aus dem Schrifttum ganz oder annährend übernommen sind, als solche kenntlich gemacht und nach ihrer Herkunft unter Bezeichnung der Fundstelle einzeln nachgewiesen habe.

Ich erkläre des Weiteren, dass die hier vorgelegte Dissertation nicht in gleicher oder ähnlicher Form bei einer anderen Stelle zur Erlangung eines akademischen Grades eingereicht wurde.

München, 20.05.2022
Ort, Datum

Julian Dorer
Unterschrift Doktorand

Abstract

There is rising evidence that epigenetic alterations are involved in Chronic Obstructive Pulmonary Disease (COPD). Spontaneous emphysema development in high mobility group nucleosome binding domain 5 (HMGN5) deficient mice and enhanced emphysematous changes after elastase treatment in these mice compared to wild-type mice have been previously detected. HMGN5 binds to the nucleosome core particle of chromatin, competing with linker-histone H1. Upon chromatin binding, HMGN5 thus alters chromatin structure affecting cellular transcription, differentiation and DNA-repair. This work seeks to explore the involvement of HMGN5 in the development and progression of emphysema.

Human lung samples from COPD patients and healthy donors were assessed for HMGN5 expression and immunofluorescence staining performed to identify the cellular localization of HMGN5. To assess underlying molecular mechanisms siRNA knock-down of HMGN5 in the human alveolar-type-II (AT II)-like cell line A549 was undertaken. Cells were additionally exposed to cigarette smoke extract (CSE) and assessed for cell death by Annexin V-staining, cell proliferation by woundhealing and WST-1 assay and cell cycle by propidium iodide (PI)-staining and transfection of Fluorescence Ubiquitin Cell Cycle Indicator (FUCCI). Expression of cell death and cell cycle associated genes was measured by qPCR.

RNA sequencing data from COPD patient lung samples revealed reduced HMGN5 expression compared to healthy individuals and immunofluorescent analysis demonstrated that HMGN5 is located in bronchial epithelial cells and AT II cells in the human lung. In addition, in vitro studies demonstrated that siRNA-mediated downregulation of HMGN5 caused A549 cells to be more susceptible to induced cell death. Cell cycle analysis of HMGN5 deficient cells revealed more cells in the early cell cycle stages compared to control cells but additional exposure to CSE did not affect this. Proliferation and migration of HMGN5 deficient cells was slightly impaired.

Taken together, this human data suggests that reduced expression of the epigenetic modulator HMGN5 is associated with emphysema development, via increased apoptosis and impaired cell cycle progression. This novel link between epigenetic regulation and emphysema, brings forth a new therapeutic target for impeding emphysema development in COPD.

Zusammenfassung

Es gibt immer mehr Hinweise darauf, dass epigenetische Veränderungen bei COPD eine Rolle spielen. Wir konnten bereits spontane Emphysementwicklung bei „high mobility group nucleosome binding domain 5“ (HMGN5) defizienten Mäusen, sowie verstärkte emphysematöse Veränderungen in diesen Mäusen verglichen mit Wild-Typ Mäusen nach Verabreichung von Elastase feststellen. HMGN5 bindet an das Nukleosom und konkurriert dabei mit dem Linker-Histon H1. Nachdem HMGN5 an Chromatin angedockt ist, verändert es die Chromatinstruktur und beeinflusst die zelluläre Transkription, Differenzierung und DNA-Reparatur. Die vorliegende Arbeit soll die Beteiligung von HMGN5 an der Entwicklung und Progression des Emphysems untersuchen.

Humane Lungenproben von COPD-Patienten und gesunden Spendern wurden auf HMGN5-Expression untersucht. Eine Immunfluoreszenzfärbung wurde durchgeführt, um die zelluläre Lokalisation von HMGN5 in der Lunge zu identifizieren. Um die zugrunde liegenden molekularen Mechanismen zu erforschen, wurde HMGN5 in der humanen Alveolarepithel-Typ-II (AT II)-Zelllinie A549 durch siRNA herunterreguliert. Die Zellen wurden zusätzlich einem Zigarettenrauch-Extrakt (CSE) ausgesetzt und auf Zelltod durch Annexin V-Färbung, Zellproliferation durch Wundheilungs- und WST-1-Assay und Zellzyklus durch Propidiumiodid (PI)-Färbung und Fluoreszenz-Ubiquitin Cell Cycle Indicator (FUCCI) untersucht. Die Expression von Zelltod- und Zellzyklus-assoziierten Genen wurde mithilfe quantitativer Polymerase-Kettenreaktion (qPCR) gemessen.

Die RNA-Sequenzierung der Lungenproben von COPD Patienten zeigte eine verminderte HMGN5-Expression im Vergleich zu gesunden Individuen. Die Immunofluoreszenzfärbung veranschaulichte, dass sich HMGN5 in bronchialen Epithelzellen und AT II-Zellen der menschlichen Lunge befindet. Darüber hinaus zeigten In-vitro-Versuche, dass eine verminderte Expression von HMGN5 in A549-Zellen eine erhöhte Anfälligkeit für induzierten Zelltod zur Folge hat. Die Analyse des Zellzyklus von HMGN5-defizienten Zellen ergab, dass sich verglichen mit den Kontrollzellen mehr Zellen in den frühen Zellzyklusphasen befinden. Die zusätzliche Behandlung mit CSE hatte hier keinen Effekt. Die Proliferation und Migration von HMGN5-defizienten Zellen zeigte sich geringfügig beeinträchtigt.

Zusammenfassend deuten diese Daten darauf hin, dass der epigenetische Modulator HMGN5 durch Beeinflussung der Apoptose und des Zellzykluses mit der Entwicklung des Emphysems assoziiert ist. Dieser Zusammenhang zwischen epigenetischer Regulation und Emphysem zeigt einen neuen therapeutischen Ansatzpunkt zur Verhinderung der Emphysementwicklung bei COPD auf.

Table of Content

Eidesstattliche Versicherung **3**
Abstract **5**
Zusammenfassung **6**
Table of Content **8**
List of Figures **10**
List of Tables **12**
Part I: Introduction **13**
1 Chronic Obstructive Pulmonary Disease (COPD) 13
1.1 Diagnosis and current therapeutic approaches for COPD 14
1.1.1 Diagnosis of COPD 14
1.1.2 Therapeutic approaches for COPD 15
1.2 Pathological Hallmarks in COPD 21
1.2.1 Emphysema 22
1.2.2 Small airway remodeling 22
1.2.3 Chronic bronchitis 23
1.2.4 Pulmonary hypertension 23
1.3 Pathogenesis of COPD 24
2 Epigenetics 27
2.1 Linker histone H1 30
2.2 High Mobility Group Nucleosome Proteins 31
2.2.1 High mobility group nucleosome protein 5 (HMGN5) 33
3 HMGN5 and Emphysema 38
4 Aim of Research 39
Part II: Material and Methods **41**
5 Material 41
5.1 Cell line 41
5.2 Chemicals and reagents 41
5.3 Buffer and solutions 42
5.4 Antibodies 43
5.5 Oligonucleotides 43
5.6 Commercial kits 44
5.7 Devices 44

5.8 Consumables 45
5.9 Software 46
6 Methods 47
6.1 Cell culture 47
6.2 RNA Interference 47
6.3 Cigarette smoke extract 49
6.4 Gene expression analysis 49
6.5 Cell apoptosis 51
6.6 Cell proliferation and migration 52
6.7 Cell cycle analysis 53
6.8 Human samples 55
6.9 Protein expression analysis 56
6.10 Immunofluorescence 58
6.11 Statistical analysis 59
Part III: Results 61
7 HMGN5 expression and localization in COPD patients 61
8 Silencing of HMGN5 in human alveolar type II like cell line A549 63
9 HMGN5 silencing of A549 cells affects susceptibility to cell death 65
10 Impairment of cell cycle in response to HMGN5 downregulation 68
11 Proliferation and migration of A549 cells after HMGN5 downregulation 72
12 Gene expression of other HMGN family members 75
Part IV: Discussion 77
References 83
Acknowledgments - Danksagung 97

List of Figures

Figure 1: Current version of the COPD assement tool. 15
Figure 2: Smoking cessation reduces lung function decline independent of disease stage. 16
Figure 3: Pharmacological treatment algorithms according to the GOLD committee' proposed ABCD classification. 18
Figure 4: Pathological changes in the lung of COPD patients. 21
Figure 5: Simplified representation of inflammatory and structural cells involved in COPD. 25
Figure 6: Mechanisms of epigenetic regulation. 27
Figure 7: Family members of HMG protein superfamily. 31
Figure 8: Human and mouse HMGN5 (NSBP1). 34
Figure 9: Interaction of HMGN5 and linker histone H1 affect chromatin compaction. 36
Figure 10: HMGN5 RNA and protein expression in various tissues. 37
Figure 11: siRNA transfection of A549 cells. 48
Figure 12: Gating of FACS-sorted propidium-iodide stained A549 cells..... 54
Figure 13: Gating of FACS-sorted A549 cells expressing geminin-GFP and Cdt1-RFP 55
Figure 14: COPD patients show reduced expression of HMGN5. 61
Figure 15: HMGN5 is predominantly expressed in alveolar epithelial type-II cells and bronchial epithelial. 62
Figure 16: Silencing of HMGN5 in human alveolar type II like cell line A549. . 64
Figure 17: HMGN5 silenced AT-II cells are more susceptible to induced cell death. 66
Figure 18: Apoptosis and necrosis related genes after HMGN5 downregulation and exposure to CSE. 67
Figure 19: HMGN5 silencing impairs cell cycle in AT-II cells. 68
Figure 20: HMGN5 silencing causes accumulation of AT-II cells in early cell cycle phases. 70
Figure 21: Changes of cell cycle associated genes after HMGN5 downregulation and exposure to CSE. 71

Figure 22: Woundhealing ability of AT-II cells is affected by CSE, but hardly by HMGN5 deficiency. 73
Figure 23: Effect of HMGN5 silencing and CSE in A549 cells. 74
Figure 24: HMGN5 knockdown affects expression of its family protein HMGN1. 75

List of Tables

Table 1: List of chemicals, reagents and solutions used in this study 42
Table 2: Composition of buffers and stock solutions 43
Table 3: Primary and secondary antibodies used for Western Blot and Immuno-flourescence 43
Table 4: List of primers used for gene expression analysis 44
Table 5: List of kits used in this study 44
Table 6: List of devices used in this study 45
Table 7: List of consumables used in this study 46
Table 8: List of software used in this study 46
Table 9: Composition of reagents for cDNA master mix 50
Table 10: Composition of reagents for qPCR master mix 51
Table 11: Demographics and clinical characteristics of COPD transplant patients (mean ± SEM). 56

Part I: Introduction

1 Chronic Obstructive Pulmonary Disease (COPD)

Chronic obstructive pulmonary disease (COPD) is one of the leading causes of morbidity and mortality worldwide and remains a major public health challenge (Vogelmeier et al. 2017). Although researchers intensely investigate COPD, our current knowledge is not sufficient to causally treat the disease (Burney 2017). This might be due to its complexity as COPD is not just – as its term suggests – a single disorder. It is characterized by a progressive airflow limitation caused by small airway remodeling, chronic bronchitis and parenchymal lung destruction termed emphysema (Rabe and Watz 2017). The manifestation of these pathological abnormalities can differ between patients and clinical symptoms can range from chronic cough to dyspnea and excessive sputum production (Vogelmeier et al. 2017).

The Global Burden of Disease Study 2015 has ranked COPD as the third leading cause of death worldwide with over 3 million patients dying of the disease annually (Mortality and Causes of Death 2016). The number of COPD cases is varying regionally and has been estimated to reach a global prevalence of 11,7% of the people aged 30 years and over in 2010 with a higher prevalence in men (14,3%) compared to women (7,6%) (Adeloye et al. 2015). However, there is also data suggesting a prevalence almost equal between the sexes (Landis et al. 2014).

COPD usually results from long-term exposure to noxious particles or gases (Vogelmeier et al. 2017). While cigarette smoking is considered as the most common risk factor for COPD, only about 20% of smokers develop COPD (Mannino and Buist 2007; Lange et al. 2015; Salvi and Barnes 2009). This suggests other environmental factors including air pollution caused by biomass fuels as well as genetic variations associated with lung development during childhood, aging and nicotine addiction contributing to disease development (Brusselle and Bracke 2015). In recent years epigenetic mechanisms such as DNA methylation and histone modifications have been attracting growing attention and might explain the variable susceptibility between humans to develop COPD (Cheng et al. 2016; Schamberger et al. 2014; Sundar et al. 2014; Wain et al. 2017).

1.1 Diagnosis and current therapeutic approaches for COPD

1.1.1 Diagnosis of COPD

COPD is most commonly diagnosed in individuals aged 40 years and over as the disease is generally developing slowly (Raherison and Girodet 2009). Especially in the elderly patient, COPD occurs in conjunction with other chronic diseases such as cardiovascular disease or musculoskeletal dysfunction, thus increasing the morbidity at higher ages (Mannino et al. 2015). Patients presenting symptoms like dyspnea, chronic cough or sputum production and/or a history of exposure to risk factors must be accurately examined considering a diagnosis of COPD. However, spirometry is required to identify the presence of airflow limitation in order to enable a formal diagnosis of COPD to be made, because chronic respiratory symptoms might occur in patients having non-pathological spirometry values. Spirometry allows the determination of airflow limitation by measuring the maximum volume, a patient can exhale in 1sec after deep inspiration, known as forced expiratory volume in 1sec (FEV_1). For the diagnosis of COPD, a post-bronchodilator FEV_1 <70% of the forced vital capacity (FVC = the maximum volume a patient can exhale after deep inspiration) is required (Vogelmeier et al. 2017).
Spirometry is not only used to establish the diagnosis of COPD, it is further applied to assess disease severity based upon airflow limitation by comparing the patients FEV_1 to a healthy reference group (GOLD spirometric grades 1-4, Figure 1). However, to achieve the best therapy and outcome for each individual, it is paramount to assess all symptoms and exacerbation risks (Vogelmeier et al. 2017). Hence, the Modified British Medical Research Council (mMRC) questionnaire allowing the determination of dyspnea (Bestall et al. 1999; Fletcher 1960) and the COPD Assessment Test (CAT) providing a comprehensive assessment of symptoms (Jones, Tabberer, and Chen 2011), are important tools in COPD assessment. To evaluate the risks of exacerbations earlier treated events in the patient history must be recorded as they act as a reliable predictor (Hurst et al. 2010). The combination of spirometry, with the assessment of patient symptoms and history of exacerbation is essential for the diagnosis and adequate prognosis and is implemented in the GOLD Report as a refined ABCD assessment scheme (Figure 1) (Vogelmeier et al. 2017).

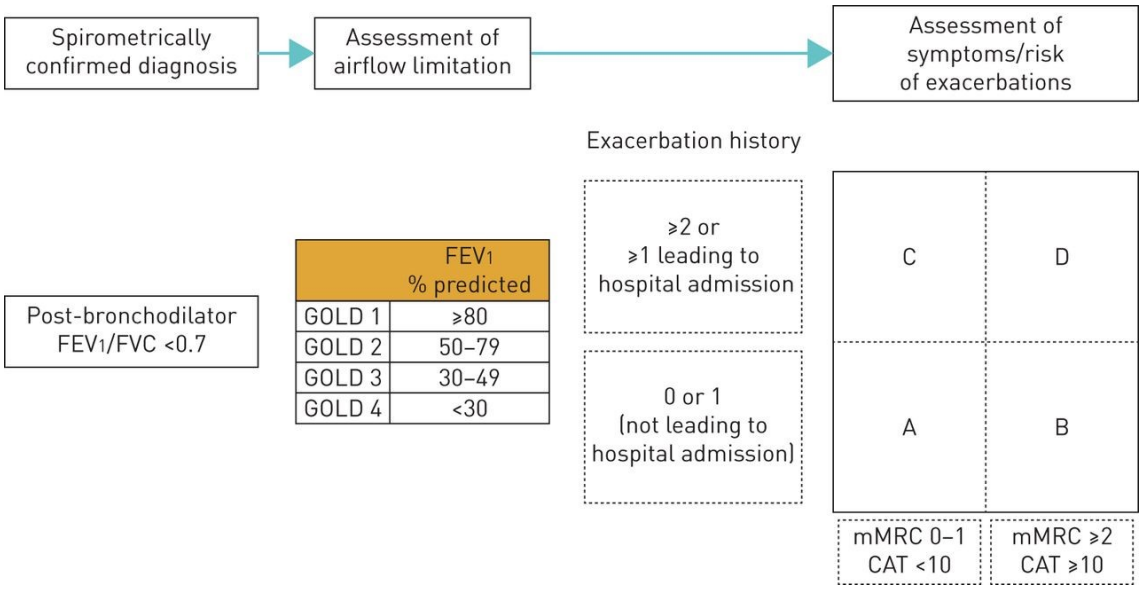

Figure 1: Current version of the COPD assement tool. Spirometry is required to establish the diagnosis of COPD by measuring post-bronchodilatator FEV_1/FVC and to assess airflow limitation classified by the GOLD stages 1-4 using FEV_1 as % of predicted. Each patient is assigned to one of the group A-D based on symptoms recorded by the mMRC and/or the CAT and exacerbation history. FEV_1 = forced expiratory volume in 1sec; FVC = forced vital capacity; GOLD = Global Initiative for Chronic Obstructive Lung Disease; mMRC = modified Medical Research Council; CAT = COPD Assessment Test. Figure reference (Vogelmeier et al. 2017).

1.1.2 Therapeutic approaches for COPD

Although at the present time COPD is an incurable disease, effective and individual disease management and therapy allow improvement in patient's health related quality of life. The COPD assessment scheme provides the basis for optimal therapy for each patient. According to the severity of symptoms and the risk of exacerbations patients are classified in groups (A-D) and receive personalized treatment based on their group affiliation and FEV_1 (graded in GOLD stages 1-4) ranking (see Figure 1) (Vogelmeier et al. 2017).

1.1.2.1 Smoking cessation

Given that cigarette smoking is the main risk factor for the development of COPD, smoking cessation plays an essential role in attenuating disease development and reducing exacerbations as well as comorbidities related to smoking (Jimenez-Ruiz et al. 2015; Scanlon et al. 2000). As most of the patients find it difficult to quit smoking, cessation intervention programs should be encouraged and can be highly effective (Anthonisen et al. 2005). Accordingly, regular supervision supported by interventions such as nicotine replacement therapy or treatment with varenicline, bupropion or nortriptyline improve smoking cessation rates (Vogelmeier et al. 2017; Stead et al. 2016).

Fletcher and Peto illustrated the decline in lung function (represented by FEV_1) over lifetime in smokers, non-smokers and those who have stopped smoking at a certain age. Although smoking cessation cannot recover lung function, it allows the further decline in FEV_1 to slow down (Figure 2) (Fletcher and Peto 1977).

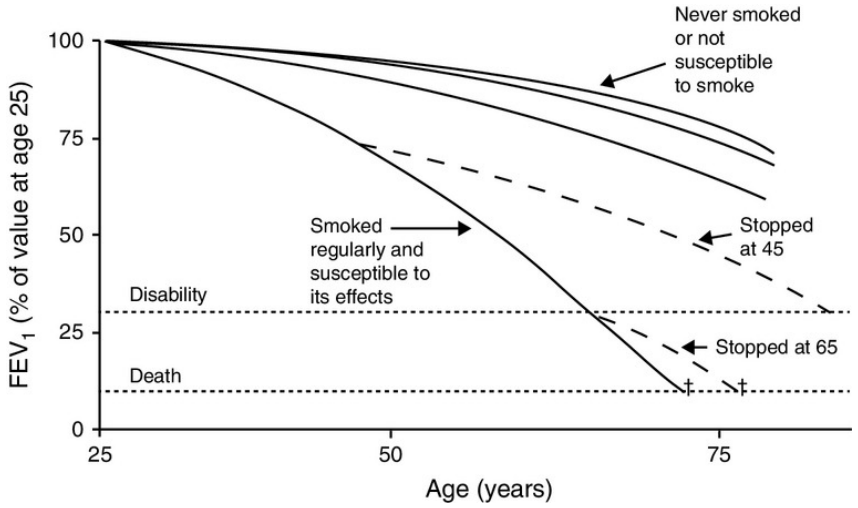

Figure 2: Smoking cessation reduces lung function decline independent of disease stage. Decline of lung function over lifetime in smokers, non-smokers and those who have stopped smoking at a certain age**.** Smoking causes a more rapid decline of FEV_1 in patients susceptible to cigarette smoke. If smoking is stopped at a certain age, the further decline in FEV_1 slows down and gets closer to the course of the natural decline due to aging. FEV_1 = forced expiratory volume in 1sec. Figure reference (Welte, Vogelmeier, and Papi 2015) reproduced from (Fletcher and Peto 1977).

1.1.2.2 Pharmacotherapy

The severity of symptoms, airflow limitation and risk of exacerbations are the basis for individualized pharmacologic therapy in COPD. Pharmacologic treatment aims to relieve symptoms, the risk of exacerbations and to improve exercise tolerance and health-related quality of life (HRQOL) (Vogelmeier et al. 2017).

Bronchodilatators

Bronchodilatators including beta($ß_2$)-agonists and antimuscarinic drugs are crucial COPD drugs and are known to increase FEV_1, reduce lung hyperinflation and improve exercise endurance (O'Donnell et al. 2004; O'Donnell et al. 2006).
$ß_2$-agonists act through $ß_2$-adrenergic receptors ($ß_2$-ARs) and increase the levels of cyclic AMP (cAMP) whereas antimuscarinic drugs block the binding of acetylcholine (ACh) to the muscarinic receptor, both resulting in airway smooth muscle relaxation (Nardini et al. 2014). Both $ß_2$-agonists and antimuscarinic drugs comprise short acting and long acting drugs (Vogelmeier et al. 2017).
Short acting $ß_2$-agonists (SABAs) and short acting muscarinic antagonists (SAMAs) has been shown to improve the patient' FEV_1 and symptoms (Sestini et

al. 2002; Appleton et al. 2006). However, the GOLD guidelines recommend to not use short acting bronchodilators on a regular basis but using long acting bronchodilators as the baseline therapy for COPD. Studies have shown that both long acting ß$_2$-agonists (LABAs) and long acting muscarinic antagonists (LAMAs) have positive effects on lung function, dyspnea, health status and exacerbation frequency (Vogelmeier et al. 2017). However, treatment with the LAMA tiotropium exhibited a greater effect in reducing exacerbations compared to LABAs (Decramer et al. 2013; Vogelmeier et al. 2011).

For patients where monotherapy is not sufficient to control the disease, treatment with a combination of bronchodilators in particular as LABA and LAMA is recommended (Vogelmeier et al. 2017). This combination has been shown to exhibit greater improvements on patient outcomes including lung function, symptoms and health status compared to monotherapy (Cazzola and Molimard 2010; Singh et al. 2015; van der Molen and Cazzola 2012; Mahler et al. 2015). Moreover, LABA/LAMA combinations have been shown to prevent exacerbations more effectively than LABA monotherapy alone does (Wedzicha et al. 2013).

As it is illustrated in Figure 3 the recommended pharmacological treatment of stable COPD is based on the patient symptoms and risk of exacerbations according to GOLD groups A-D. However, if airflow limitation is not in line with the level of symptoms, further evaluation and strategies should be taken into consideration (Vogelmeier et al. 2017).

In addition to ß$_2$-agonists and antimuscarinic drugs the xanthine derivate theophylline appears to have small effects on bronchodilation in stable COPD patients (Ram et al. 2002).

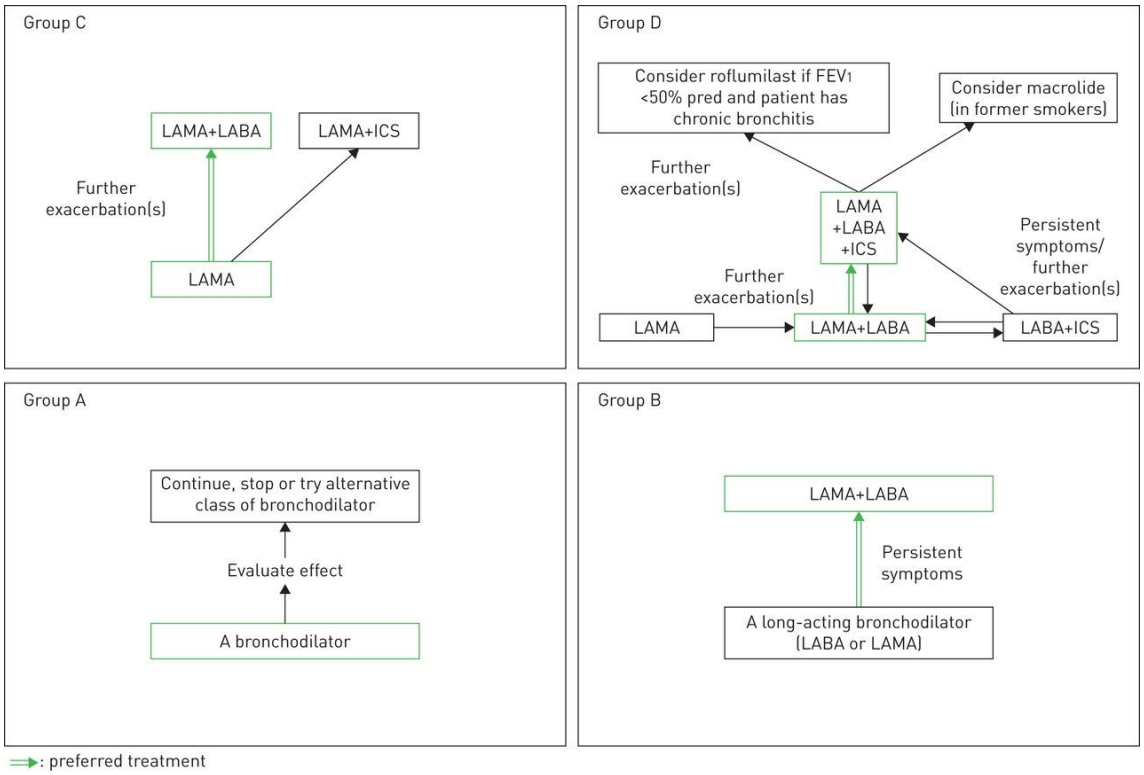

Figure 3: Pharmacological treatment algorithms according to the GOLD committee' proposed ABCD classification. The ABCD classification is based on the assessment of symptoms and exacerbation risks and is key for individualized management of COPD patients. Preferred treatment options are indicated by highlighted boxes and doubled arrows. GOLD = Global Initiative for Chronic Obstructive Lung Disease; LABA = long acting β2-agonist; LAMA = long acting muscarinic antagonist; ICS = inhaled corticosteroid; FEV1 = forced expiratory volume in 1sec. Figure reference (Vogelmeier et al. 2017).

Anti-inflammatory therapy

In patients with moderate to severe COPD and a history of exacerbations the use of anti-inflammatory drugs mostly inhaled corticosteroids (ICS) can be an effective therapeutic option (Vogelmeier et al. 2017).

However, there are some limitations. Some evidence revealed a stronger reduction of exacerbations for LABA/LAMA compared to LABA/ICS combination (Wedzicha et al. 2016). Moreover, LABA/ICS combination was found to be not superior in reducing exacerbation rate compared to monotherapy with the LAMA tiotropium (Wedzicha et al. 2008).

There is contradictory data regarding mortality in COPD patients taking ICS (Soriano et al. 2003; Calverley et al. 2007) and monotherapy with ICS does not impact the long-term decline in FEV_1 in those patients (Soriano et al. 2007). Nevertheless, LABA/ICS combination has demonstrated a beneficial effect on lung function, exacerbation rate and quality of life, which seem to be further increased by triple inhaled therapy comprising LABA/LAMA/ICS (Vogelmeier et al. 2017). In addition, several studies revealed that patient blood eosinophil counts had an impact on the effect of ICS in conjunction with bronchodilator therapy (Watz et al. 2016; Siddiqui et al. 2015; Pascoe et al. 2015).

Other anti-inflammatory drugs that may be considered to reduce exacerbations in COPD patients are phosphodiesterase-inhibitors (PDE4-Inhibitors) e.g. roflumilast for those with chronic bronchitis in a severe or very severe disease stage, antibiotics such as the macrolides azithromycin and erythromycin and mucolytics/antioxidants such as carbocysteine and N-acetylcystein (Vogelmeier et al. 2017).

Alpha 1-Antitrypsin augmentation

Although alpha 1-Antitrypsin (AAT) deficiency occurs in a low frequency, the WHO recommends to screen all patients with a diagnosis of COPD to initiate appropriate therapy in case of deficiency (Tsechkovski, Boulyjenkov, and Heuck 1997).

Vaccination

It is recommended to administer Influenza and pneumococcal vaccines to COPD patients as it reduces the risk of exacerbations and severe illness (Vogelmeier et al. 2017).

1.1.2.3 Non-pharmacological treatments

Pulmonary rehabilitation, education and self-management

Pulmonary rehabilitation including disease education and self-management is an indispensable element of effective disease management in all patients with relevant symptoms and/or high exacerbation risk. Pulmonary rehabilitation is a multidisciplinary approach aiming to improve physical and mental status, symptoms and HRQOL (Spruit et al. 2013). Educational support and self-management as an integrated part of rehabilitation target, among others, smoking cessation, self-recognition of exacerbations, appropriate use of inhaler device, disease understanding and explanation of therapeutic procedure. There is conflicting data for the duration of these programs, however according to GOLD, patients benefit the most from programs over a period of 6 to 8 weeks (Vogelmeier et al. 2017; Spruit et al. 2013). Although such treatment strategies exert beneficial impact on patient outcome and additionally seem to be cost-effective, they are too little used (Rabe and Watz 2017; Rochester et al. 2015).

Oxygen and ventilation therapy

Long-term oxygen therapy is recommended in patients having severe resting hypoxemia, however it provides limited to no benefit in patients with stable COPD (Stoller et al. 2010; Vogelmeier et al. 2017). Ventilatory support may be indicated

in patients hospitalized due to exacerbation and in patients suffering from COPD and obstructive sleep apnea (Vogelmeier et al. 2017).

Interventional therapies

In some patients with severe emphysema lung volume reduction surgery (LVRS) and/or bronchoscopic interventions can be indicated (Vogelmeier et al. 2017; Shah et al. 2017). Finally, if the disease is extensively progressed lung transplantation is considered as a substantial treatment option to improve quality of life and functional lung capacity (Vogelmeier et al. 2017).

1.2 Pathological Hallmarks in COPD

It has long been recognized, that several pathological changes in the lung of COPD patients can be observed and can lead to progressive airflow limitation, the main feature of COPD (Vogelmeier et al. 2017). Processes such as infiltration of inflammatory cells, and impaired injury-repair mechanisms of the lung tissue and cells can cause lung abnormalities associated with emphysematous destruction, small airway remodeling, chronic bronchitis and lung hypertension (Figure 4). The site, where these pathological features occur may vary and comprise airways, the parenchymal compartment and/or the pulmonary vasculature (Hogg and Timens 2009). Also, the extent, in which each of these pathological features occur may vary from patient to patient leading to different phenotypes of COPD (Castaldi et al. 2014).

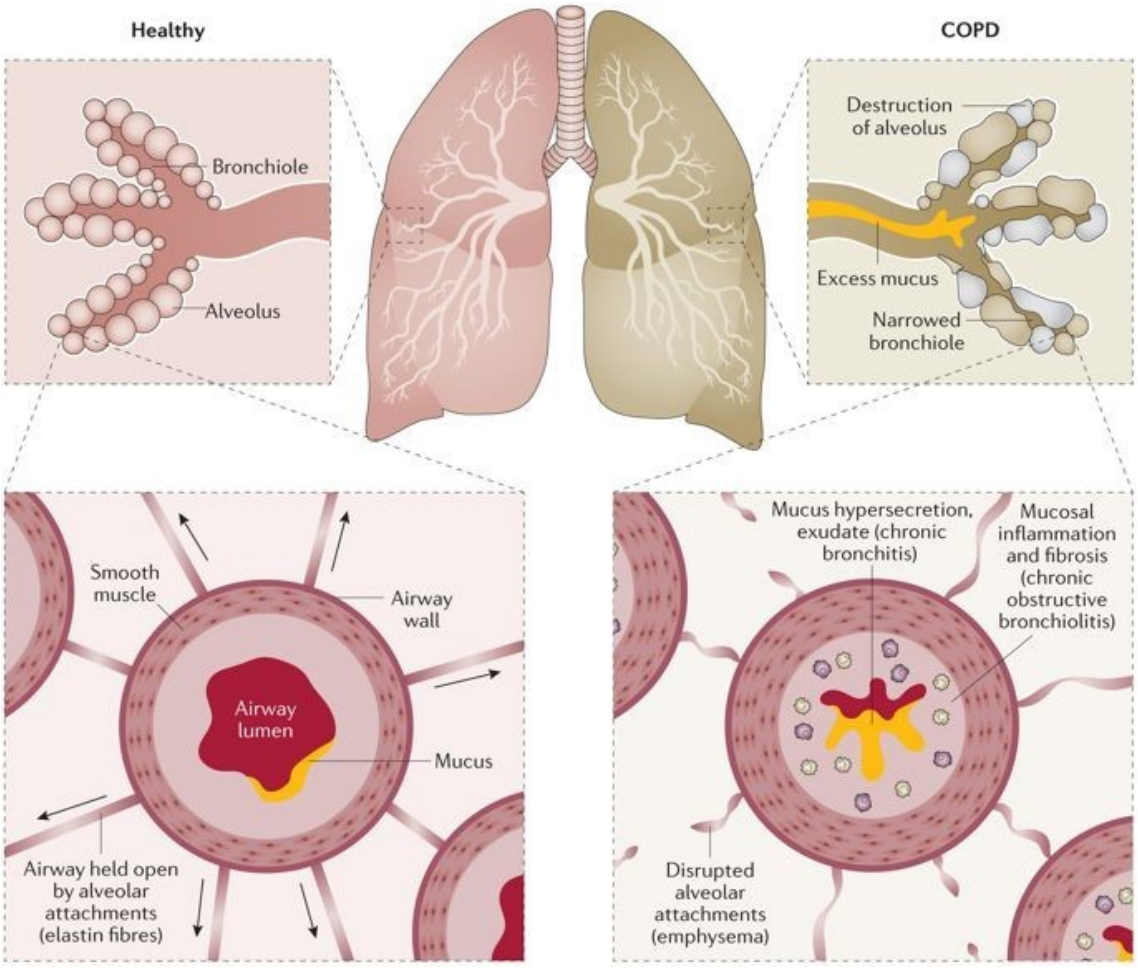

Figure 4: Pathological changes in the lung of COPD patients. Some of the pathological features occurring in the lung of COPD patients are shown on the right. These may include destruction of alveoli and disrupted alveolar attachments during emphysema development, mucus hypersecretion defined as chronic bronchitis and small airway remodeling with mucosal inflammation and fibrosis. For comparison a healthy lung is displayed on the left. Figure reference (Barnes et al. 2015).

1.2.1 Emphysema

The American Thoracic Society has defined emphysema “as a condition of the lung characterized by abnormal, permanent enlargement of airspaces distal to the terminal bronchiole, accompanied by the destruction of their walls, and without obvious fibrosis” (Snider et al. 1985). Emphysema is commonly associated with a smoking history, chronic airway obstruction, dyspnea and the occurrence of airway lesions (Snider et al. 1985). Although, emphysema usually appears first in the respiratory bronchioles (Hogg et al. 2009) it is mainly characterized by the destruction of the alveolar structures consisting primarily of alveolar type I (AT-I) and type II (AT-II) cells, in conjunction with endothelial and fibroblastic cells (Sirianni, Chu, and Walker 2003; Tuder et al. 2006). Consequently, emphysematous destruction leads to a decrease in alveolar surface area and a reduction in lung elastic recoil resulting in impaired gas-exchange and expiratory flow. However, it has also been found that emphysema can occur in patients who do not have impaired lung function, this raises the question whether the occurrence of emphysematous lesions without airflow limitation applies as a risk factor for the development of COPD at a later stage (Hogg and Timens 2009).
For a long time, detection and quantification of emphysema was limited to autopsy, but the establishment of computed tomography (CT) has made it possible to assess the site and severity of emphysema radiologically (Pare and Camp 2012). Subsequently, several studies have identified distinct disease phenotypes and significant correlation to clinical and pathological features related to COPD (Castaldi et al. 2014; Martinez et al. 2012; Nakano et al. 2000).

1.2.2 Small airway remodeling

COPD is defined by limited expiratory airflow which has been reported to result aside from reduced lung elastic recoil, small airway thickening, fibrosis-induced luminal constriction and mucus-induced occlusion of small airways (Hogg and Timens 2009). In addition to this, it has been shown that increased airflow resistance in distal airways correlated with the loss of small airways detectable before emphysematous destruction occurs (McDonough et al. 2011). The pathological changes of the smaller airways stated above have been reported to correlate with the clinical severity of COPD (Hasegawa et al. 2006; Hogg et al. 2007). There is conflicting data about the vasculature at the site of small airways during remodeling processes in the lung of COPD patients. Whereas one study has reported small vessels to be not increased in number in the walls of small airways (Hasegawa et al. 2006), another study has revealed enlarged vascular area in these distal airways (Hashimoto, Tanaka, and Abe 2005).

1.2.3 Chronic bronchitis

The prevalence of chronic bronchitis in COPD patients varies considerably among different population-based studies ranging from 14 to 74% (Kim and Criner 2013). Chronic bronchitis has been defined as a “chronic or recurrent increase in the volume of mucoid bronchial secretion sufficient to cause expectoration” (Medical Research Council 1965) for a minimum of three months in each of two successive years (Kim and Criner 2013). Chronic bronchitis is clinically demonstrated by increased bronchial mucus production which is commonly reflected by productive cough (Medical Research Council 1965). It has been demonstrated that COPD patients exhibiting a phenotype of chronic bronchitis show a higher decline in lung function, undergo a higher number of exacerbations with increased severity and are affected by a higher risk of mortality (Burgel et al. 2009; Kim et al. 2011; Vestbo, Prescott, and Lange 1996; Lahousse et al. 2017). Cigarette smoke is considered as the main risk factor for the development of chronic bronchitis and contributes to excessive mucus production (Ebert and Terracio 1975).

1.2.4 Pulmonary hypertension

Pulmonary hypertension has been shown to develop in patients with COPD, especially in advanced stages, most commonly due to hypoxic conditions (Sakao, Voelkel, and Tatsumi 2014). However, it has also been reported to appear in patients with mild COPD under non-hypoxemic conditions (Wright et al. 1983). Additionally, the loss of pulmonary vessels has been indicated to correlate with the magnitude of pulmonary hypertension (Matsuoka et al. 2010). Nevertheless, it has been shown that increased pulmonary artery pressures in COPD patients can occur independently of emphysematous changes and loss of pulmonary vessels (Sakao, Voelkel, and Tatsumi 2014). Oswald-Mammosser et al. reported a 5-year survival rate of 36% among COPD patients with a mean pulmonary artery pressure (mPAP) above 25mmHg and considered the level of PAP to be the most suitable prognostic value in oxygen-treated COPD patients (Oswald-Mammosser et al. 1995). Long-term oxygen therapy has been suggested in patients with severe COPD as it can stop the progression of pulmonary hypertension and even decreases PAP values, albeit not to the expected physiological level (Weitzenblum et al. 1985).

1.3 Pathogenesis of COPD

The pathogenesis of COPD is based on complex pathobiological mechanisms and interactions triggered by the body's exposure to noxious particles or gases. Cigarette smoke is considered as the major etiologic factor for the development of COPD. It contains a combination of over 4700 chemical compounds and generates an enormous number of radicals and other oxidants (MacNee 2001). However, there is strong evidence that also non-smokers may develop the disease (Lamprecht et al. 2011), though it has been shown that they exhibit a milder disease with less symptoms, lower inflammatory response and lower risk for cardiovascular comorbidities compared to former and current smokers with COPD (Thomsen et al. 2013). This implies other factors than cigarette smoke play a role in the pathogenesis of COPD. Svanes et al. have demonstrated "childhood disadvantage factors" such as maternal smoking, childhood asthma and childhood respiratory infections to be significantly associated with reduced FEV_1 and with a higher risk of COPD later in life. Indeed, they could observe a similar impact of these "childhood disadvantage factors" and cigarette smoking (Svanes et al. 2010). Lange et al. reported that low levels of FEV_1 in early adulthood must be considered as a critical factor for the development of COPD and that patients affected by that, do not necessarily demonstrate an accelerated decline in FEV_1 (Lange et al. 2015). Furthermore, outdoor air pollution, occupational exposures, biomass smoke and dietary factors as well as chronic asthma and tuberculosis seem to be associated with COPD formation, however to suggest that these factors significantly cause COPD requires further research (Eisner et al. 2010).
COPD is also known to be caused by genetic syndromes such as alpha-1 antitrypsin (AAT) deficiency which affects a small group of patients (Tsechkovski, Boulyjenkov, and Heuck 1997). AAT protects the lung from proteolytic processes mainly by inhibiting neutrophil elastase, that induces lung tissue damage upon AAT deficiency (Edgar et al. 2017). The heterogeneity and susceptibility of COPD is further associated with genetic variations that have been detected in genome-wide association studies (GWAS) such as AGER-PPT2, ELN, SFTD, TERT, NAF1, HHIP, FAM13A and IREB2. (Lee et al. 2014; Hancock et al. 2010; Pillai et al. 2009; Brusselle and Bracke 2015). Other factors that modify the risk of developing COPD are sex, age, socioeconomic status and residential area (Gershon et al. 2011). Accordingly, the interaction between genes, environmental and other factors may lead to multifactorial processes that predispose an individual to COPD.

Lung inflammation plays a crucial role in the pathogenesis of COPD particularly since normal inflammatory responses were observed to be modified by cigarette smoke and other noxious particles (Barnes 2016). Both innate and adaptive

immune responses are involved in the inflammatory response of COPD in the course of which circulating neutrophils, monocytes and lymphocytes are attracted to the lungs (Figure 5) (Barnes 2016). Also in smokers without obvious airflow limitation such an inflammatory pattern can be observed (Barnes 2016). However, the inflammatory response is intensified in COPD patients and appears to be modified by genetic and epigenetic alterations (Barnes 2016). Neutrophils release serine proteases (neutrophil elastase) and metalloproteinases (MMP8 and MMP9) that degrade matrix components destroying the alveolar walls. Additional to the innate and adaptive immune system, structural cells including airway and alveolar epithelial cells, endothelial and fibroblastic cells are getting activated and release inflammatory mediators such as IL-1β, IL-6, TNF-α or CXCL8 magnifying the response (Gao et al. 2015). Moreover, other factors including TGF- β, known to trigger fibrosis and VEGF, a key factor in maintaining cell integrity are reported to shape the pathological response in COPD (Barnes 2016).

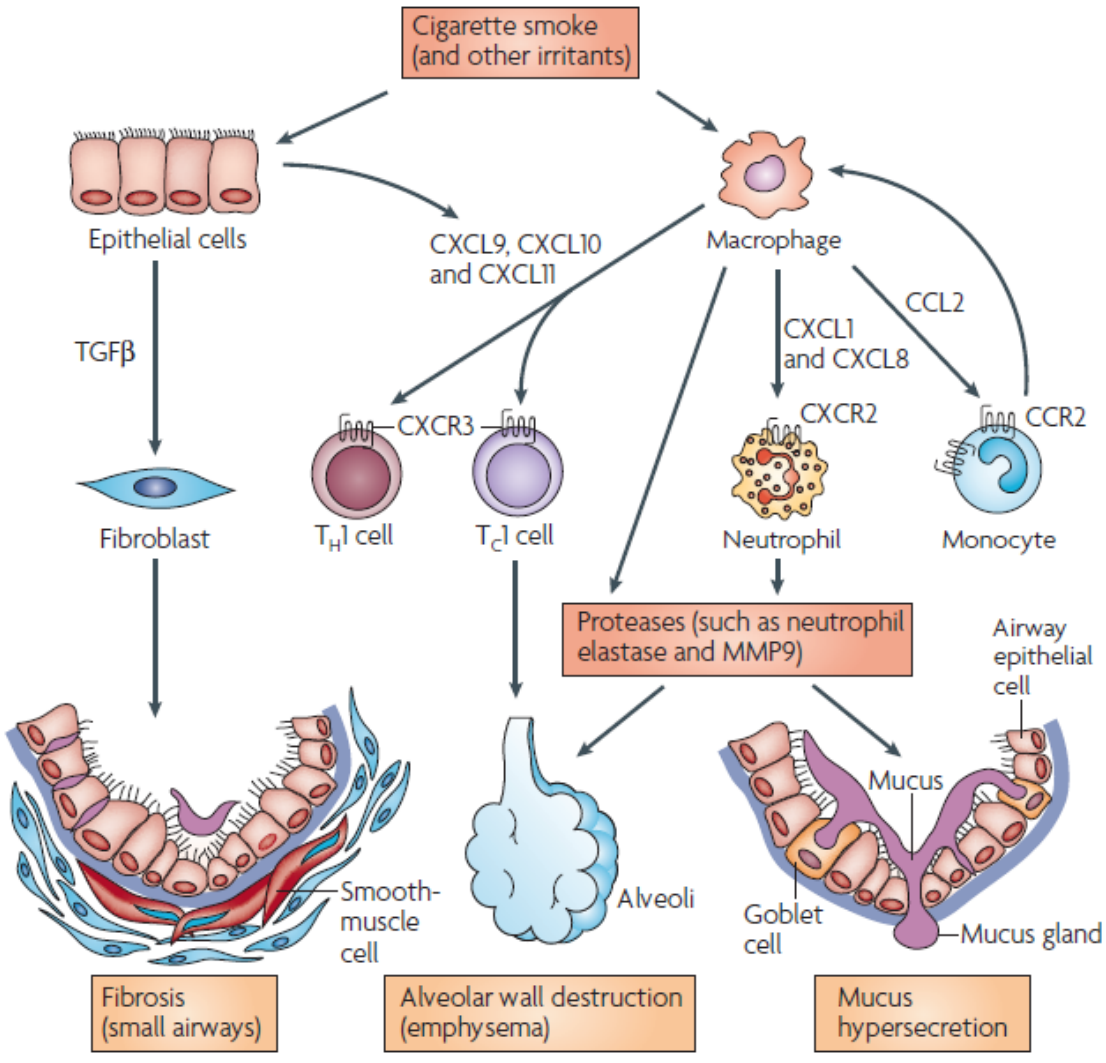

Figure 5: Simplified representation of inflammatory and structural cells involved in COPD. Epithelial cells and macrophages get activated by cigarette smoke and other noxious particles

and release several cytokines whereof some attract inflammatory cells to the lungs. These inflammatory cells together with epithelial cells and fibroblasts shape the pathological response in COPD resulting in fibrosis, alveolar wall destruction and mucus hypersecretion. Figure reference (Barnes 2008).

Airway epithelial cells are the primary defense line against extrinsic substances by releasing antioxidants, antiproteases, defensins and producing mucus. More distal, alveolar type I (AT-I) and type II (AT-II) cells, in conjunction with endothelial and fibroblastic cells build a close cellular network that is important in maintaining the alveolar structure (Sirianni, Chu, and Walker 2003; Tuder et al. 2006). Although AT-II cells only cover about 5% of the alveolar surface area they play a decisive role as progenitors for AT-I cells during injury repair, synthesize and secret the lung protective surfactant and release pro-inflammatory cytokines and chemokines. Upon exposure to cigarette smoke and other noxious particles alveolar cells undergo injury leading to impaired surfactant production, as a result of increased oxidative stress and protease release (Zhao et al. 2010). As a consequence, this repetitive injurious response of alveolar cells and increased cell death can cause the development of emphysema.

The pathological processes underlying alveolar destruction and inflammation in emphysema are shaped by a complex interaction of molecular and cellular events including oxidative stress, protease-antiprotease imbalance and cell death and repair, all of which play a key contributing role in COPD (Tuder et al. 2006). These interactive processes may be mutually reinforced and are promoted by risk factors that influence disease formation and progression (see previous section) (Tuder et al. 2006). As stated before, inflammatory and structural changes still persist after smoking cessation (Barnes 2016), which strengthens the assumption of amplified feed forward loops that are generated by endogenous signaling even in absence of cigarette smoke exposure (Tuder et al. 2006). Nevertheless, the fact that only a minority of smokers suffer from COPD and that disease development varies considerably among individuals imply that the presence and interaction of multiple factors and processes determine the susceptibility of each individual to COPD formation (Barnes 2016). In respect to this variable susceptibility a substantial role is devoted to epigenetic alterations.

2 Epigenetics

There is existing evidence that epigenetic regulation plays a notable role in COPD development and may partially explain the heterogenous vulnerability of each individual to COPD (Cheng et al. 2016; Schamberger et al. 2014; Sundar, Yao, and Rahman 2013; Wain et al. 2017; Qiu et al. 2012). The term “epigenetics” means “in addition to changes in the genetic sequence” and implies that gene activity is not only regulated by changes in the DNA sequence, but also by processes that do not alter the underlying genetic sequence (Weinhold 2006). Waddington introduced this term in 1942 and by now epigenetic regulation has been attracting growing attention and importance. Epigenetic processes are known to modify gene expression, thus leading to a particular phenotype (Allis and Jenuwein 2016). Epigenetic modifications are potentially heritable but can also be reversed and are known to be dynamically influenced by environmental factors, aging or nutrition (Schamberger et al. 2014). Many types of epigenetic regulation have been identified comprising histone modification, DNA-methylation or RNA-associated silencing, all of which can interact with each other (Figure 6) (Schamberger et al. 2014).

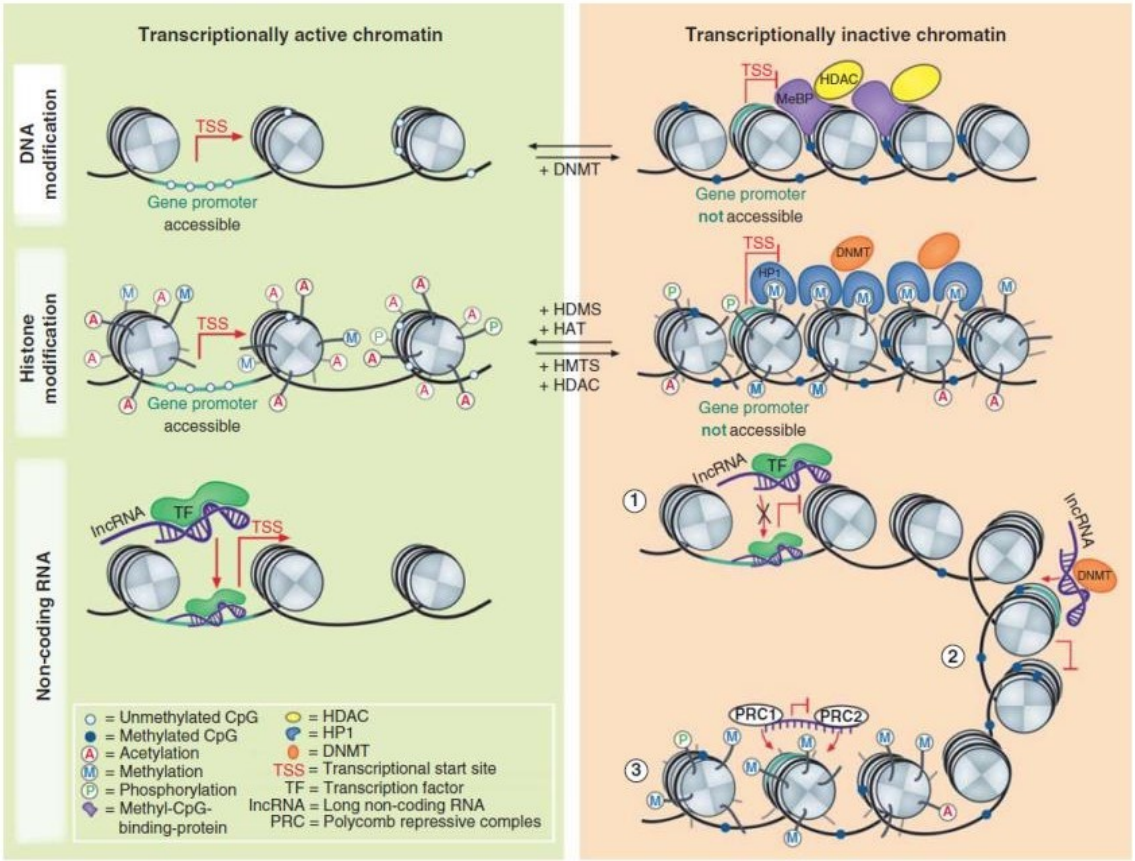

Figure 6: Mechanisms of epigenetic regulation. Gene transcription is modified epigenetically

through distinct mechanisms. The left panel shows the architecture of the transcriptionally active chromatin, whereas in the right panel the transcriptionally inactive chromatin is displayed. (1) DNA modification: DNA methyltransferases (DNMTs) regulate the methylation of DNA, more precisely of cytosine residues at cytosine-phosphate-guanine (CpG) sites. Increased methylation leads to transcriptional repression, that is reinforced by methyl-CpG-binding proteins (MeBPs) that recruit histone deacetylases (HDACs). (2) Histone modification: Histones can be modified at specific amino acids at their N-terminal. Such posttranslational modifications including among others methylation, acetylation or phosphorylation are catalyzed by various enzymes such as histone methyltransferases (HMTS), histone acetytransferases (HATs) or kinases and are removed by histone demethylases (HDMS), HDACs or phosphatases. Other enzymes and complexes can bind to these posttranslational modifications and regulate the chromatin accessibility and thus gene transcription. (3) Non-coding RNA (ncRNA): ncRNAs, especially long ncRNAs (lncRNAs) function as regulators of gene expression by recruiting other chromatin remodeling complexes such as polycomb repressive complexes (PRCs) or DNMTs. Figure reference (Schamberger et al. 2014).

Epigenetic regulation is required for many biological functions and ensures normal development and health, however if these mechanisms are disturbed, it can result in significant changes in health and behavior leading to diseases such as cancer, mental retardation, chromosomal abnormalities or lung diseases (Simmons 2008). There is existing evidence that cigarette smoke, the major risk factor for COPD is linked with epigenetic modifications found in the airway epithelium and that lung inflammation is markedly affected by epigenetic regulation (Adcock et al. 2007). Genome wide studies demonstrated global changes in the DNA-methylation pattern of lymphoblasts and macrophages (Monick et al. 2012), as well as in small airways (Vucic et al. 2014). These changes were significantly associated with smoking status (Monick et al. 2012). Furthermore, reduced expression and activity of histone modifying enzymes such as histone deacetylases (HDACs) (Ito et al. 2005) or sirtuins (SIRTs) (Rajendrasozhan et al. 2008), that have anti-inflammatory function were found in COPD patients. Schamberger et al. summarized the main epigenetic modifications found in COPD models and COPD patients (Schamberger et al. 2014).

Epigenetic regulation implies the dynamic remodeling of chromatin and regulation of gene expression, DNA replication and repair (Cuvier and Fierz 2017). The dynamic interaction of numerous proteins and the chromatin within the nucleus regulates the accessibility of the DNA and therefore affects the transcriptional program of mammalian cells. Chromatin is built by a complex of DNA and distinct proteins, forming an elementary unit of which all chromosomes consist of. Whereas the term euchromatin is used for open and accessible chromatin, heterochromatin represents the transcriptionally suppressed chromatin state. The basic unit of chromatin is the nucleosome, which is composed by a protein octamer wrapped by an approximately 147 base pair (bp) long DNA strand. The protein octamer consists of two copies each of the histones H2A, H2B, H3 and

H4. The nucleosomes are stabilized by the interaction of multiple proteins and are connected by short fragments of “linker” DNA (Annunziato 2008).

2.1 Linker histone H1

The linker histone H1, that binds to the DNA entry/exit sites of the nucleosomes stabilizes both the nucleosome complex and higher ordered structures of the chromatin by forming chromatin fibers (Luger, Dechassa, and Tremethick 2012). Several linker H1 subtypes are known to exist in mammalian cells with a highly conserved globular domain and more variable positively charged tails among the subtypes within a distinct species (Hergeth and Schneider 2015). It has been shown, that histone H1 is not as initially thought, an absolute repressor of transcription, it rather affects the regulation of specific genes (Shen and Gorovsky 1996). Histone H1 acts in a dynamic manner by changing its binding site to chromatin continuously. Misteli et al. discovered that most of the H1 molecules in living cells stick to a chromatin site for a mean time of about 220 seconds before rapidly moving to another available binding site (Misteli et al. 2000). Furthermore, linker histone H1 was shown to be post-translationally modified by acetylation, phosphorylation and/or methylation, leading to alterations in the chromatin structure and thus affecting nuclear activities and biological processes (Wisniewski et al. 2007). Such processes are also influenced by a group of non-histone architectural proteins, known as high mobility group (HMG) proteins, devoting their attention as potential regulators in disease development.

2.2 High Mobility Group Nucleosome Proteins

The high mobility group nucleosome (HMGN) proteins belong to the high mobility group (HMG) superfamily including nuclear proteins that are the most commonly expressed chromosomal non-histone proteins in living cells (Bianchi and Agresti 2005). The HMG family comprises three subgroups: HMGA, HMGB and HMGN. All members of these are known to affect DNA-dependent processes through chromatin modulation (Bianchi and Agresti 2005). A negatively charged C-terminal domain can be found in all HMG proteins, however, each family contains specific functional motifs. The HMGA family is characterized by AT-hooks, the HMGB family is characterized by HMG boxes whereas the members of the HMGN family exhibit a positively charged nucleosome binding domain to specifically target nucleosomes (Figure 7) (Bianchi and Agresti 2005; Hock et al. 2007). All HMG proteins bind to chromatin independently of the underlying DNA sequence (Postnikov and Bustin 2010). The acidic tail occurring in all HMG proteins has been reported to both regulate the binding properties of HMG proteins and to be involved in interactions with other proteins (Catez and Hock 2010). Furthermore there is existing evidence that HMG proteins affect the posttranslational modification of histone proteins supporting their role as modulators of epigenetic processes (Lange, Mitchell, and Vasquez 2008; Lim et al. 2004; Lim et al. 2005).

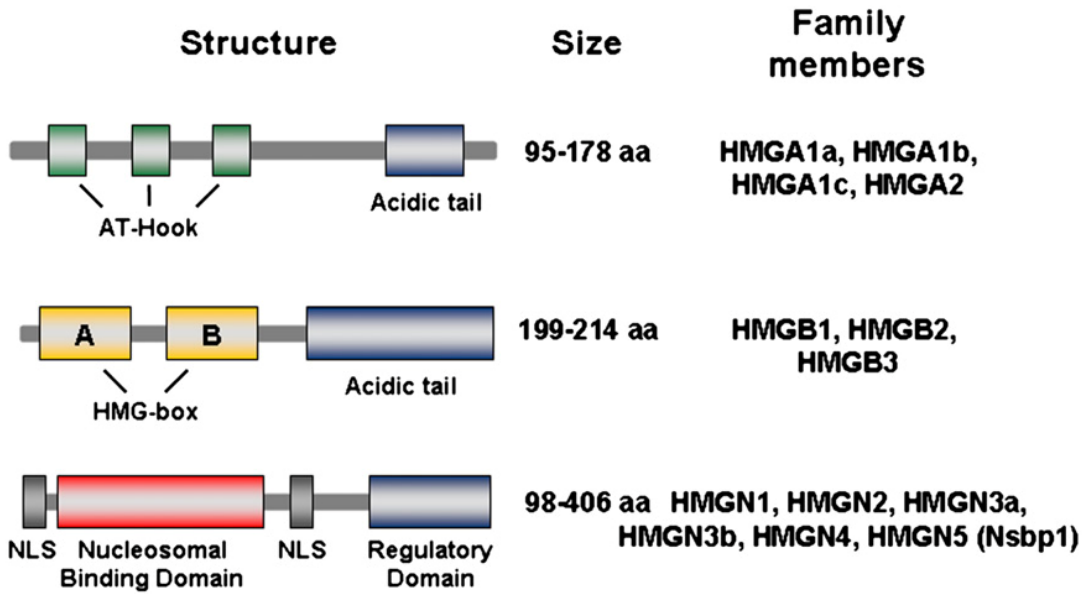

Figure 7: Family members of HMG protein superfamily. The HMG superfamily is subdivided into three groups: HMGA (upper panel), HMGB (middle panel) and HMGN (lower panel). Each family is characterized by specific functional motifs indicated by colors (green, yellow, red) whereas an acidic C-terminal tail (blue) can be found in all HMG proteins. Members of each family are listed on the right and their various size is indicated by the range of amino acids (aa). Figure reference (Catez and Hock 2010)

Among all the HMG proteins, HMGN have the unique feature of binding to the nucleosome core particle (CP). To do so, they have a highly conserved nucleosome binding domain (NBD), a core octapeptide enabling binding to the nucleosome core particle (CP) (Ueda et al. 2008). Furthermore, HMGN proteins contain a bipartite nucleosome localization signal (NLS) (Hock, Scheer, and Bustin 1998) and exhibit a less conserved C-terminal domain, enriched in highly acidic residues acting as regulatory domain (RD) (Trieschmann et al. 1995). HMGN proteins exist in all vertebrates (Kugler, Deng, and Bustin 2012) and are known to modify the chromatin architecture globally and locally (Kugler, Deng, and Bustin 2012). They act by binding to the nucleosome and regulating the access of regulatory factors to chromatin and the underlying DNA (Hock, Scheer, and Bustin 1998). Through their distinct domains, HMGN proteins have the potential to interfere with the binding of both other HMGN proteins and the linker histone H1. Additionally, they can interact with histones within the nucleosome and affect their posttranslational modifications (Kato et al. 2011; Trieschmann et al. 1995). It has been shown that two molecules of the same HMGN protein bind to the CP to form a complex restricted to one HMGN variant (Alfonso et al. 1994). It has also been shown that two serine residues within the NBD of HMGN proteins are phosphorylated during metaphase impeding the formation of such a HMGN-dimer-DNA complex (Cherukuri et al. 2008). Moreover, HMGNs were the first non-histone proteins identified as acetylated by histone acetylases (Kugler, Deng, and Bustin 2012). Similar to histone H1, HMGN proteins bind dynamically to nucleosomes and continuously change between the chromatin binding sites (Postnikov and Bustin 2010). The time HMGN proteins reside bound to a nucleosome CP is significantly longer than their transition between the nucleosomes. As a consequence, in terms of time, most of the HMGN proteins are bound to the nucleosomes (Postnikov and Bustin 2010). Only about 1% of the nucleosome CPs can be occupied due to the limited amount of HMGN proteins existing in the nucleus (Postnikov and Bustin 2010). However, the dynamic behavior of HMGN proteins enables every nucleosome to be potentially targeted (Postnikov and Bustin 2010).

Changes in the chromatin architecture induced by HMGN proteins affect the transcriptional regulation. Recent studies in genetically altered mice have shown that the expression of a non-functional HMGN variant, in which the NBD was deleted to prevent the ability to bind to the nucleosome CP, leads to variant and tissue specific changes in the transcriptional profile (Kugler et al. 2013). However, the tissue specific pattern of gene expression was not altered in the presence of a non-functional HMGN variant, indicating that HMGN proteins exert their role in modulating the fidelity of the transcriptional profile already preexisting in a tissue (Kugler et al. 2013). The impaired fidelity of gene expression due to a non-functional HMGN variant did not result in pronounced phenotypes of the mice,

however, if the mice were subjected to certain stress the development of specific phenotypes and symptoms could be observed (Kugler et al. 2013). Thus, it is likely that biological processes that were affected by the presence of a non-functional HMGN variant made these mice vulnerable to further genetic processes and environmental stress (Kugler et al. 2013). In this regard, it has been shown that mice exhibiting non-functional HMGN1 develop behavioral abnormalities and show impaired repair processes after DNA damage (Abuhatzira et al. 2011; Birger et al. 2005; Birger et al. 2003; Kugler et al. 2013) and that mice exhibiting non-functional HMGN3 show a mild diabetic phenotype (Ueda et al. 2009; Kugler et al. 2013).

2.2.1 High mobility group nucleosome protein 5 (HMGN5)

As a member of the HMGN family, HMGN5 (also known as NSBP1) exhibits structural similarity to other HMGN proteins, however HMGN5 contains a considerably longer C-terminal tail, that additionally differs among various species (Rochman, Malicet, and Bustin 2010). The C-terminus of the mouse Hmgn5 comprises around 300 amino acids, whereas in human HMGN5 it comprises around 200 amino acids (Figure 8) (Rochman, Malicet, and Bustin 2010). The gene coding for HMGN5 is located on the X-chromosome in a single copy in both mouse (X D) and human (Xq13.3) and comprises 6 exons and 5 introns (King and Francomano 2001). Unlike *Hmgn5,* that encodes a 406 amino acid long protein, *HMGN5* encodes a 282 amino acid long protein, resulting from the difference in the number of amino acids encoded by exon 6 (King and Francomano 2001). According to the structural features of the HMGN family, the positively charged N-terminal domain of HMGN5 contains a nuclear localization signal (NLS) followed by the nuclear binding domain (NBD) (Ueda et al. 2008). The NBD is characterized by a highly conserved functional sequence (RRSARLSA), that enables HMGN5 to bind to the nucleosome CP (Ueda et al. 2008). The decisive role of this sequence is reflected by studies that have demonstrated that modifications in just two serine residues within the sequence abolish the ability of HMGN5 and other HMGN proteins to interact with the nucleosome CPs (Prymakowska-Bosak et al. 2001; Shirakawa et al. 2000; Ueda et al. 2008).

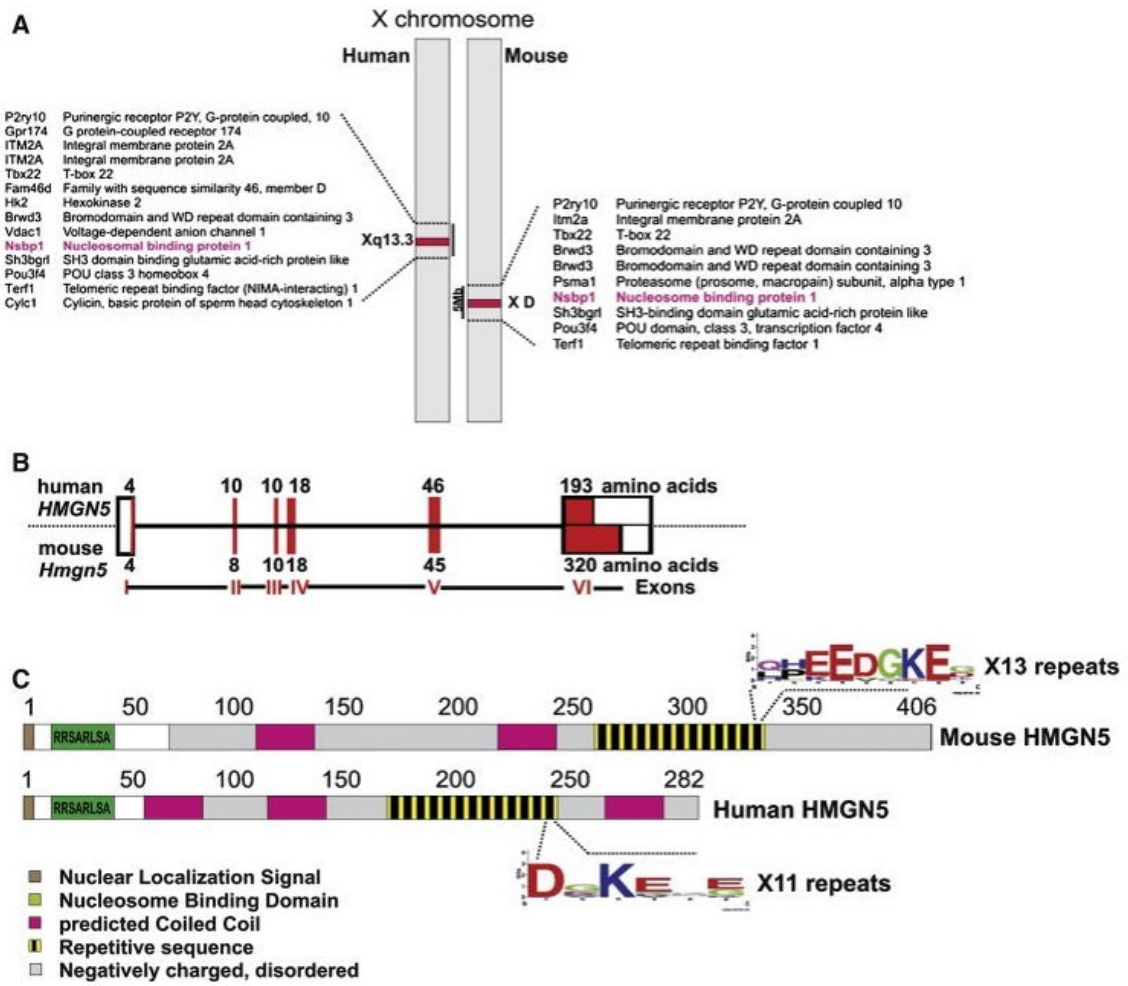

Figure 8: Human and mouse HMGN5 (NSBP1). (A) Both in human and mouse the gene encoding for HMGN5 is located on the X-chromosome and (B) is composed of 6 exons. The number of amino acids encoded by each exon is almost the same, except for exon 6, that is decisive for the different length of the HMGN5 protein in human and mouse. (C) Human and mouse HMGN5 share similar structural motifs: a nuclear localization signal (NLS) and nucleosome binding domain (NBD) in the N terminus and a highly acidic C-terminus containing repeats of an amino acid sequence. Figure reference (Rochman, Malicet, and Bustin 2010).

The long acidic C-terminal tail of HMGN5 contains several repeats of an amino acid sequence and differs in the sequence and number of repeats between human and mouse; 13 repeats could be detected in mouse HMGN5, 11 repeats in human (Figure 8) (Shirakawa et al. 2000). It has been shown, that the C-terminal tail directs HMGN5 to distinct chromatin domains and plays an essential role in the interaction with other proteins (Rochman, Malicet, and Bustin 2010; Rochman et al. 2009). Thus, human HMGN5 localizes to both eu- and heterochromatin like other HMGN proteins do, whereas mouse HMGN5 specifically targets euchromatin. Studies suggest that this is due to the sequence of the HMGN5 C-terminal tail, rather than to the negative charge. (Malicet et al. 2011).

Like other HMGN proteins, HMGN5 dynamically moves within the nucleus, interacts with nucleosomes and linker histone H1 (Rochman et al. 2009). Given

that the binding sites on the nucleosome for HMGN5 and H1 partially overlap, these two proteins compete for their binding on the nucleosomes (Rochman, Malicet, and Bustin 2010). Moreover, HMGN5 and H1 interact through their differently charged tails (Figure 9, A) (Rochman, Malicet, and Bustin 2010). As the C-terminal domain of H1 is essential to stabilize chromatin compaction (Woodcock, Skoultchi, and Fan 2006), the interaction of the negatively charged tail of HMGN5 with the positively charged C-terminal domain of H1 diminishes the ability of H1 to maintain chromatin compaction (Figure 9, B) (Rochman et al. 2009). Nevertheless, it has been demonstrated, that the correct binding of HMGN5 to the nucleosome CP is required to induce chromatin decondensation, as HMGN5 mutants lacking the ability to bind to nucleosomes failed to cause chromatin decondensation (Rochman et al. 2009). Thus, it can be concluded that both molecular mechanisms, the competition for the nucleosome binding sites and the interaction through their C-terminal tails play an essential role in affecting chromatin compaction (Rochman et al. 2009). In addition, Rochman et al. demonstrated that it is the interaction of HMGN5 with nucleosomes that enables HMGN5 to impact the cellular transcription profile (Rochman et al. 2009).

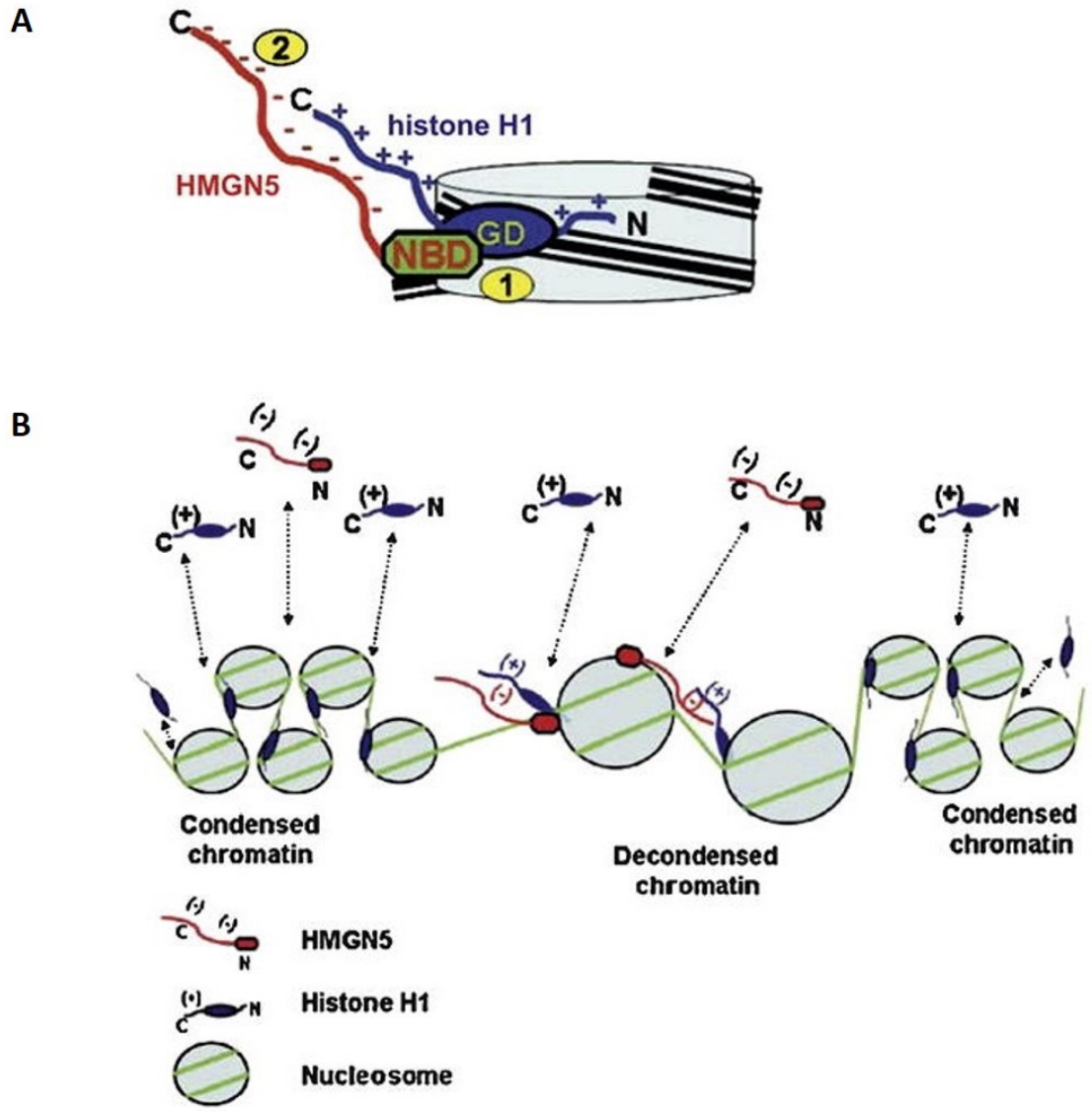

Figure 9: Interaction of HMGN5 and linker histone H1 affect chromatin compaction. (A) HMGN5 and H1 interact in two ways: The nuclear binding domain (NBD) of HMGN5 competes with the globular domain (GD) of H1 at their binding site to the nucleosome (1) and the negatively charged C-terminal domain of HMGN5 interacts with the positively charged C-terminal domain of H1 (2). (B) Both HMGN5 and H1 act in a dynamic manner by changing their binding sites to chromatin continuously. Thereby HMGN5 counteracts the H1-mediated compaction of chromatin resulting in loosened chromatin structure. Figure reference (Rochman, Malicet, and Bustin 2010)

HMGN5 is ubiquitously expressed and its function in various organs has not yet been sufficiently explored. The Human Protein Atlas (HPA) RNA dataset revealed HMGN5 to be highly expressed in testis and epididymis (Figure 10), other data suggest also a very high RNA expression in the pituitary gland (FANTOM5 dataset, not shown) (The Human Protein Atlas). Moreover, protein expression analysis by the HPA demonstrate a high expression of HMGN5 in many tissues (Figure 10) (The Human Protein Atlas). The expression of HMGN5 was shown to vary during embryonic development and HMGN5 likely plays a role in differentiation and function of the placenta (Shirakawa et al. 2009). HMGN5 was

demonstrated to affect cellular regulation and differentiation by modifying the expression of various genes (Rochman et al. 2011). Overexpression of HMGN5 was found to be associated with many cancer types such as prostate cancer (Song et al. 2006), bladder cancer (Wahafu et al. 2011), clear cell renal cell carcinoma (Ji et al. 2012) and breast cancer (Li et al. 2006). Moreover, a study has revealed that downregulation of HMGN5 inhibits proliferation of human lung cell cancer cells (Chen et al. 2012).

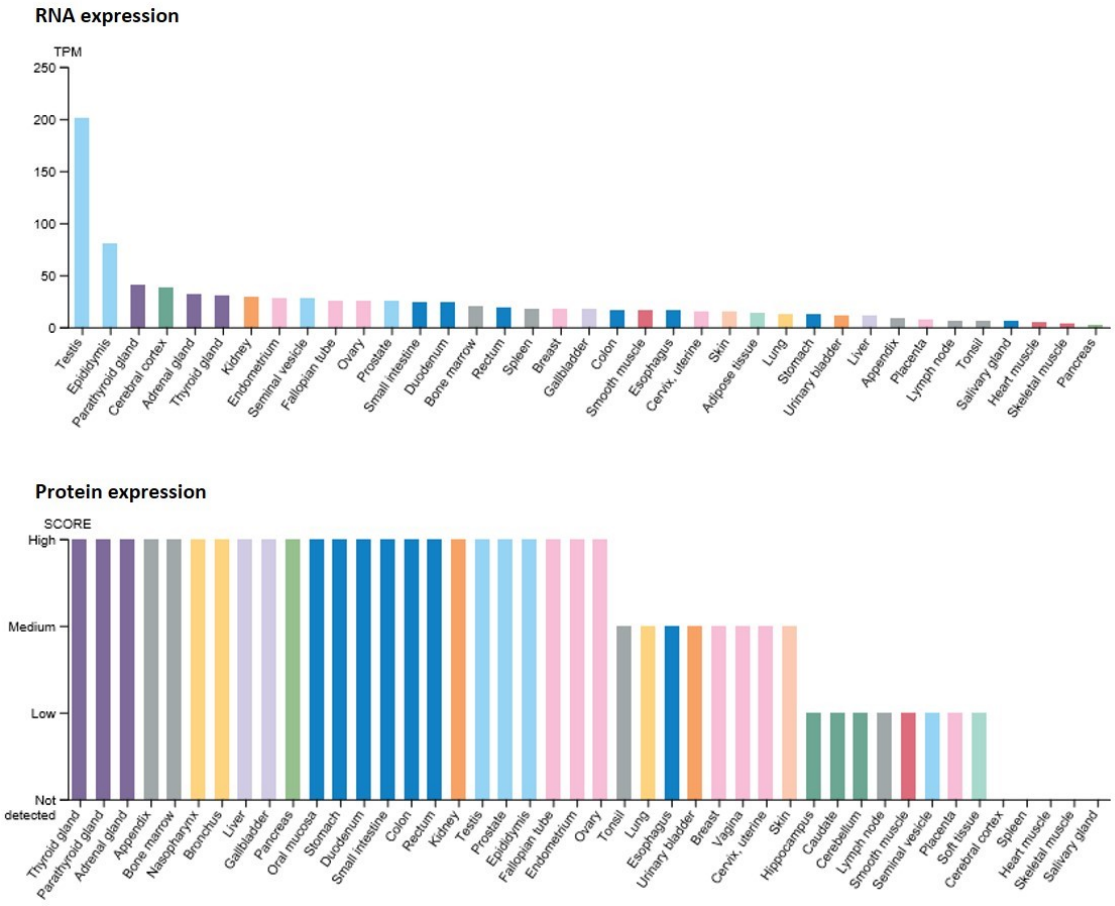

Figure 10: HMGN5 RNA and protein expression in various tissues. HMGN5 is ubiquitously expressed in several tissues indicated by its RNA (upper panel) and protein expression (lower panel). Data analysis was performed by the Human Protein Atlas. TPM = transcripts per million. Plots shown were taken from (The Human Protein Atlas).

3 HMGN5 and Emphysema

It has been previously shown that HMGN (Adcock et al. 2007)proteins affect the fidelity of the cellular expression profile dependent on the tissue and HMGN variant examined. It was observed that mice expressing a HMGN5 mutant protein unable to bind to the nucleosome CP (hereinafter referred to as HMGN5$^{-/-}$ mice), demonstrated emphysematous changes in their lungs (Kugler et al. 2013). To investigate the impact of HMGN5 deficiency both WT and HMGN5$^{-/-}$ mice were subjected to pancreatic porcine elastase (PPE) treatment which is known to induce emphysematous changes in the lungs (Sarker et al. 2015; Suki, Bartolak-Suki, and Rocco 2017). HMGN5$^{-/-}$ mice showed a more severe emphysema compared to their WT littermates as assessed by lung function and histological analysis of airspace enlargement (unpublished observations from our lab). Moreover, in WT mice exposed to CS smoke, that did show features of COPD like emphysema, airway remodeling and inducible bronchus-associated lymphoid tissue (iBALT) (Jia et al. 2018; Conlon et al. 2020), expression of HMGN5 RNA was downregulated (unpublished observations from our lab). Similarly, the application of PPE in WT mice resulted in lower levels of HMGN5 RNA and protein (unpublished observations from our lab).

4 Aim of Research

As mentioned in the previous chapter, emphysematous mice showed reduced expression of HMGN5 and HMGN5$^{-/-}$ mice demonstrated enhanced emphysema development. Investigations with the mouse alveolar type II cell line LA-4 indicate that this may result from reduced cellular proliferation and increased apoptosis of ATII cells (unpublished observations from our lab). This work follows up on these recent observations with a translational approach. In order to determine whether COPD patients reveal any differences in HMGN5 expression compared to healthy subjects, HMGN5 expression and localization in the lungs was determined. HMGN5 was reported to affect chromatin compaction and thus the cellular transcription profile (Rochman et al. 2009). To explore its effect on physiological processes that are known to be impaired in emphysema development the human alveolar-type-II-like cell line A549 was used. Cell death, proliferation and cell cycle were investigated in HMGN5 deficient cells. Kugler et al. demonstrated that HMGN deficiency impairs the fidelity of gene expression but leads to pronounced effects only by additional exposure to stress (Kugler et al. 2013). Therefore, cigarette smoke, the main etiologic factor of COPD, was assessed in addition to HMGN5 deficiency. Although HMGN5 was shown to be associated with disease development, very less is known about the cellular processes HMGN5 regulates and the underlying mechanisms. This work therefore aims to provide further knowledge of the epigenetic regulator HMGN5 in the field of COPD and the potential mechanisms underlying its role in emphysema development.

Part II: Material and Methods

5 Material

5.1 Cell line

The human alveolar-type-II-like cell line A549 was purchased from the American Type Culture Collection (ATCC, Manassas, VA, USA).

5.2 Chemicals and reagents

Substance	Company
0,25% Trypsin-EDTA Solution	Sigma-Aldrich, St. Louis (USA)
0,4% (w/v) Trypan Blue	Sigma-Adrich, St. Louis (USA)
4x Laemmli Loading Buffer	Bio-Rad, Hercules (USA)
Acrylamide: N,N'- Methylene-Bisacrylamide 40% (29:1)	Carl Roth, Karlsruhe (GER)
AllStars Neg. Control siRNA (scrambled siRNA)	Qiagen, Hilden (GER)
Ammoniumsulfate (APS)	Carl Roth, Karlsruhe (GER)
Bovine Serum Albumin (BSA)	Sigma-Adrich, St. Louis (USA)
Cell Proliferation Reagent WST-1	Roche, Mannheim (GER)
Citrate Buffer	Zytomed Systems, Berlin (GER)
cOmplete, Mini, EDTA-free Protease Inhibitor	Roche, Mannheim (GER)
Dimethyl Sulfoxide (DMSO)	Sigma-Adrich, St. Louis (USA)
Distilled water	Helmholtz-Muenchen (GER)
DNase/Rnase-free water	Thermo Fisher Scientific, Waltham (USA)
dNTP Mix 10mM 1ml	Thermo Fisher Scientific, Waltham (USA)
Dulbecco's Modified Eagle Medium (DMEM)	Thermo Fisher Scientific, Waltham (USA)
Ethanol	Carl Roth, Karlsruhe (GER)
Fetal Bovine Serum (FBS)	Biochrom, Berlin (GER)
FlexiTube GeneSolution GS79366 for HMGN5	Qiagen, Hilden (GER)
HiPerFect Transfection Reagent	Qiagen, Hilden (GER)
Isopropanol	Carl Roth, Karlsruhe (GER)
Methanol	Merck, Darmstadt (GER)
$MgCl_2$ 50mM	Thermo Fisher Scientific, Waltham (USA)
Minimum Essential Media (MEM)	Thermo Fisher Scientific, Waltham (USA)
MuLV Reverse Transcriptase 5000U, 50U/µl	Thermo Fisher Scientific, Waltham (USA)

Substance	Company
N,N,N',N'-Tetramethylethylendiamin (TEMED)	Bio-Rad, Hercules (USA)
Non-Essential Aminoacids (NEA)	Biochrom, Berlin (GER)
PCR-Buffer II	Thermo Fisher Scientific, Waltham (USA)
Penicillin/Streptomycin (P/S)	Sigma-Aldrich, St. Louis (USA)
Phosphatase Inhibitor (Vanadate)	New England Biolabs, Ipswich (USA)
Phosphate Buffered Saline (PBS)	Thermo Fisher Scientific, Waltham (USA)
Precision Plus Protein Standard	Bio-Rad, Hercules (USA)
Random Hexamers 50µM	Thermo Fisher Scientific, Waltham (USA)
Restore PLUS Western Blot Stripping Buffer	Thermo Fisher Scientific, Waltham (USA)
RNase Inhibitor 2000U, 20U/µl	Thermo Fisher Scientific, Waltham (USA)
Roswell Park Memorial Medium 1640 (RPMI)	Biochrom, Berlin (GER)
Roti-Block	Carl Roth, Karlsruhe (GER)
SensiFast Sybr Green	Thermo Fisher Scientific, Waltham (USA)
Sodium Dodecyl Sulfate (SDS)	AppliChem, Darmstadt (GER)
ß-Mercaptoethanol	Sigma-Adrich, St. Louis (USA)
Staurosporine	Santa Cruz Biotechnology, Dallas (USA)
Triton X-100	Sigma-Adrich, St. Louis (USA)
Tween 20	Sigma-Adrich, St. Louis (USA)
Xylol	Carl Roth, Karlsruhe (GER)

Table 1: List of chemicals, reagents and solutions used in this study

5.3 Buffer and solutions

Buffer/Solution	Composition
10x PBS	Na2HPO4 KH2PO4 NaCl KCl
10x Transfer Buffer	Glycine 150 mM Tris 20 mM 20 % Methanol
5x Running Buffer	Tris (25mM) Glyzin (250mM) 0,5% SDS
PBS-T (Washing Buffer)	1x PBS 1 % Tween
Permeabilization Buffer	1x PBS 0,5 % Triton X-100

Buffer/Solution	Composition
RIPA Buffer	NaCl 150 mM Tris pH 7,2 10 mM SDS 0,1 % Triton X-100 1 % Deoxycholate 1 % EDTA 5 mM
MACS Buffer	0,5 % FBS 2 mM EDTA

Table 2: Composition of buffers and stock solutions

5.4 Antibodies

Primary Antibody	Company
Anti-HMGN5 antibody produced in rabbit (HPA000511)	Sigma-Aldrich, St. Louis (USA)
Anti-SP-C antibody (sc-7705)	Santa Cruz Biotechnology, Dallas (USA)
Anti-β-actin antibody	Abcam, Cambride (UK)
Secondary Antibody	**Company**
Anti-rabbit IgG, HRP-linked Antibody (#7074)	Cell Signaling, Danvers (USA)
Anti-DAPI antibody	Thermo Fisher Scientific, Waltham (USA)
Anti-goat antibody 568 nm	Thermo Fisher Scientific, Waltham (USA)
Anti-rabbit antibody 488 nm	Thermo Fisher Scientific, Waltham (USA)

Table 3: Primary and secondary antibodies used for Western Blot and Immunoflourescence

5.5 Oligonucleotides

Gene name	Forward primer (5'->3')	Reverse primer (3'->5')
BAX	TGGCAGCTGACATGTTTTCTGAC	TCACCCAACCACCCTGGTCTT
BCL2	TTTGAGTTCGGTGGGGTCAT	TGACTTCACTTGTGGCCCAG
CASP3	CTGTACCAGACCGAGATGTCA	CTGTACCAGACCGAGATGTCA
CCNB1	GCCTCTACCTTTGCACTTCC	GTAGAGTTGGTGTCCATTCACC
CCND1	GAGGAGCTGCTGCAAATGG	GCGGATGATCTGTTTGTTCTCC
CCNA2	TGGAAAGCAAACAGTAAACAGCC	GGGCATCTTCACGCTCTATTT
CCNE1	GCCAGCCTTGGGACAATAATG	CTTGCACGTTGAGTTTGGGT
C-JUN	CCAAAGGATAGTGCGATGTTT	CTGTCCCTCTCCACTGCAAC
HMGN1	CGGAAAACGGGGAAACGAAG	GAAGGGAGACAGGGACCACT
HMGN2	ACGAACCACAGAGAAGATCCG	TTTTGGCATCTCCATTTTCTGC

Gene name	Forward primer (5'->3')	Reverse primer (3'->5')
HMGN5	CAACAATGCCCAAAAGAAAGGC	GCATAGCAGACAACCTGGC
HPRT	AGGAAAGCAAAGTCTGCATTGTT	GGTGGAGATGATCTCTCAACTTTAA
KI67	ACGCCTGGTTACTATCAAAAGG	CAGACCCATTTACTTGTGTTGGA
PCNA	ACACTAAGGGCCGAAGATAACG	ACAGCATCTCCAATATGGCTGA
LDH-A	ATGGCAACTCTAAAGGATCAGC	CCAACCCCAACAACTGTAATCT
MB	AGTCAGAGGACGAGATGAAGG	GATGCATTCCGAGATGAACTCC
PPIA	ACCGTGTTCTTCGACATTGC	GTCTTTGGGACCTTGTCTGC
PPIB	GATAGAGCCAAGCTGCAACC	AATCCTTGCCATCCTTGAGC

Table 4: List of primers used for gene expression analysis

5.6 Commercial kits

Kit	Company
Amersham ECL Prime Western Blotting Detection Reagent	GE Healthcare, Buckinghamshire (UK)
eBioscience Annexin V Apoptosis Detection Kit	Thermo Fisher Scientific, Waltham (USA)
peqGOLD Total RNA Kit	PEQLAB Biotechnology, Erlangen (GER)
Pierce BCA Protein Assay Kit	Thermo Fisher Scientific, Waltham (USA)
SuperSignal West Femto Maximum Sensitivity Substrate	Thermo Fisher Scientific, Waltham (USA)

Table 5: List of kits used in this study

5.7 Devices

Device	Company
BDK Sterile Hood	Weisstechnik, Reiskirchen (GER)
Centrifuge 5430	Eppendorf AG, Hamburg (GER)
Centrifuge Galaxy 16 DH	VWR International, Darmstadt (GER)
Centrifuge Mini Spin Plus	Eppendorf AG, Hamburg (GER)
ChemiDoc XRS + Molecular Imager	Bio-Rad, Hercules (USA)
Cool Centrifuge, Mikro 220R	Andreas Hettich, Tuttlingen (GER)
Cool Centrifuge, Rotina 35R	Andreas Hettich, Tuttlingen (GER)
Coulter Mixer	Coulter Electronics Limited, Luton (GBR)
Decloaking Chamber	Biocare Medical, Pike Line (USA)
FACSCanto II Flow Cytometer	BD Biosciences, Franklin Lakes (USA)
Glass Cylinder	Lenz Laborglas, Wertheim (GER)

Device	Company
Haemocytometer Neubauer	Brand, Wertheim (GER)
Heat Block HBT 130	Ditabis, Pforzheim (GER)
Heat Block Thermomixer Compact	Eppendorf AG, Hamburg (GER)
Heating Cabinet	Memmert, Schwabach (GER)
Incubator MCO-20AK	SANYO Component, München (GER)
Magnetic Steerer COMBIMAG RET	IKA Werke, Staufen im Breisgau (GER)
Mastercycler Nexus Eco/ Nexus Gradient	Eppendorf AG, Hamburg (GER)
MicroAmp 96-Well Base	Thermo Fisher Scientific, Waltham (USA)
Microscope Axioskop	Carl Zeiss, Oberkochen (GER)
Microscope Axiovert 135	Carl Zeiss, Oberkochen (GER)
Microscope Axiovert 25	Carl Zeiss, Oberkochen (GER)
Microtome Hyrax m55	Carl Zeiss, Oberkochen (GER)
Multifix Constant MC 1000 FEC	Semikron, Nürnberg (GER)
Multipipette E3	Eppendorf AG, Hamburg (GER)
NanoDrop® ND-1000 Spectrophotometer	PEQLAB, Erlangen (GER)
Pipetboy	INTEGRA Biosciences, Zisers (SUI)
qRT – PCR Thermocycler StepOne™ Plus	Thermo Fisher Scientific, Waltham (USA)
Scale CP6201	Sartorius, Göttingen (GER)
Scanner Mirax Desk	Carl Zeiss, Oberkochen (GER)
Shaking Incubator	IKA Werke, Staufen im Breisgau (GER)
Systec Autoclave DE-23	Systec, Linden (GER)
Tecan Nanoquant Infinite 200 Pro	Tecan Group AG, Männedorf (SUI)
Unitwist 3D	UniEquip, Planegg (GER)
Vortexer NeoLab D6012	IKA Werke, Staufen im Breisgau (GER)
Vortexer VF2	IKA Werke, Staufen im Breisgau (GER)
Waterbath	GFL, Burgwedel (GER)
Western Blot (all devices)	Bio-Rad, Hercules (USA)

Table 6: List of devices used in this study

5.8 Consumables

Consumable	Company
Cellstar 24-well Culture Plate	Greiner Bio-One, Kremsmünster (AUT)
Cellstar Cell Culture Flask 75cm^2	Greiner Bio-One, Kremsmünster (AUT)

Consumable	Company
Dako Fluorescence Mounting Medium	Dako, Carpinteria (USA)
Dako Pen	Dako, Carpinteria (USA)
Eppendorf Tubes 0,5/1,5/2,0ml	Eppendorf AG, Hamburg (GER)
Falcon Tubes 15/50ml	Corning Science, Corning (USA)
Glass Pipettes 5/10/25ml	Greiner Bio-One, Kremsmünster (AUT)
Immun-Blot PVDF Membrane 0,2µm	Bio-Rad, Hercules (USA)
Injekt® – Syringes 20ml	B.Braun, Melsungen (GER)
MicroAmp™ Fast Optical 96-Well Ahesive Film	Thermo Fisher Scientific, Waltham (USA)
MicroAmp™ Fast Optical 96-Well Reaction Plate	Thermo Fisher Scientific, Waltham (USA)
Microscope Slides 76x26mm	VWR International, Darmstadt (GER)
Multitips automatic	Eppendorf AG, Hamburg (GER)
Nunc Cryo Tube Vials	Thermo Fisher Scientific, Waltham (USA)
Pasteurpipettes 230mm	Hirschmann, Eberstadt (GER)
RNase AWAY®	Carl Roth, Karlsruhe (GER)
SafeSeal Pipette Tips 10µm	Biozym, Hessisch Oldendorf (GER)
Syringefilter 0,22µm	TPP, Trasadingen (SUI)
TipOne® Pipette Tips 20/100/200/1000µm	Starlab, Hamburg (GER)

Table 7: List of consumables used in this study

5.9 Software

Software	Company
Axio Vision v1.9	Carl Zeiss, Oberkochen (GER)
FACS Diva Software v6.1.3	BD Biosciences, Franklin Lakes (USA)
GraphPad Prism v5.0	GraphPad, La Jolla (USA)
Image Lab v5.1	Bio-Rad, Hercules (USA)
StepOne Software v2.3	Thermo Fisher Scientific, Waltham (USA)
Tecan Magellan Software	Tecan, Männerdorf (SUI)
FlowJo v10	FlowJo LLC, Ashland (USA)
ZEN v2.3 (blue edition)	Carl Zeiss, Oberkochen (GER)

Table 8: List of software used in this study

6 Methods

6.1 Cell culture

A549 cells were cultured in Roswell Park Memorial Medium 1640 (RPMI) supplemented with 10% Fetal Bovine Serum, 1% Non-essential amino acids and 1% Penicillin/Streptomycin. Cells were grown in 75cm^2 cell culture flasks at 37°C in a humidified atmosphere with 5% CO_2 and split into new passage after reaching approximately 90-95% confluency. Cells were washed with 10ml of pre-warmed PBS and subsequently incubated with 3ml of 0,25% Trypsin-EDTA solution for 5min at 37°C to get the cells detached. Trypsinization was stopped by adding 7ml of medium and the desired volume of cell suspension was transferred to a new flask containing fresh culture medium.

6.2 RNA Interference

FlexiTube GeneSolution GS79366 comprising four different siRNAs targeting HMGN5 (HMGN5-siRNA) was used to perform RNA-Interference in A549 cells. All siRNAs were provided lyophilized. Upon delivery the siRNAs were dissolved in DNase/RNase-free water to obtain a 1µM stock solution of each single siRNA. Aliquots were prepared and stored at -20°C. Prior to transfection all four siRNAs were mixed and incubated for 30min in optiMEM-medium together with HiPerfect transfection reagent resulting in a 10nM-siRNA transfection master mix. Control cells (ctrl) were treated with optiMEM-medium only, however, to ensure that observations do not result from transfection itself a negative control siRNA (ctrl-siRNA) non-homologous to any known mammalian gene was utilized.
Cells grown in a 75cm^2 cell culture flask were processed as described in “6.1 Cell culture”. Whole suspension was transferred to a 50ml Falcon tube and centrifuged for 5min at 1500rpm at room temperature. Supernatant was discarded and cells were resuspended in 5ml of fresh medium prior to counting.
20µl of cell suspension was mixed in a 96-well-plate well with equal volume of 0,4% (w/v) Trypan Blue and 10µl were pipetted into a Neubauer chamber. Cell number was calculated using the following equation:

$$\frac{\textit{Cells counted in all four quadrants}}{4} \; x\; 2\; x\; 10^4 = n\; cells\; per\; ml$$

Based on the calculated number of cells a cell suspension containing 80 000 cells/ml was prepared.

The transfection of cells was carried out as “Reverse Transfection” in a 24-well plate as illustrated in Figure 11.
A volume of 125µl of transfection master mix containing either ctrl-siRNA or HMGN5-siRNAs or simply opti-MEM medium was added to each respective well. Subsequently 375µl of cell suspension, thus 30 000 cells were added to each well, resulting in a total volume of 500µl per well. Time of transfection was selected as the initial time of 0h. The plates were placed into the incubator and shaken ensuring the cells were evenly distributed. Unless otherwise stated, for each condition/culture medium a ctrl, ctrl-siRNA and HMGN5-siRNA were prepared in triplicate, respectively and transfection medium was replaced by 500µl of fresh culture medium after 24hours.

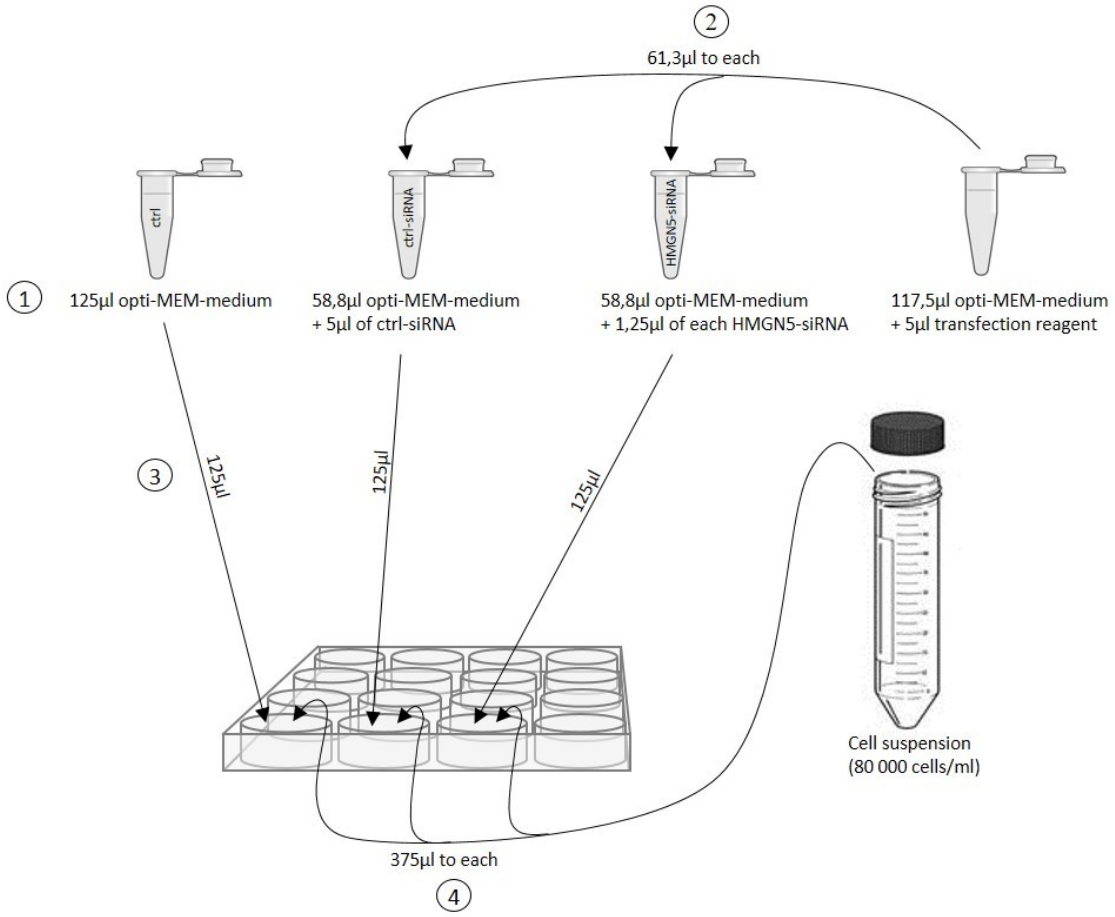

Figure 11: siRNA transfection of A549 cells. (1) Eppendorf tubes for each ctrl, ctrl-siRNA and HMGN5-siRNA were prepared using a 1µM stock of ctrl-siRNA and HMGN5-siRNAs. Transfection reagent was mixed separately with opti-MEM medium. Vials were vortexed and incubated for 5min. (2) Transfection reagent-containing opti-MEM media was added to the respective vials giving a ctrl-siRNA- and HMGN5-siRNA-transfection master mix. After vortexing samples were incubated for 30min. (3) Equal volume from each transfection master mix, as well as from the ctrl vial were transferred to the respective wells. (4) Cells were immediately added to each well. Volumes indicated are based on the calculation for one sample and were adapted to the respective n number.

6.3 Cigarette smoke extract

Commercially available Research 3R4F cigarettes from the Kentucky Tobacco Research Center at the University of Kentucky were used to prepare cigarette smoke extract containing medium (CSE-medium). Mainstream smoke from three cigarettes was bubbled at a rate of 5min per cigarette into 30ml of RPMI medium without additional supplements added. CSE-medium was filtered through a 0,22µm pore filter to eliminate large particles and bacteria. This preparation was considered as 100% CSE. Aliquots were prepared and stored at -20°C and were used once upon thawing. Prior to each experiment the desired concentration of CSE was freshly prepared by diluting the stock with RPMI medium and adding FBS to obtain a CSE-medium with a final concentration of 25% CSE.

6.4 Gene expression analysis

A standard procedure was applied to measure gene expression of specific genes at the mRNA level. RNA was isolated from the cells; complementary DNA was prepared and quantitative PCR analysis was run.

6.4.1 RNA-Isolation

The PeqGOLD Total RNA Kit was used to isolate RNA from untreated and treated A549 cells. Cells were seeded into 24-well plates and were transfected with siRNA as described in “6.2 RNA Interference”. 42h later the transfection culture medium was replaced by 500µl of fresh culture medium or 500µl of 25%-CSE-medium. Under these conditions cells were cultured for 6h. RNA was isolated at the time of 48h. In detail, cells were washed with PBS to remove cell debris and old medium. A volume of 400µl of RNA Lysis Buffer T was added to each well. Cell lysates were immediately transferred to a DNA removing column placed in a 2,0ml Eppendorf tube and centrifuged for 1min at 12 000 x g at room temperature. DNA removing columns were discarded and 400µl of 70% ethanol was added to the flow through to precipitate the RNA. The samples were vortexed and whole lysates were transferred to PerfectBind RNA columns placed in 2,0ml collection tubes followed by centrifugation for 1min at 10 000 x g. Collection tubes including the flow through were discarded and RNA columns were placed into new 2,0ml collection tubes for the following three wash steps: First 500µl of RNA Wash Buffer I was added to the RNA columns followed by two wash steps with 600µl of RNA Wash Buffer II. After each wash step the samples were centrifuged for 15sec at 10 000 x g and the flow through were discarded. Prior to the elution of RNA, a drying step was carried out by centrifuging for 2min at 10 000 x g to ensure that all ethanol was removed from the column matrix. Once RNA columns were placed into fresh Eppendorf tubes, 50µl of RNase free water was added to

each column. After incubation for 3min the samples were centrifuged for 1min at 5000 x g. Eluted samples were stored at -80 °C for further use

6.4.2 Quantitation of RNA

To assess nucleic acid yield and purity absorbance was measured with a NanoDrop spectrophotometer. RNA concentration values were calculated based on the absorbance at 260nm and given in ng/µl. The purity of RNA was determined by the ratio of absorbances at 260/280nm and 260/230nm. A 260/280nm ratio of ~2,0 was accepted as pure.

6.4.3 cDNA-Synthesis

Complementary DNA (cDNA) was prepared by a reverse transcriptase mediated synthesis using RNA as a template. A volume equivalent to 800ng of RNA was taken and DNase/RNase-free water was added to obtain a total volume of 20µl. Samples were exposed to 70°C for 10min to denature RNA and incubated on ice for 5min, followed by a short spin. Meanwhile 20µl of cDNA master mix was prepared by mixing the reagents according to the following table (Table 9)

Reagent	Volume
10 x PCR Buffer II	4
25 mM $MgCl_2$	4
10 mM each type of dNTPs	2
50 µM random hexamers	2
dH20	5,5
10 U RNase Inhibitor	0,5
50 U MuLV RT	2
total volume	20

Table 9: Composition of reagents for cDNA master mix

A volume of 20µl of cDNA master mix was added to each sample. Reverse transcription was carried out in a PCR thermocycler under the following conditions: 10min at 20°C, 75min at 43°C, 5min at 99°C. The cDNA samples were cooled to 4°C and unless immediately used stored at -20°C.

6.4.4 Real Time Quantitative PCR (qPCR)

Amplification of the cDNA was conducted using SYBR Green fluorescent dye and run on a StepOne PCR Thermocycler. SYBR Green fluorescent dye is binding to double-stranded DNA so that the intensity of fluorescent signal is correlating with the amount of amplified DNA. Hypoxanthine-guanine phosphoribosyl transferase (HPRT) was used as a reference housekeeping gene. Each sample was run in

duplicate and the mean cycle threshold (C_t) values were taken for further calculations. Relative gene expression of each target gene was determined by calculating $2^{-\Delta C_t}$ ($\Delta C_t = C_t^{reference} - C_t^{target}$). $2^{-\Delta C_t}$ values of samples were normalized to the mean $2^{-\Delta C_t}$ of ctrl-siRNA in normal culture medium. Results were analyzed in the GraphPad Prism software and illustrated as bar graphs.

Reagent	Volume
dH20	8
Primer (0,5 µl Fwd, 0,5 µl Rv)	1
$MgCl_2$	1
SYBR green	13
total volume	23

Table 10: Composition of reagents for qPCR master mix

A volume of 23µl of qPCR master mix and 2µl of sample were put in each well of a 96-well reaction plate. Primers used are listed in Table 4. A negative control for each primer was run without any template. The PCR reaction was performed using the thermocycler under following thermal conditions: 5min at 95°C; 45 cycles with 1) 5sec at 95°C 2) 5sec at 59°C 3) 30sec at 72°C; 15sec at 95°C. Melt curves and amplification plots were assessed with the StepOne software and expression of the respective genes was calculated as described above.

6.5 Cell apoptosis

Apototic and necrotic cell death was examined using the eBioscience Annexin V Apoptosis Detection Kit. Cells were seeded into 24-well plates and transfected with siRNA as described in “6.2 RNA Interference”. Each sample was run in duplicate. 48h after transfection culture medium was replaced by 500µl of either fresh culture medium, 25%-CSE-medium or 1µM staurosporine containing medium (STR-medium). Under these conditions the cells were cultured for 6h. Cells were harvested as follows: First they were washed with 500µl of PBS, then 200µl of trypsin was put into each well. After 4min of incubation trypsin activity was stopped by adding 500µl of MACS-Buffer. Everything, including the old medium was collected in FACS tubes and centrifuged. Centrifugation steps were run for 5min at 400 x g at room temperature and the supernatant was discarded right after. Cells were resuspended in 1ml of 1X Annexin V binding buffer (1 part of 10X Annexin binding buffer mixed with 9 parts of distilled water) and centrifuged. Staining for Annexin V was performed mixing 5µl of APC conjugated Annexin V dye and 100µl of 1X binding buffer in each tube. Samples were shortly vortexed and incubated for 15min at room temperature protected from light to ensure that Annexin V binds to phosphatidylserine. After the incubation, 2ml of 1X binding buffer was added to each tube and samples were centrifuged. Cells

were resuspended in 5µl of propidiume iodide (PI) mixed with 200µl of 1X binding buffer. Tubes were immediately put on ice and protected from light ready for flow cytometric analysis.

A FACSCanto II Flow Cytometer was used for flow cytometric analysis of cells applying the following settings: Parameters (FSC 220V, SSC 308V, PI 325V, APC 456V). Data was processed and visualized using the FACS Diva Software. For each sample 10 000 cells were analyzed by flow cytometry.

6.6 Cell proliferation and migration

6.6.1 Wound healing assay

The wound healing assay is a suitable method to study cell migration and proliferation in vitro. Cells grown in a monolayer were “scratched” and wound closure was assessed at certain time points to determine the rate of cell migration and proliferation. Seeding and siRNA transfection of cells was performed in 24-well plates as described in “6.2 RNA Interference”. An artificial gap was generated 48h after transfection by “scratching” the cell monolayer top down in the middle of the wells using 1ml pipette tips. Old culture medium was removed and cells were washed once with 500µl of PBS. A volume of 500µl of either fresh culture medium or 25%-CSE-medium was added to each well. Images were captured with an Axiovert microscope 0, 6, 18 and 24h after “scratching”. Meanwhile, the plates were put into the incubator allowing the cells to proliferate and migrate across the wound. The Axio Vision software was used to measure wound size in pixel area. The rate of migration and proliferation was determined by calculating the ratio of wound size at a certain time to the time of 0h (“scratch”).

6.6.2 WST-1 cell proliferation assay

To determine the effects of HMGN5 knockdown and additional CSE exposure on cell proliferation a colorimetric assay based on the tetrazolium salt WST-1 was applied. Once WST-1 is added to the cells it gets cleaved to formazan, a product that allows spectrophotometric quantification of cell proliferation. Thereby metabolically active cells exhibit a higher amount of formazan resulting in elevated absorbance values (Berridge et al. 1996). Cells were seeded and transfected as described above (“6.2 RNA Interference”). 42h after transfection culture medium was replaced by 500µl of fresh culture medium or 25%-CSE-medium. Cells were cultured under these conditions for 6h. A volume of 30µl of WST-1 reagent was added to each well and plates were incubated for additional 2h. Absorbance measurements were carried out using a Tecan Nanoquant Infinite 200 Pro spectrophotometer with the Tecan Magellan software. The

absorbance of samples was measured against a background control at a wavelength of 450nm and a reference wavelength of 650nm. The absorbance value of each sample was normalized to the mean absorbance of ctrl-siRNA in normal culture medium.

6.7 Cell cycle analysis

6.7.1 Propidiumiodide(PI)-staining

Flow cytometric analysis of PI-stained cells was conducted to examine whether the cell cycle is affected once HMGN5 is depleted. Propidium iodide is a stoichiometric dye that binds DNA and offers the possibility to quantify the DNA content. Cells that are in the replication phase (S-phase) contain more DNA compared to the ones in growth phase G_1. Cells in G_2-phase, in turn, have doubled their DNA expecting the fluorescent signal to be twice as high as in G_1-phase. Hence, PI enables the identification of cell populations at different interphase stages (Krishan 1975).
Seeding and siRNA transfection of cells were done as described in “6.2 RNA Interference”. 42h after transfection the culture medium was replaced by 500µl of fresh culture medium or 25%-CSE-medium. Cells were harvested 6h later and stained with PI. In detail, cells were washed with 500µl of PBS and detached by adding 200µl of trypsin to each well. After 4min of incubation a volume of 500µl of MACS buffer was added to stop the trypsin activity. Suspensions were collected in 5ml FACS tubes and centrifuged for 5min at 400 x g at room temperature. Cells were fixed in ethanol to prevent PI to be actively pumped out of the cell. Therefore, 1ml of cold 70% ethanol was added drop wise under repeated vortexing and the samples were immediately stored on ice for 30min. Cells were centrifuged for 10min at 850 x g at 4°C and supernatant was discarded. Cells were washed once with 1ml of PBS, centrifuged and supernatant was discarded. As PI binds to all nucleic acids, cells were treated with Ribonuclease A (RNase A) prior to staining. A volume of 0,5µl of RNase A (10mg/ml) was diluted with 49,5µl of cold PBS and added to each tube containing the fixed cells. A mixture made up of 10µl of PI (1mg/ml) and 190µl of cold PBS was added and samples were shortly vortexed. Samples were incubated on ice protected from light for 10min and analyzed by flow cytometry.

A FACSCanto II Flow Cytometer together with the FACS Diva Software was used for flow cytometric analysis of cells. The following settings were applied: Parameters (FSC 203V; SSC 286V; PI 360V).
Gating of cells was applied as shown below (Figure 12). The “FSC-A/PI-A subset” comprised 30 000 cells for each sample. The cell cycle histogram was generated

using the FlowJo-software and the percentage of cells in each cell cycle phase was calculated based on the Watson Pragmatic algorithm.

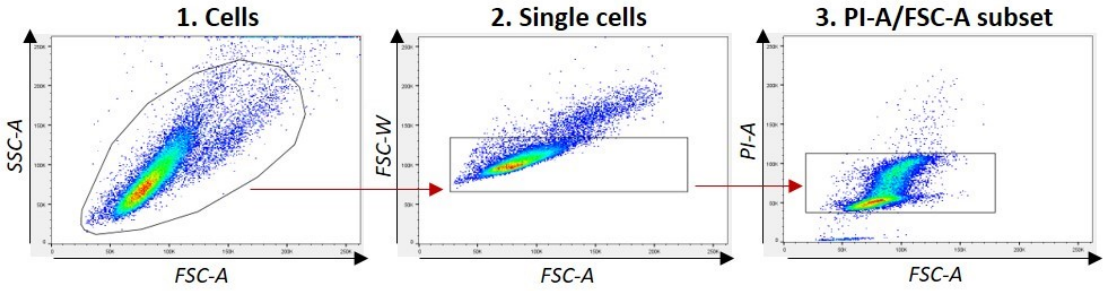

Figure 12: Gating of FACS-sorted propidium-iodide stained A549 cells

6.7.2 Fluorescence Ubiquitin Cell Cycle Indicator (FUCCI)

An additional independent analysis of the cell cycle was undertaken using a relatively novel method based on two fluorescent protein tagged regulators that are expressed in cells after transfection of a baculovirus-vehicle.
Cells were seeded and transfected with siRNA as described in "6.2 RNA Interference". 24h after siRNA transfection cells were transfected with the FUCCI sensors and subsequently incubated for 18h before medium was replaced either by 500µl of fresh culture medium or 500µl of 25%-CSE-medium. Six hours later cells were harvested and analyzed by flow cytometry. The volume of Premo-geminin-GFP and Premo-Cdt1-RFP was calculated according to the manufacture's protocol considering cell number, PPC (particles per cell) and the number of viral particles the reagent contains per ml. The number of cells present upon transfection was estimated counting the cells once 24h after seeding and the PPC number was taken as recommended for A549 cells. The following equation was used to calculate the volume needed:

$$\frac{\textit{(number of cells) x (PPC)}}{1\ x\ 10^8} = volume\ of\ Premo\text{-}geminin\text{-}GFP\ or\ Premo\text{-}Cdt1\text{-}RFP$$

A volume of 500µl of fresh culture medium was mixed with 24µl of each Premo-reagent and the total volume of 548µl was applied to each well. Prior to flow cytometric analysis cells were harvested as follows: Cells were washed with 500µl of PBS and detached by adding 200µl of trypsin to each well. After 4min of incubation trypsin activity was stopped by adding 500µl of MACS-Buffer. The suspension was collected in a 5ml FACS tube and centrifuged for 5min at 400 x g at room temperature. The supernatant was discarded. To detect dead cells when analyzing by flow cytometry a Viability 405/520 Fixable Dye was used. This lyophilized dye was reconstituted by adding 100µl of DMSO and aliquots were stored at -20°C. Cells were resuspended in 50µl of PBS mixed with 0,4µl of Viability Fixable Dye and incubated for the following 15min. Cells were washed

once with 500µl of PBS, centrifuged for 10min at 300 x g at room temperature and the supernatant was removed. A volume of 200µl of MACS-Buffer was added to resuspend the cells. The whole procedure was performed under minimal light exposure.

Flow cytometric analysis of cells was performed using the following settings: Parameters (FSC 165V; SSC 300V; PE 390V; FITC 357V; AmCyan 360V), Compensation (FITC-PE 3,10; AmCyan-PE 2,30; PE-FITC 15,50; AmCyan-FITC 7,00; PE-AmCyan 3,00; FITC-AmCyan 2,40). Cells were gated as shown in (Figure 13). In total 50 000 cells within the “Live-subset” were analyzed from each sample.

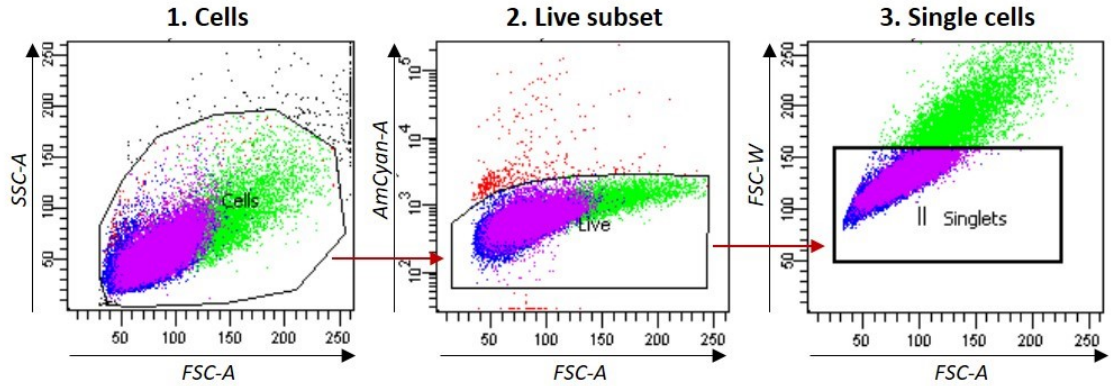

Figure 13: Gating of FACS-sorted A549 cells expressing geminin-GFP and Cdt1-RFP that were additionally stained with Viability Fixable Dye for exclusion of dead cells.

6.8 Human samples

Lung core samples were provided by Dr. Stijn Verleden (University of Leuven, Belgium) and obtained from explanted lungs of COPD patients undergoing lung transplantation. Both emphysematous and healthy regions originate from the same lungs. Ethical approval was provided by the University of Leuven Institutional Review Board (ML6385) and all participants have given written consent. Experiments were performed according to the principles stated in the Declaration of Helsinki. Patient demographics are highlighted in Table 11. Immediately after transplantation, lungs were air-inflated at a pressure of 10cm H2O and fixed in liquid nitrogen under constant pressure. Once fixed, lungs were sliced using a band saw and sampled using a core bore. Upon receipt, lung cores were portioned and subsequently fixed in 4% paraformaldehyde followed by paraffin embedding or used for protein isolation.

	COPD
Subjects (n)	16
Men age years	57.06 ± 1.23
Sex Male Female	 7 9
Height (cm)	165 ± 2
Weight (kg)	59.44 ± 3.18
Smoking (packs/year)	39.00 ± 7.55
FEV_1 (%)	34.38 ± 5.55
FVC (%)	82.73 ± 5.84
FEV_1/FVC (%)	31.01 ± 5.07

Table 11: Demographics and clinical characteristics of COPD transplant patients (mean ± SEM).

6.9 Protein expression analysis

6.9.1 Protein Isolation

Lung cores used for protein were homogenized under liquid nitrogen using metal bead dissociation in a microdismembrator for 1min at 1600 x g. Unless not immediately used homogenates were stored at -80°C. Proteins were isolated taking two spoons of lung homogenate and adding 500µl of RIPA lysis buffer containing complete protease inhibitor (1:20) and sodium orthovanadate (1:100). Samples were incubated at 4°C for 30min and vortexed periodically. Afterwards, samples were centrifuged at 4°C and 30 000 x g for 15min and the supernatant was kept for further use.

6.9.2 Quantitation of Protein

Protein concentration was determined using the Pierce BCA Protein Assay Kit consisting of two reagents. The working reagent was prepared by mixing reagent B with reagent A in a 1:50 ratio. Samples were diluted 1:5 with RIPA buffer and a volume of 25µl was given to each respective well of a 96-well microplate. To compile a standard curve, distinct bovine serum albumin (BSA)-concentrations (2000, 1500, 1000, 750, 500, 250, 125, 25 and 0µg/ml) were prepared by diluting BSA with RIPA buffer. A volume of 25µl of each concentration was put to an empty microplate well, respectively. Samples and standards were applied in duplicate. After adding 200µl of working reagent to each well, the plate was incubated for 30min at 37°C. Next, absorbance was measured at 562nm with the Tecan Nanoquant Infinite 200 Pro. Protein concentrations were calculated with the help of the standard curve and values were between 1,1 and 4,2µg/µl.

6.9.3 Gel electrophoresis and Transfer

Sodium dodecyl sulfate polyacrylamide gel electrophoresis (SDS-PAGE) was undertaken to separate proteins according to their molecular weight. Therefore, a gel comprising two different layers, a stacking and a separating layer, was prepared. The separating gel with a concentration of 12% of acrylamide containing 2,8ml of H_2O; 2,1ml of TRIS 1,5M/pH 8,8; 3,3ml of acrylamide 30%; 82,5µl of SDS 10%; 11µl of TEMED and 11µl of APS 25% was poured into the gel casting apparatus and allowed to polymerize. To obtain an even gel surface some isopropanol was put on top of the gel for the time of polymerization. Meanwhile, the stacking gel consisting of 2,9ml of H_2O; 1,25ml of TRIS 0,5M/pH 6,8; 0,85ml of acrylamide 30%; 50µl of SDS 10%; 10µl of TEMED and 10µl of APS 25% was prepared. Isopropanol was removed and the stacking gel was poured onto the separating gel. A comb was immediately inserted into the stacking gel and removed once polymerization took place. The gel was placed into an electrophoresis chamber that was filled with 1X running buffer (5X running buffer diluted with distilled water).

A volume equivalent to 20µg of protein of each sample was topped up with RIPA buffer resulting in an equal total volume of all samples. Loading buffer (containing 1 part of β-mercaptoethanol and 9 parts of Laemmli loading buffer) was added in a 1:4 ratio. Samples were incubated at 95C for 10min, put on ice for 5min and shortly spun down. Samples were then equally loaded into the wells of the SDS-polyacrylamide gel. A protein standard was run on each gel to assess protein size later. Electrophoresis was run at 100V for 15min, followed by 120V for 1h. In order to enable immunodetection of the proteins, the separated proteins were transferred onto a polyvinylidene difluoride (PVDF)-membrane. A “sandwich” consisting of the following layers soaked in 1X transfer buffer (1 part of 10X transfer buffer, 2 parts of methanol and 7 parts of distilled water) was built: sponge, filter paper, gel, PVDF-membrane, filter paper, sponge. This “sandwich” was placed into an electrophoresis chamber filled with 1X transfer buffer. Transfer was run at 100V for 60min.

6.9.4 Immunostaining of PVDF-membrane

Immunostaining was performed with the following steps: blocking, incubation with primary antibody, washing, incubation with secondary antibody, washing. To prevent non-specific binding of antibodies the PVDF-membrane was blocked by placing it in 1X Roti-Block (10X Roti-Block diluted 1:10 with RNase/DNase free water) for 1h on an Orbital Shaker. Primary antibody (Anti-HMGN5) was diluted in 1X Roti-Block in a 1:500 ratio. The membrane was incubated with the primary antibody in a 50ml Falcon tube placed in a rotator at 4°C overnight. The next day, the membrane was washed in PBS-Tween (PBS-T) 3 x 10min. A horse radish peroxidase (HRP)-conjugated antibody (1:300 in 1X Roti-Block) was used to

incubate the membrane with the secondary antibody for 1h at room temperature. The membrane was washed (as before) and subsequently used for immunodetection.

6.9.5 Chemiluminescent detection

The Amersham ECL Prime Western Blotting Detection Kit was used for chemiluminescent detection of the antibodies. The provided solutions, ECL solution A and B were mixed equally and applied on the membrane. Following incubation for 3min, the bands were visualized by capturing images with a ChemiDoc XRS Molecular Imager using the Image Lab v5.1 software. Densitometry of bands was performed using the Image Lab v5.1 software. The data was transferred to Graph Pad Prism for statistical analysis.

6.9.6 Beta-actin detection

Beta-actin was detected as a control protein to normalize loading. Detection was carried out as follows: The membrane was washed 3 x 5min, stripped with Restore Plus Western buffer and washed again 3 x 5min. After blocking for 30min, the membrane was incubated with anti-β-actin antibody (1:50 000 in 1X Roti-Block) for 1h. Prior to detection with the Imager, the membrane was washed again 3 x 10min.

6.10 Immunofluorescence

Immunofluorescent staining was performed on formalin-fixed paraffin embedded (FFPE) lung tissue sections from COPD patients and healthy individuals (6.8 Human samples). For each group, sections from four different individuals were stained for HMGN5, SPC and DAPI using the commercial antibodies listed in “5.4 Antibodies”. Prior to staining, the lung tissue slides were incubated at 60°C overnight. Deparaffinization was implemented subjecting the slides to the following steps: Xylol for 5min (x2), 100% EtOH for 2min (x2), 90% EtOH for 2min, 80% EtOH for 2min, 70% EtOH for 2min and briefly distilled water. Antigen retrieval was achieved heating the slides in 1:10 citrate buffer (180ml of distilled water mixed with 20ml of citrate buffer). A box containing the buffer and all slides was placed into a pressure cooker and incubated as follows: Temperature was increased to a maximum of 125°C within 20min. Once maximum was reached temperature was held for 30sec and subsequently lowered to 90°C within 25min. After 10sec at 90°C heating process was finished. Slides were cooled down by discarding some of the buffer and replacing it with 1X PBS. This step was repeated a few times to ensure that the temperature was gradually lowering. Cells were permeabilized by incubating the slides in 0,5% Triton X-100 for 5min and

washed with 1X PBS 3 x 5min. Tissue sections on each slide were encircled using a Dako pen. Slides were placed into a wet chamber and blocked in 5% BSA for 30min. Meanwhile, the primary antibody dilution was prepared mixing HMGN5 antibody (1:100) and SPC-antibody (1:200) with 1% BSA. Slides were incubated with a volume of 50µl per section at 4°C overnight in a wet dark chamber. This chamber was used for all the following steps. The next day, sections were washed with 1X PBS 3 x 5min. The secondary antibody dilution was prepared mixing anti-goat antibody (1:500), anti-rabbit antibody (1:20) and anti-DAPI antibody (1:4000) in 1% BSA. Each section was incubated with 100µl of secondary antibody dilution for 1h at room temperature. Washing was repeated as done before. In a final step, prior to microscopy, slides were mounted using the Dako mounting media and left to dry. For visualization, a laser scanning microscope (LSM710) was used and images were captured and analyzed using the ZEN software.

6.11 Statistical analysis

Graph Pad Prism 6 was used to prepare all graphs and to run statistical analysis on the data. In the presence of one variable unpaired student's t-test was used when comparing two groups, one way-ANOVA followed by Boniferroni post-test when comparing more than two groups. Two way-ANOVA followed by Boniferroni post-test was applied for experiments comprising two variables. All data is presented as mean ± SD and $p < 0,05$ is considered as statistically significant. N numbers are stated in the figure legends as well as in the method descriptions.

Part III: Results

7 HMGN5 expression and localization in COPD patients

It was previously shown that HMGN5 deficient mice demonstrated emphysematous lungs (Kugler et al. 2013) and emphysematous mice had reduced HMGN5 expression in the lungs (unpublished observations from our lab). To assess, whether HMGN5 is also less expressed in patients suffering from COPD its expression was analyzed by comparing lungs of COPD patients with healthy individuals. Although it was not possible to detect a difference in the protein expression level of HMGN5 comparing COPD patients' lungs, that did show an emphysematous phenotype, with healthy individuals (Figure 14, A), RNA analysis showed distinct changes. Five different publicly available microarray datasets (Figure 14, B) demonstrated reduced HMGN5 expression in lungs of COPD patients compared to healthy individuals. Similar results were obtained by RNA-sequencing from our COPD patient cohort (Figure 14, C).

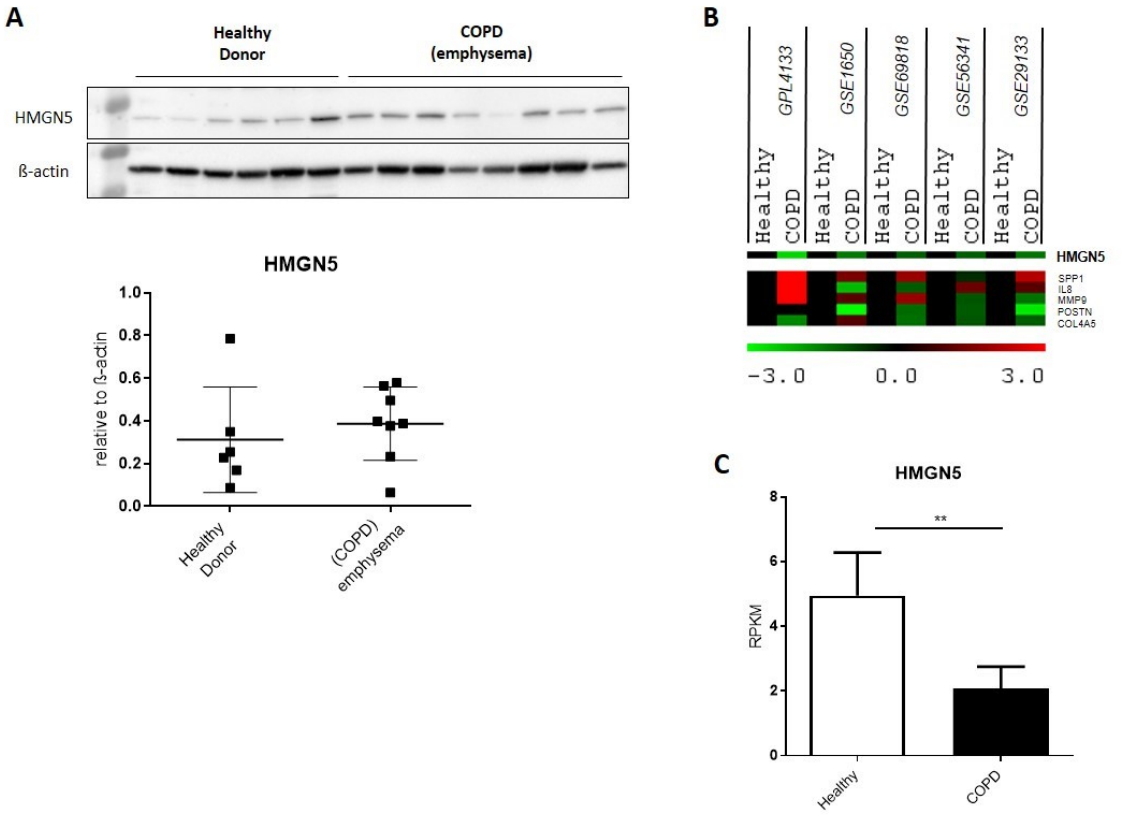

Figure 14: COPD patients show reduced expression of HMGN5. A) Protein expression analysis by Western Blot of whole lung extracts from six healthy individuals and eight emphysematous COPD patients. ß-actin was used as a loading control. (B) Five different publicly accessible microarray datasets were analyzed for HMGN5 gene expression in COPD patients compared to healthy individuals, along with genes strongly associated with COPD. (C) RNA-Seq

of whole lung from our COPD patient cohort with n = 4 per group. Kindly provided by Dr. K. Heinzelmann CPC-M BioArchive, Helmholtz Zentrum München. Values are given as mean ± SD (**p<0.01, two-tailed t test).

Previously our lab identified HMGN5 to be expressed in the nucleus of alveolar epithelial type II (AT-II) cells and bronchial epithelial cells from mice (unpublished observations). To verify whether there is a similar expression pattern in human lung cells, immunofluorescence staining of HMGN5 on lung sections from COPD patients and healthy individuals was performed. Similar to findings in mice, HMGN5 localized to the nucleus of mainly AT-II cells (Figure 15, white triangles and co-localization with the AT-II marker SPC) and bronchial epithelial cells in both groups. Moreover, HMGN5 appeared to be less expressed in AT-II cells from COPD patients compared to healthy individuals (Figure 15).

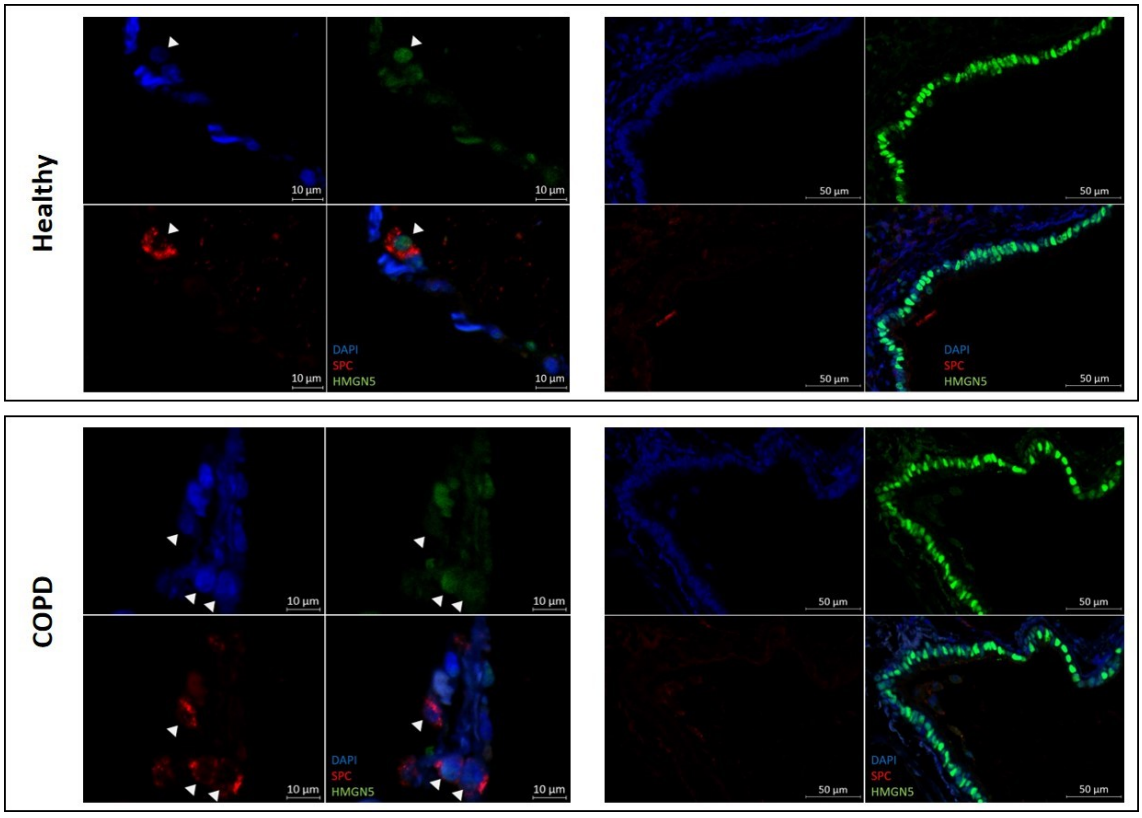

Figure 15: HMGN5 is predominantly expressed in alveolar epithelial type-II cells and bronchial epithelial cells. Paraffin sections from Healthy subjects (upper panel) and COPD patients (lower panel) were immunostained for HMGN5 (green), SPC (red) and DAPI (blue). Representative pictures are shown and focusing on alveolar region (left side of each panel, scale bar = 10µm) and bronchial epithelium (right side of each panel, scale bar = 50µm). White triangles are indicating AT-II cells.

8 Silencing of HMGN5 in human alveolar type II like cell line A549

As COPD patients demonstrated reduced expression of HMGN5 the role HMGN5 plays during disease development was investigated. HMGN5 expression was observed in AT-II cells (Figure 15). AT-II cells play an important role in maintaining the alveolar structure and enabling efficient gas exchange (Zhao et al. 2010). In emphysematous lungs a destruction of alveolar structures occurs and alveolar cells undergo death (Yoshida and Tuder 2007). The loss of AT-II cells impairs regeneration and repair, thus affecting tissue homeostasis in COPD patients exhibiting an emphysematous phenotype. But whether altered HMGN5 expression is contributing to these processes remain to be examined. Therefore, HMGN5 expression in the human AT-II-like cell line A549 was downregulated. In this study *HMGN5* was silenced using RNA Interference as described in “6.2 RNA Interference”. As shown in Figure 16, siRNA silencing of *HMGN5* caused a downregulation of *HMGN5* RNA expression of more than 80% compared to negative control siRNA (ctrl-siRNA).

Kugler et al. (2013) previously reported that reduced expression of HMGN variants in mice affect the transcriptional profile but only leads to distinct changes in the phenotype, if the mice are subjected to certain stress (Kugler et al. 2013). Accordingly, our previous unpublished data from mice showed that HMGN5 deficiency enhances emphysematous changes that were triggered by elastase treatment, whereas an effect of HMGN5 deficiency alone was not detectable (unpublished observations). Considering these findings, A549 cells were placed under stress using the main etiologic factor of COPD, that is cigarette smoke (CS). Here, gene expression of HMGN5 was also downregulated more than 80% compared to ctrl-siRNA (Figure 16, B).

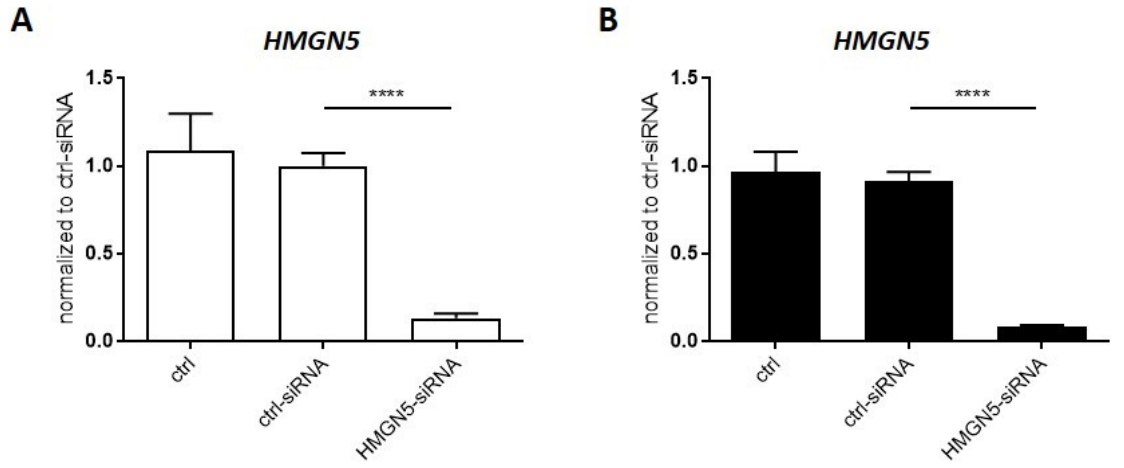

Figure 16: Silencing of HMGN5 in human alveolar type II like cell line A549. *HMGN5* mRNA expression was measured by quantitative PCR to assess knockdown efficiency of HMGN5 48h after siRNA transfection. 6h prior to RNA isolation cells were grown in normal culture medium (A) or 25%-CSE- medium (B). 2^-ΔCT values were calculated with HPRT as housekeeping gene and were then normalized to ctrl-siRNA. Data were combined from two independent experiments (n=3 per group and per experiment) and are given as mean values ± SD. 1-way ANOVA following Bonferroni posttest was run for statistical analysis with ****$p < 0{,}0001$.

9 HMGN5 silencing of A549 cells affects susceptibility to cell death

The destruction of alveolar walls which leads to enlarged airspace is the main pathophysiological characteristic that occurs in emphysema development (Snider et al. 1985). It is known, that cellular injury can cause alveolar cell death (Kosmider et al. 2011). Thereby alveolar cells can undergo apoptosis or necrosis (Kosmider et al. 2011; Segura-Valdez et al. 2000; Park, Ryter, and Choi 2007; van der Toorn et al. 2007; Zeng et al. 2012; Aoshiba and Nagai 2003; Petrache and Serban 2016). However, the exact mechanisms remain to be further investigated.

In light of this, the main aim was to explore the involvement of HMGN5 in cellular death of AT-II cells in the context of emphysema. To identify apoptotic and necrotic cells an Annexin V/ PI-staining was performed, and cells were analyzed using flow cytometry (Figure 17). As shown, there was no observable effect of HMGN5 downregulation alone in A549 cells, neither on apoptotic nor on necrotic cell death (Figure 17, A upper row and B).

However, based on our labs findings that elastase induced emphysematous changes in HMGN5 deficient mice were enhanced compared to their littermates, it was important to determine whether HMGN5 downregulation in A549 cells enhances the effect of external stimuli that are known to induce cell death. Here cigarette smoke extract (CSE) and staurosporine was used. First, it was confirmed that both CSE and staurosporine were initiating cell death. Whereas cells treated with 25% CSE became necrotic (Figure 17, A middle row and B), cells treated with 1µM staurosporine underwent apoptosis (Figure 17, A lower row and B).

By treating HMGN5 silenced cells with staurosporine, the number of cells undergoing apoptosis was drastically increased compared to siRNA-negative control transfected cells. Furthermore, a higher number of cells that were exposed to CSE became necrotic when HMGN5 was downregulated, although this did not reach significance (Figure 17, A middle row and B).

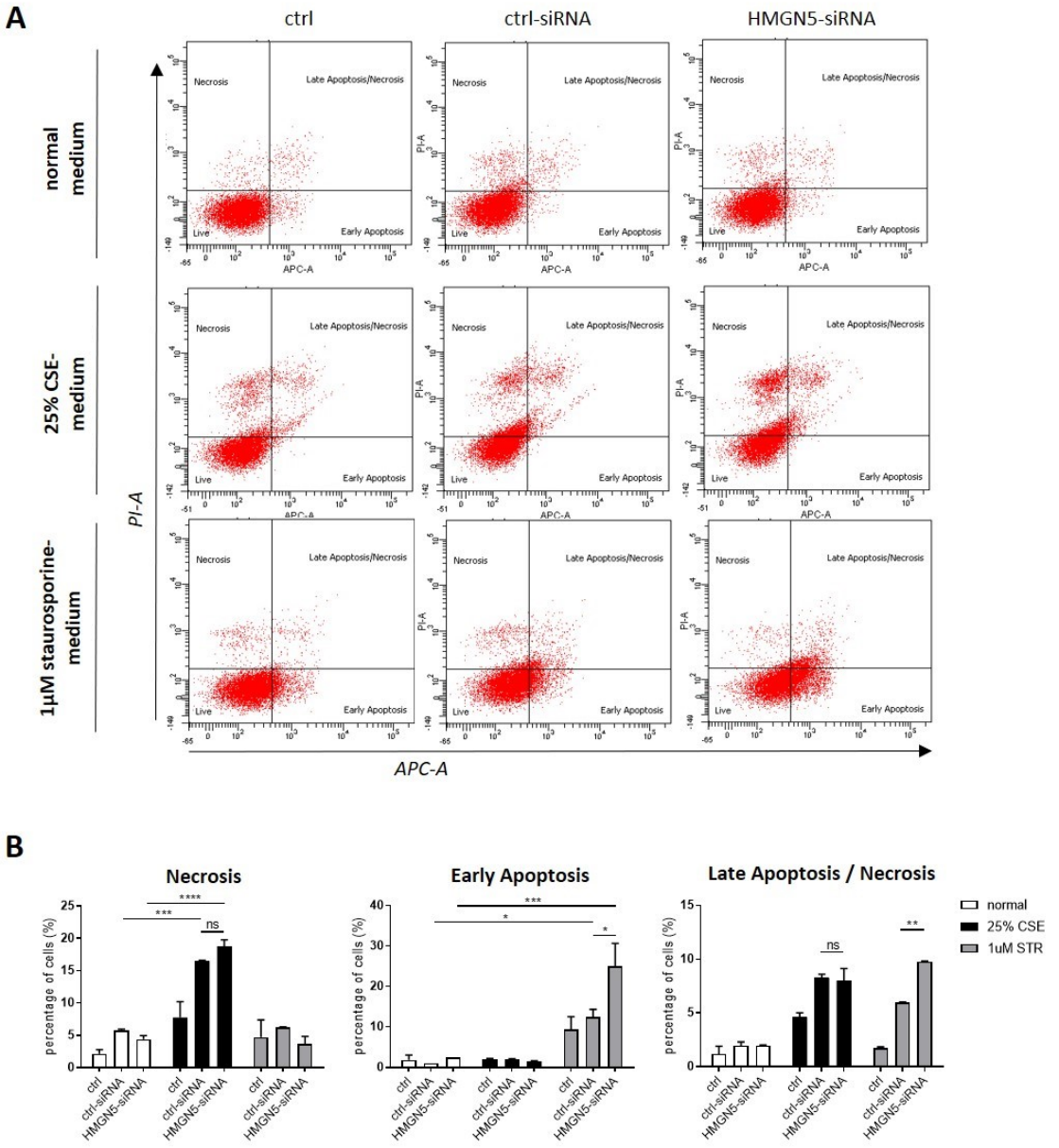

Figure 17: HMGN5 silenced AT-II cells are more susceptible to induced cell death. Flow cytometrical analysis of Annexin-V-APC/Propidium-Iodide (PI) double stained A549 cells 54h after HMGN5 siRNA Transfection. Prior to staining cells were treated with either normal medium, 25%CSE-containing- or 1µM staurosporine-containing medium for 6h. (A) Representative dot plots from flow cytometry analysis showing an increased number of necrotic cells after CSE treatment (middle panel), that is further increased by HMGN5 knockdown (middle panel, right). Likewise, HMGN5 silenced cells demonstrate a stronger response to staurosporine induced apoptosis (lower panel, right). (B) Quantification of flow cytometry analysis. Experimental data is shown from a single experiment representative for two independent experiments (n=2 per group and experiment). Values are given as mean ± SD; 2-way ANOVA following Bonferroni posttest was run for statistical analysis with *p < 0,05, **p < 0,01, ***p < 0,001 and ****p < 0,0001.

In order to assess how HMGN5 downregulation affects cellular death, gene expression of genes associated with apoptosis or necrosis were measured using qPCR. Even though there was no increased cellular apoptosis and necrosis in siRNA-HMGN5 transfected cells not subjected to any cell death inducing stimuli, gene expression changes in the transcriptional profile could be detected.

Increased levels of the caspase family member *CASP3* in siRNA-HMGN5 transfected cells accompanied by a tendency of increased expression of the proapoptotic gene *BAX* (Figure 18, A, white bars) was observed. In addition, transcriptional levels of cyclophilin D (also known as PPID), a mediator of necrotic cell death (Nakagawa et al. 2005; Ying and Padanilam 2016), were elevated in siRNA-HMGN5 transfected cells (Figure 18, B, white bars). Likewise, gene transcription of cyclophilin A (also known as PPIA), that was described as a marker for necrosis (Christofferson and Yuan 2010), appeared to be slightly upregulated (Figure 18, B, white bars). Changes in gene expression of *BCL-2*, *MB* and *LDH-A* were not detectable. Also, treating HMGN5 silenced cells additionally with CSE didn't reveal significant changes in the expression of the examined genes (Figure 18, A and B, black bars).

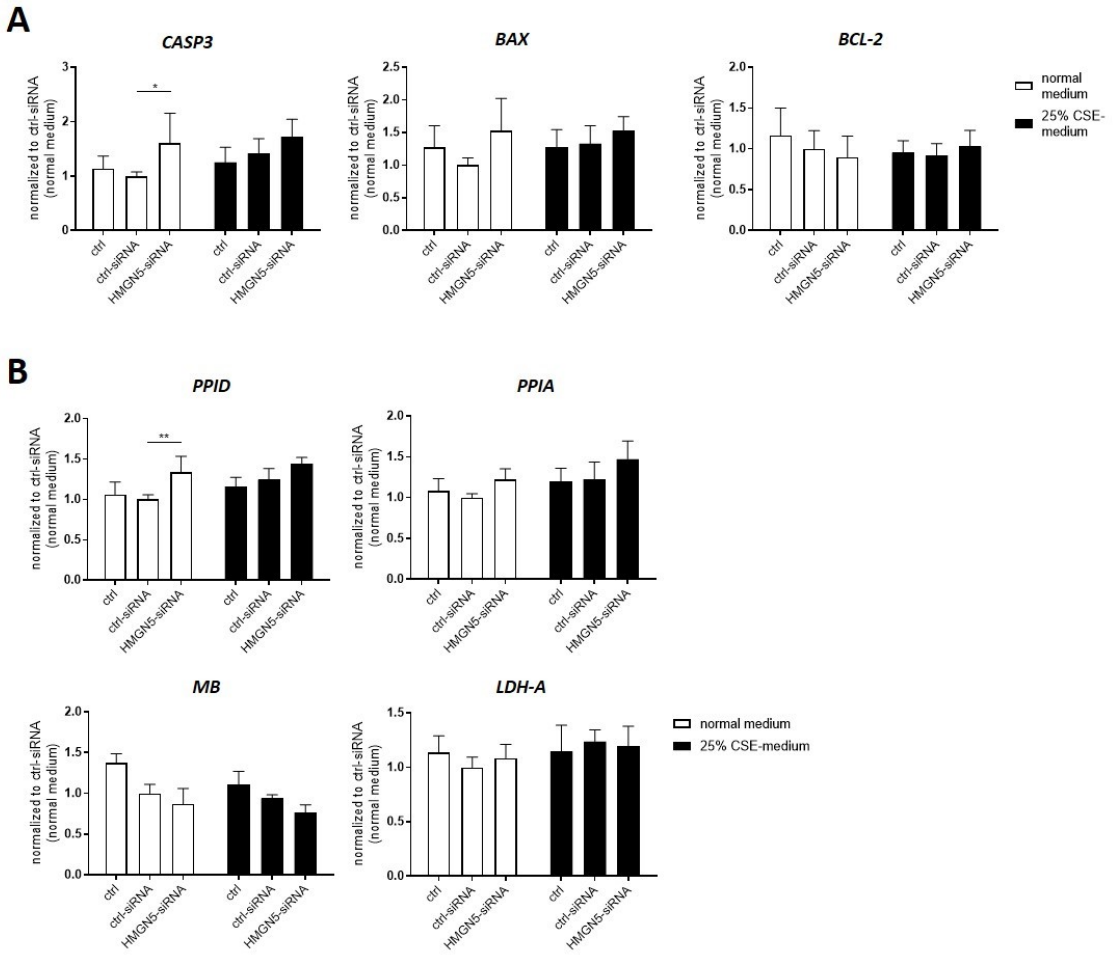

Figure 18: Apoptosis and necrosis related genes after HMGN5 downregulation and exposure to CSE. mRNA expression of different genes was measured by quantitative PCR 48h after siRNA transfection. 6h prior to RNA -Isolation cells were grown in normal medium (white bars) or 25% CSE-containing medium (black bars). 2^-ΔCT values were calculated with HPRT as housekeeping gene and were then normalized to "scrambled complete medium". Data were combined from two independent experiments (n=3 per group and per experiment) and are given as mean values ± SD. 2-way ANOVA following Bonferroni posttest was run for statistical analysis with *p < 0,05, **p < 0,01

10 Impairment of cell cycle in response to HMGN5 downregulation

Tissue homeostasis is based on a complex network including biological processes such as cell proliferation and division, cell death and survival, DNA repair and recombination, all of these influencing each other (Zhivotovsky and Orrenius 2010). As HMGN5 is known to affect the compaction of chromatin (Malicet et al. 2011) it is likely that it also plays a role during such processes. Several studies have already reported HMGN5 to be involved in cell cycle regulation (Chen et al. 2012; Ji et al. 2012; Jiang, Zhou, and Zhang 2010). Here two different approaches were used to evaluate the effect of HMGN5 downregulation on cell cycle progression. First, the percentage of cells in each cell cycle phase by staining their DNA with PI and analyzing the cells using flow cytometry was determined (Figure 19).

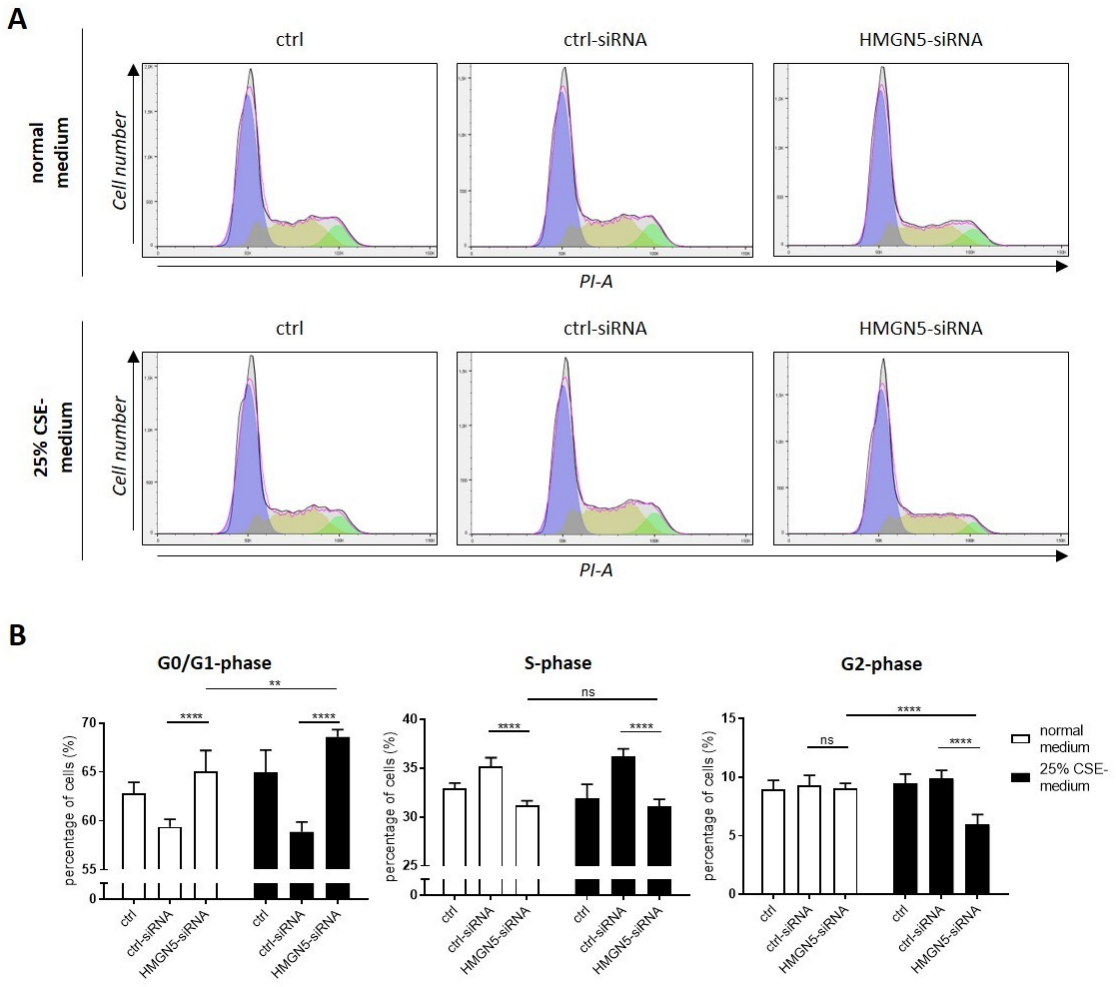

Figure 19: HMGN5 silencing impairs cell cycle in AT-II cells. Knockdown of HMGN5 in A549 cells leading to an increased number of cells in early cell cycle stage G1 and a lower number of cells in replication phase S. Cells were cultured in either normal medium or 25%CSE-containing medium for 6h prior to harvesting at 48h after transfection. Cell cycle was assessed by Propidium-Iodide (PI) staining followed by flow cytometry. Results were analyzed using FlowJo-Software. (A) Representative graphs showing populations of cells in different cell cycle stages (purple: G1-phase; yellow: S-phase; green: G2-phase). (B) Quantification of FACS data combined from two

independent experiments (n=3 per group and per experiment). Values are given as mean ± SD. 2-way ANOVA following Bonferroni posttest was run for statistical analysis with ****p < 0,0001.

Cell cycle analysis of HMGN5 silenced cells revealed more cells in early cell cycle phase G0/G1 (65,1% vs 59,4%), whereas less cells were detected in synthesis phase S (31,2% vs 35,2%) (Figure 19). A change in the percentage of cells in G2 phase was not observed. To investigate if CS exhibits an additional effect to HMGN5 silencing on cell cycle progression, cells were further exposed to CSE. Here, a similar pattern compared to HMGN5 silencing alone was observed. However, even more HMGN5-siRNA transfected cells were halted in G0/G1 when exposed to CSE compared to HMGN5-siRNA transfected cells grown in normal medium (68,6% vs 65,1%) (Figure 19). There was no difference between the latter two groups in S phase, but there was a lower number of CSE treated HMGN5-siRNA transfected cells in G2 phase (6,0% vs 9,0%) (Figure 19).

To verify these results, a relatively novel method the fluorescent ubiquitination cell cycle indicator (FUCCI) system was utilized. It is based on two fluorescent tagged proteins Geminin and Cdt1 that are ubiquitinated by specific ligases in a cell cycle phase dependent manner. In the G1 phase of the cell cycle, GFP tagged Geminin is degraded, allowing the identification of cells in G1 by their red nuclei due to RFP tagged Cdt1 that is still present in these cells. On the contrary, in the S/G2/M phases RFP-Cdt1 is broken down and GFP tagged geminin is accountable for the green color of the nuclei. During the transition from G1 to S phase both fluorescent tagged proteins are present causing the cells nuclei to appear yellow (Sakaue-Sawano et al. 2008). Thus, these cyclic color changes allow the separation of cell populations into G1, G1/S-transition and S/G2/M phases.

Flow cytometry analysis revealed most cells to be in cell cycle phase S, G2 or M. However, while 82,6% of the ctrl-siRNA transfected cells were in the S/G2/M phase, only 71,2% of the HMGN5-siRNA transfected cells were in this phase (Figure 20). On the contrary, the percentage of HMGN5-siRNA transfected cells in the early cell cycle phase G1 (8,0%) and G1/S transition (19,6%) was higher compared to the percentage of negative control-siRNA transfected cells (3,7% in G1 phase and 12,4% in G1/S transition phase) (Figure 20). When additionally exposed to CSE, the distribution of cells showed a similar pattern as it did without CSE, although there were a little less HMGN5-siRNA transfected cells in the G1 phase under CSE exposure (6,0%) compared to HMGN5-siRNA transfected cells grown in normal medium (8,0%) (Figure 20).

Taken together this data reveal distinct changes in cell cycle progression in HMGN5-siRNA transfected cells. A downregulation in HMGN5 expression appears to halt the cells in the early phase of the cell cycle.

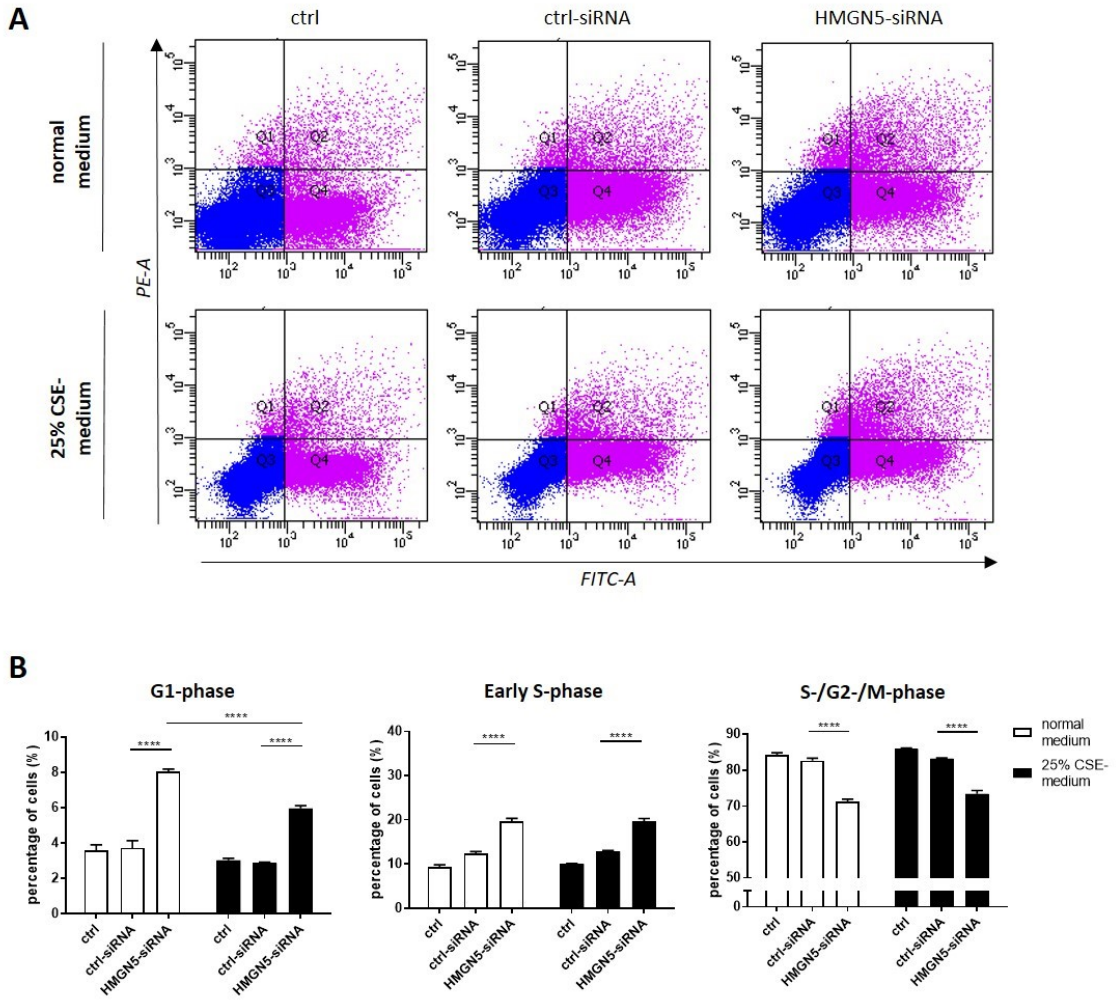

Figure 20: HMGN5 silencing causes accumulation of AT-II cells in early cell cycle phases. Fluorescence Ubiquitin Cell Cycle Indicator (FUCCI) technology was employed for cell cycle analysis of HMGN5 silenced A549 cells. Flow cytometry analysis indicate a higher number of cells in G1- and early S-phase when transfected with HMGN5-siRNA, whereas in the following cell cycle stages the percentage of cells is decreased. FUCCI cell cycle sensor was added to the cells 24h after siRNA transfection and medium was changed to either normal medium or 25%CSE-containing medium 18h later. Cells were harvested 48h after siRNA transfection. (A) Representative dot plots showing the populations of cells in different cell cycle phases. Q1: G1-phase, Q2: early S-phase, Q3: S-/G2-/M-phase, Q4: non-transfected cells or M-/G-1 transition. (B) Quantification of FACS data shown from a single experiment representative for two independent experiments (n=3 per group and experiment). Values are given as mean ± SD; 2-way ANOVA following Bonferroni posttest was run for statistical analysis with ****p < 0,0001.

It is well known, that cell cycle progression is regulated by cyclins which are periodically expressed and degraded during the cell cycle and sequentially activate cyclin-dependent kinases (Johnson and Walker 1999). To evaluate whether the observed changes in the cell cycle of HMGN5-siRNA transfected cells are associated with altered gene expression of cyclins, qPCR analysis was performed (Figure 21). In comparison to cells transfected with negative control-siRNA, HMGN5-siRNA transfected cells exhibited increased expression of *CYCLIN-D* (1,5-fold) and *CYCLIN-A* (1,4-fold), whereas changes in the expression of *CYCLIN-E* and *-B* could not be detected (Figure 21, A). CS

exposure diminished the effect of HMGN5 downregulation on *CYCLIN-D* and *-A* expression (Figure 21, A). Furthermore, RNA expression of the transcription factor c-jun was analyzed, that has been reported to be a critical protein in early cell cycle progression (Wisdom, Johnson, and Moore 1999). Increased RNA expression of *C-JUN* in HMGN5-siRNA transfected cells both in cells cultured in normal medium and in CSE-medium was observed (Figure 21, B).

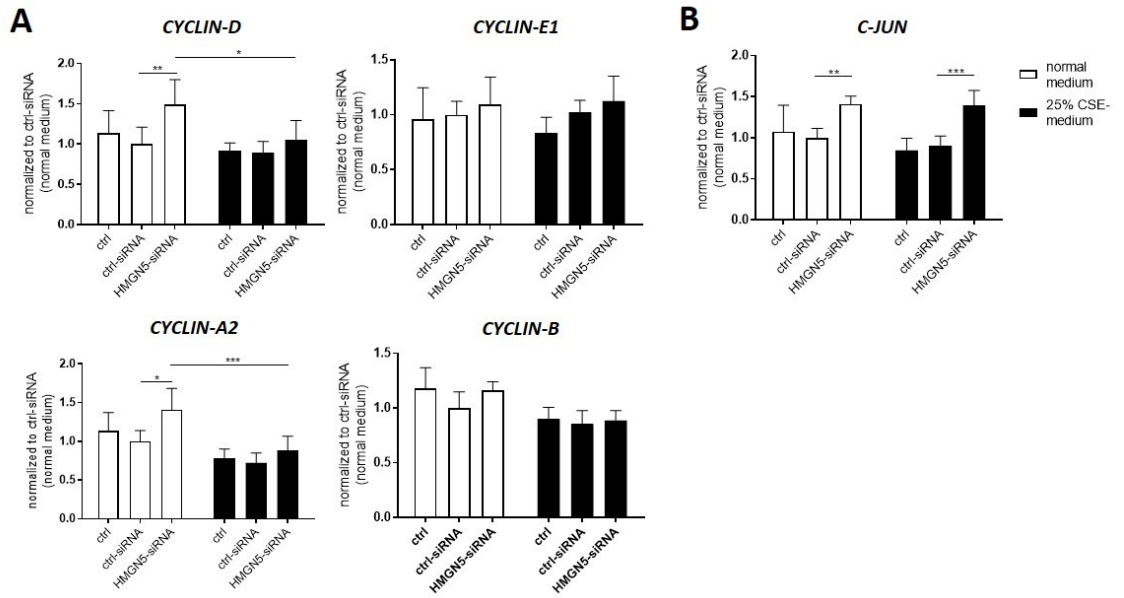

Figure 21: Changes of cell cycle associated genes after HMGN5 downregulation and exposure to CSE. Messenger-RNA expression of different genes was measured by qPCR 48h after siRNA transfection. 6h prior to RNA -Isolation cells were grown in normal medium (white bars) or 25% CSE-containing medium (black bars). 2^-ΔCT values were calculated with HPRT as housekeeping gene and were normalized to "scrambled complete medium". Data were combined from two independent experiments (n=3 per group and per experiment) and values are given as mean ± SD. 2-way ANOVA following Bonferroni posttest was run for statistical analysis with *p < 0,05, **p < 0,01, ***p < 0,001.

11 Proliferation and migration of A549 cells after HMGN5 downregulation

An intact cell cycle is essential for proliferation in the course of regeneration and repair (Zhivotovsky and Orrenius 2010). As HMGN5-siRNA transfected cells showed impaired cell cycle progression, it was conceivable that this is accompanied by reduced proliferation of the cells. Therefore, proliferation and migration in vitro using the wound healing assay was undertaken. Although CSE treatment impaired wound healing of the cells, a change in the wound healing ability of HMGN5-siRNA treated cells in comparison to ctrl-siRNA cells was not statistically distinguishable, neither if cultured in normal medium nor exposed to CSE-medium (Figure 22). However, HMGN5 silenced cells show a tendency for impaired wound healing compared to their respective control in each group. Proliferation and viability of the cells was additionally examined using the cell proliferation reagent WST-1. The effect of CSE on cell proliferation and viability was confirmed, nevertheless HMGN5-siRNA treatment did not show any effect on proliferation and viability in this assay (Figure 23).

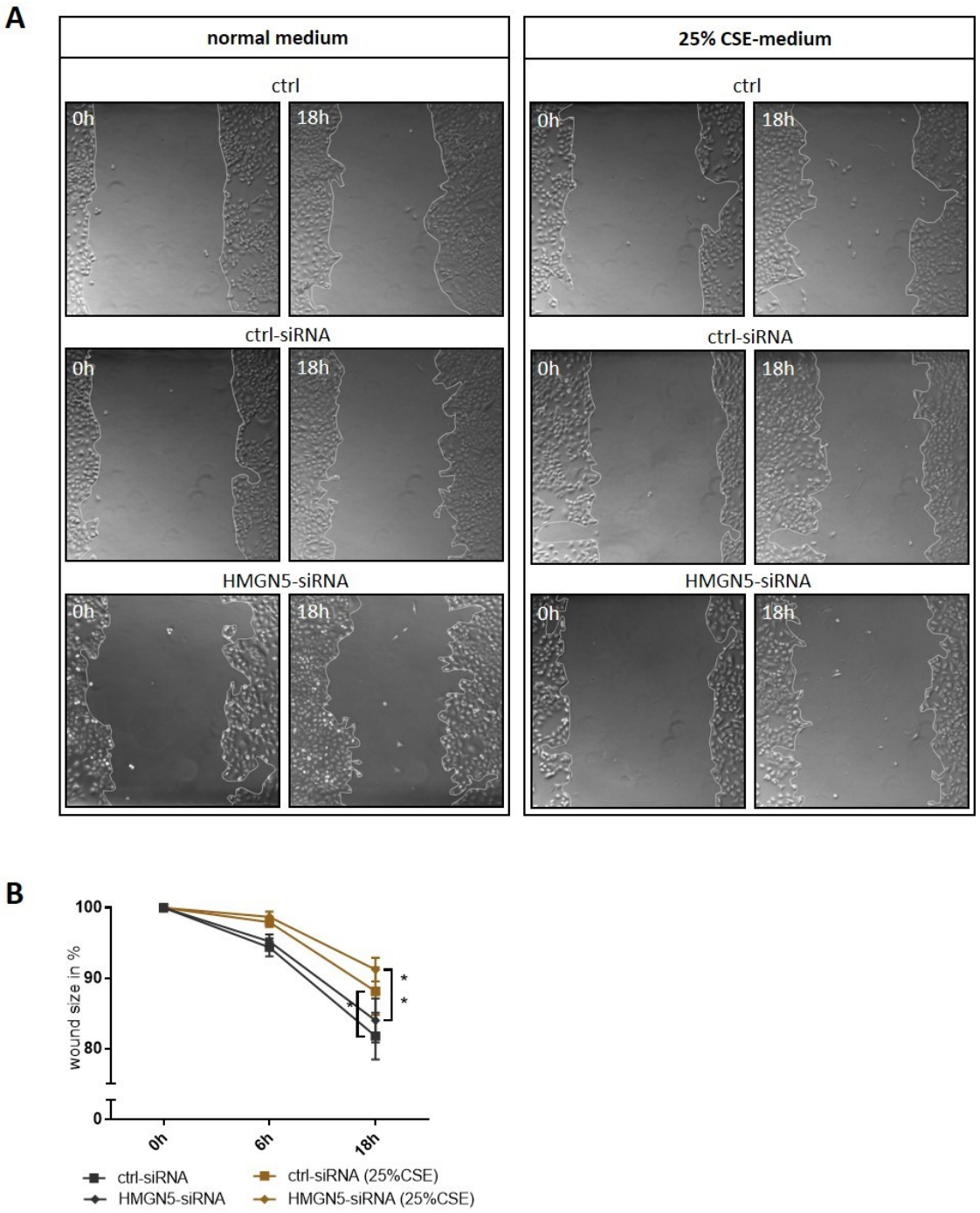

Figure 22: Woundhealing ability of AT-II cells is affected by CSE, but hardly by HMGN5 deficiency. 48h hours after siRNA transfection cell layer was scratched and culture medium was replaced either with normal medium or 25%CSE-containing medium. Pictures were taken at the indicated time points (A) Representative pictures showing wound closure at time point 18h. (B) CSE exposure of A549 cells causes less migration and/or proliferation both after 6h (significance not shown in the interest of clarity) and 18h of exposure indicated by a slower wound closure. HMGN5 silenced cells show a tendency for impaired woundhealing compared to their respective control in each group. Data were combined from two independent experiments (n=3 per group and per experiment) and are given as mean values ± SD. 2-way ANOVA following Bonferroni posttest was run for statistical analysis with *p < 0,05.

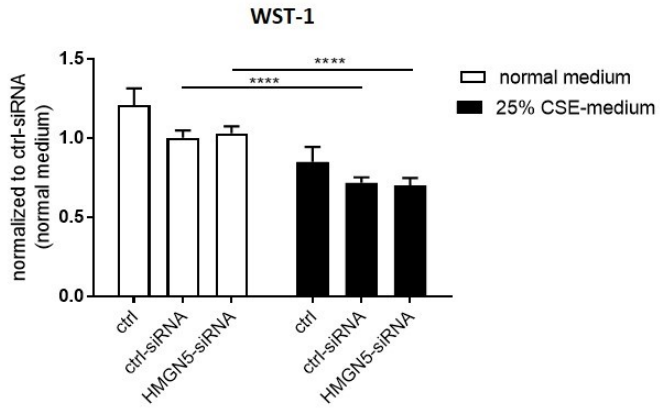

Figure 23: Effect of HMGN5 silencing and CSE in A549 cells. WST-1 cell proliferation reagent was used to assess proliferation and viability of HMGN5-siRNA transfected A549 cells. Cells were cultured in either normal medium or 25%CSE-medium for 6h before adding WST-1 reagent. Absorbance was measured after 2h of incubation, in total 50h after siRNA transfection. Data were combined from two independent experiments (n=3 per group and per experiment) and are given as mean values ± SD. 2-way ANOVA following Bonferroni posttest was run for statistical analysis with ****$p < 0{,}0001$.

12 Gene expression of other HMGN family members

In order to evaluate whether downregulation of HMGN5 is compensated by other HMGN family members, their RNA expression was measured. As it is shown in Figure 24, cells treated with HMGN5-siRNA exhibited increased expression of HMGN family member HMGN1 both in normal medium and CSE medium, whereas expression of HMGN2 was not altered.

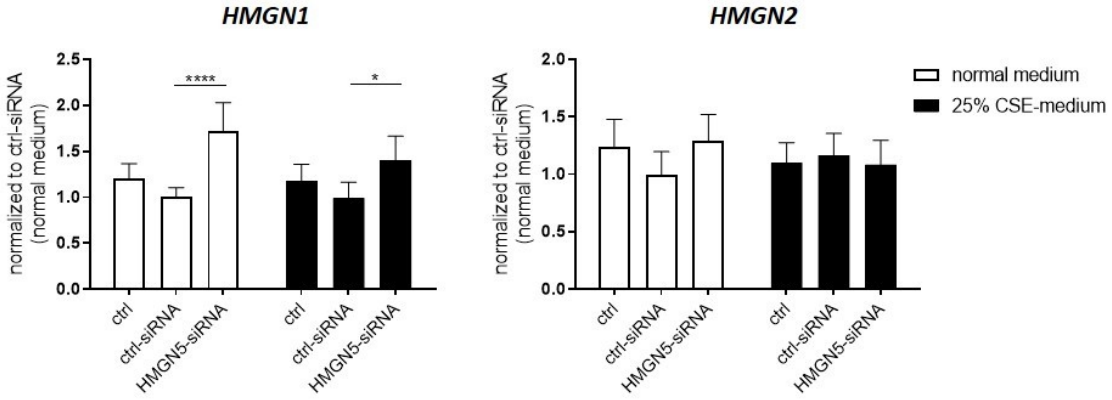

Figure 24: HMGN5 knockdown affects expression of its family protein HMGN1. HMGN1 and HMGN2 mRNA expression was measured by Quantitative PCR 48h after siRNA Transfection against HMGN5. 6h prior to RNA-Isolation cells were grown in normal medium (white bars) or 25% CSE-containing medium (black bars). 2^ΔCT values were calculated with HPRT as housekeeping gene and were then normalized to scrambled normal medium. Data were combined from two independent experiments (n=3 per group and per experiment) and are given as mean values ± SD. 2-way ANOVA following Bonferroni posttest was run for statistical analysis with *p < 0,05, ****p < 0,0001.

Part IV: Discussion

In the past two decades emerging progress has been made in the field of epigenetics. Although several epigenetic modifications and potential targets for therapy have been already described in COPD (Schamberger et al. 2014), further research is required in this broad field. We are still lacking detailed knowledge about the molecular mechanisms underlying epigenetic changes, as well as their importance in disease susceptibility, onset and development. In this study a potential role of the chromatin remodeling protein HMGN5 in COPD disease pathogenesis was identified. Firstly, lower expression of HMGN5 was found in the lungs of COPD patients, and secondly, downregulation of HMGN5 expression in the alveolar-type-II-like cell line A549 resulted in increased susceptibility to cell death inducing stimuli and impaired cell cycle progression.

High mobility group nucleosome (HMGN) proteins are known to modify chromatin architecture by dynamically binding to nucleosomes within the nucleus and interacting with linker histone H1 and other structural proteins (Postnikov and Bustin 2010; Kugler, Deng, and Bustin 2012). It has been shown, that loss of a functional HMGN variant in mice, leads to a variant-specific phenotype (Kugler et al. 2013). Mice exhibiting a non-functional HMGN5 variant demonstrated differences in lung parameters (IC, ERV, VC, TLC, FVC and FEV100), mechanical properties and showed an emphysematous phenotype (Kugler et al. 2013). Previous studies in our lab couldn't detect any of these differences in HMGN5 deficient mice. This could be explained by the different age of the mice. While Kugler et al. investigated mice at 17 weeks of age, in our lab mice where examined at 6 weeks of age. However, when HMGN5 deficient mice (6 weeks of age) were subjected to pancreatic porcine elastase, they developed severer emphysema compared to their wild-type counterparts as assessed by lung compliance and histological analysis of lung sections (unpublished observations from our lab). These findings are in line with observations by Kugler et al., that distinct changes in the phenotype of mice lacking functional HMGN variant could only be detected when mice were exposed to certain stress (Kugler et al. 2013).

Since HMGN5 deficient mice at older age developed emphysematous changes (Kugler et al. 2013) and cigarette smoke exposed wild-type mice exhibited reduced HMGN5 expression (unpublished observations from our lab) the question arose whether HMGN5 expression is also affected in COPD patients. Protein expression of HMGN5 in the lungs of COPD patients with predominant emphysema did not differ compared to healthy lungs, but RNA analysis of publicly accessible microarray and RNA-Sequencing of our COPD cohort revealed less RNA expression in COPD patients compared to healthy lungs (Figure 14).

HMGN5 has already been described in many human cancers such as prostate cancer, bladder cancer, clear cell renal cell carcinoma, breast cancer and lung cell cancer, where its expression was highly upregulated (Chen et al. 2012; Ji et al. 2012; Li et al. 2006; Song et al. 2006; Wahafu et al. 2011). Beyond that, it has been reported that COPD patients with predominant emphysema have a higher risk of lung cancer compared to patients exhibiting a predominant airway type (de Torres et al. 2007; de-Torres et al. 2015; Rabe and Watz 2017). This could explain the lack of change in HMGN5 protein expression in COPD patients with predominant emphysema, since it is unknown how HMGN5 expression is changing in the course of emphysema-cancer development. It might be that dysregulated expression of HMGN5 can contribute to emphysema development by downregulation and to lung cancer by upregulation. The time magnitude and extent of HMGN5 dysregulation to potentially provoke emphysema and lung cancer remain so far unclear.

Alveolar epithelial cells play a decisive role in emphysema development. Several pathological processes have been described in emphysema including oxidative stress, protease-antiprotease imbalance and cell death and repair leading to impaired tissue homeostasis (Tuder et al. 2006). Structural integrity of the alveolar area is maintained by alveolar epithelial type II cells that release the lung protective surfactant, function as progenitors of alveolar type I cells and secrete inflammatory cytokines (Zhao et al. 2010). Disruption of the biological function of alveolar epithelial cells occurs as a result of repetitive injury in emphysema (Zhao et al. 2010). HMGN5 expression in alveolar epithelial type II cells of COPD patient lungs (Figure 15) and previous findings in mice suggested a potential role of HMGN5 in the context of emphysema. To explore the underlying mechanism that drive emphysematous changes upon HMGN5 depletion the human alveolar type II-like cell line A549 was investigated.

HMGN5 silenced A549 cells revealed a similar pattern compared to control cells when assessing for cellular death, but additional treatment with staurosporine lead to an increased number of cells undergoing cell death (Figure 17). A similar trend, although less pronounced was observed when additionally treating HMGN5 downregulated cells with cigarette smoke extract (Figure 17). Interestingly, cigarette smoke mainly triggered cell necrosis at the dose used, whereas staurosporine induced cell death mainly via apoptosis. Zhang et al. have reported that HMGN5 downregulation induces cell apoptosis in prostate cancer cells via regulation of the caspase-related mitochondrial pathway and BCL-2 family proteins (Zhang et al. 2012). They have detected notably higher numbers of apoptotic cells after HMGN5 downregulation using the Annexin-V-APC/Propidium-Iodide assay used in this study. In addition, they have observed both increased protein expression of some pro-apoptotic proteins such as Bax, Bid and caspase 3 and decreased expression of anti-apoptotic proteins such as

Bcl-2 and Bcl-xl (Zhang et al. 2012). Here, similar findings by RNA expression analysis of some of these genes in HMGN5 downregulated A549 cells were also observed. Increased levels of CASP3 expression and a tendency of increased expression of BAX (Figure 18) were detected, but no differences in BCL-2 expression (Figure 18). Beside this, changes in necrosis related genes were detected, with higher expression of cyclophilin D and a tendency of higher expression of cyclophilin A (Figure 18). Although there is increased RNA expression of some pro-apoptotic genes, in contrast to Zhang et al. we could not detect higher numbers of apoptotic cells after HMGN5 downregulation alone (Figure 17). These observations might be explained by the following points: firstly, perhaps cell death analysis was performed at too early a stage, and secondly, the slight changes in RNA expression have been too small to induce cellular apoptosis. Taken together, some apoptosis and necrosis related changes in the transcriptional profile of siRNA-HMGN5 transfected cells were detectable, that did not affect the number of cells undergoing death. However, there is clear enhanced susceptibility to staurosporine, a known inductor of cellular apoptosis (Belmokhtar, Hillion, and Segal-Bendirdjian 2001), in HMGN5 downregulated cells.

In this study, cigarette smoke, the main toxic agent for the development of COPD, has been observed to cause cell necrosis at the dose used. A notable number of cells treated with 25% of cigarette smoke extract (CSE) underwent necrotic cell death. It has been described that CSE causes cell death in a concentration- and time-dependent manner (van Rijt et al. 2012). There is contradictory data about the characterization of cell death after cigarette smoke exposure, whereas some studies revealed induction of apoptosis (Ramage, Jones, and Whelan 2006; Hoshino et al. 2001), the findings here are consistent with other studies showing that cigarette smoke induces necrosis in human alveolar epithelial type II cells (van Rijt et al. 2012; Wickenden et al. 2003) and prevents apoptosis (Wickenden et al. 2003). Although the effect of cigarette smoke on cellular death of HMGN5 downregulated cells was not as clear as observed for staurosporine, the data is suggestive that HMGN5 silenced cells are also more susceptible to CSE. Taken together, these findings confirm what has already been observed in HMGN5 deficient mice subjected to pancreatic porcine elastase, that HMGN5 downregulation increases susceptibility to stimulation by external stress factors. On a molecular basis this might be due to the findings by Kugler et al. who have reported that HMGNs modulate the fidelity of cellular gene expression by fine tuning the transcription profile existing in a tissue or cell (Kugler et al. 2013).

Cell death and survival are strongly linked to cellular processes such as cell repair, proliferation and division in order to maintain tissue homeostasis that is disrupted in COPD development and numerous other diseases (Zhivotovsky and Orrenius 2010; Tuder and Petrache 2012). Hereby a fundamental role is

attributed to cell cycle processes and control (Rubin, Philpott, and Brooks 1993). There are several studies that have already unveiled a role of aberrant HMGN5 expression on cell cycle processes (Chen et al. 2012; Jiang, Zhou, and Zhang 2010; Wahafu et al. 2011; Ji et al. 2012). Jiang et al. have reported cell cycle arrest of prostate cancer cells after HMGN5 downregulation. They observed an increased number of cells in the G_2/M phase and a time dependent increase of cells in the S phase of the cell cycle (Jiang, Zhou, and Zhang 2010). Indeed, downregulation of HMGN5 has also been shown to induce cell cycle arrest in the human lung cancer cell line A549 (Chen et al. 2012). Chen et al. have demonstrated cell cycle arrest in early stages by detecting a higher number of cells in the G_0/G_1 phase. In accordance with these reports, HMGN5 downregulation induced cell cycle arrest in this study. These findings are consistent with the results by Chen et al. since a higher number of cells in the G_0/G_1 phase were also detected. Two different approaches were used to assess the impact of HMGN5 downregulation on cell cycle progression. One is a long time and well-known method using propidium iodide, a stoichiometric dye that binds DNA allowing the quantification of the DNA content (Krishan 1975). The other, a recently established method, is based on fluorescent tagged proteins that are ubiquitinated by specific ligases in a cell cycle phase dependent manner (Sakaue-Sawano et al. 2008). Although distinct changes between these two approaches regarding the distribution of cells trough the cell cycle were observed, both clearly demonstrated a similar pattern with accumulation of HMGN5 silenced cells in early cell cycle phases (G_0/G_1 and early S phase) and thus, lower amount of cells in the proceeding cell cycle stages (Figure 19 and Figure 20). This data suggests that HMGN5 is a crucial protein for maintaining physiological cell cycle progression.

During cell cycle progression, cyclins, that are periodically synthesized and degraded interact with cyclin dependent kinases (CDK) to maintain cell cycle progression (Johnson and Walker 1999). Others have previously shown an association between cell cycle arrest at G_2/M phase and reduced expression of cyclin B1, that is known to activate cyclin dependent kinases to initiate cell cycle transition from G_2 to M phase, in HMGN5 silenced clear cell renal cell carcinoma cells (Ji et al. 2012) and prostate cancer cells (Jiang, Zhou, and Zhang 2010). The data presented here doesn't support these findings, suggesting cell type specific effects. Firstly, cell cycle arrest was detected at earlier stages, and secondly, there was no defective expression of cyclins (Figure 21, A), notably not of those important for the progression in G_1, G_1/S transition and early S phase, that are cyclin D, E and A (Johnson and Walker 1999). Some evidence revealed a role of the transcription factor c-jun in cell cycle processes. It has been reported that c-jun is required for progress through G_1 and is able to directly control cyclin-D1 expression (Wisdom, Johnson, and Moore 1999). However, increased c-jun

expression in HMGN5 silenced cells was detected in this study. It is possible that the elevated levels of c-jun and cyclin D expression measured here were due to the increased percentage of HMGN5 downregulated cells in early cell stages of the cell cycle (Figure 20).

The integrity of the alveolar structure is based on the balance between cell repair and death (Tuder et al. 2006). One can hypothesize that cell cycle arrest after HMGN5 downregulation is accompanied by impaired cell proliferation that is consequently hindering physiological cell repair. Impaired proliferation in cells subjected to cigarette smoke extract was clearly observed, however, clear differences between HMGN5 silenced and control cells were not detected in the in vitro experiments using the wound healing and WST-1 assay (Figure 22 and Figure 23), whereas other studies have discovered disrupted proliferation in A549 cells after downregulation of HMGN5 (Chen et al. 2012; Li et al. 2016).

Despite some discrepancies between this data and previously published studies similar findings regarding cell cycle arrest after HMGN5 downregulation were clearly demonstrated. Furthermore, these results suggest enhanced susceptibility of HMGN5 silenced cells to cell death inducing stimuli. This observation is consistent with previous findings that showed a more severe emphysema in HMGN5 deficient mice compared to their wild-type controls when subjected to pancreatic porcine elastase (unpublished data from our lab). We have recently detected decreased HMGN5 RNA expression in cigarette smoke exposed mice that showed COPD features (unpublished data from our lab). In addition, it was clearly demonstrated here that there was reduced HMGN5 RNA expression in the lungs of COPD patients (Figure 14). Moreover, HMGN5 deficient mice at older age did show emphysematous changes in their lungs (Kugler et al. 2013). The aforementioned observations indicate a link between cigarette smoke exposure, COPD particularly emphysema and HMGN5 expression. However, detailed knowledge to fully understand these interactions as well as precise molecular mechanisms related to HMGN5 is still lacking. Shi et al. have pointed out some possible HMGN5 signaling pathways based on studies in cancer including the PI3K/AKT and MAPK/ERK signaling pathway and associated downstream targets such as cyclins, caspases, MMPs, VEGF and PCNA that regulate cell cycle, apoptosis, proliferation and migration, but these findings are based on only a few studies (Shi et al. 2016). HMGN proteins, so far only HMGN1 and HMGN2, have been described to modify gene expression during B cell activation (Zhang et al. 2016). B cells, that are organized in inducible bronchus-associated lymphoid tissue (iBALT), in turn, play a substantial role in emphysema development (Conlon et al. 2020; Jia et al. 2018; John-Schuster et al. 2014). Thus, it might be plausible to further consider that HMGN5 also drives emphysematous changes by affecting B cell activation. Indeed, most evidence reveals that HMGNs affect a distinct set of many genes without targeting specific

biological processes. Hence, changes in the expression of HMGNs can modulate the fidelity of cellular gene expression via interaction with the nucleosomes without any specificity for the underlying gene sequence, thereby resulting in increased susceptibility of an organism to injury (Kugler et al. 2013; Rochman et al. 2011). Given the possibility of functional redundancy among HMGN variants, the expression of other HMGN variants was examined. Increased RNA expression of HMGN1 after downregulation of HMGN5 was observed (Figure 24), raising the question whether HMGN1 is able to compensate HMGN5 function. However, most evidence suggests that HMGN variants are not fully redundant (Rochman, Malicet, and Bustin 2010; Rochman et al. 2009; Rochman et al. 2011; Kugler, Deng, and Bustin 2012).

This study and our previous experiments highlight a potential role of the epigenetic modulator HMGN5 in COPD development. Further investigations are required to unravel the mechanism by which HMGN5 might contribute to COPD pathogenesis. This study however points out that loss of HMGN5 in AT-II cells results in increased apoptosis and impaired cell cycle progression as a contributing factor to emphysema. Given the fact that HMGN5 may be a critical protein in both the pathogenesis of COPD and lung cancer, and that epigenetic modifications are mostly reversible, makes HMGN5 an interesting potential therapeutic target.

References

Abuhatzira, L., A. Shamir, D. E. Schones, A. A. Schaffer, and M. Bustin. 2011. 'The chromatin-binding protein HMGN1 regulates the expression of methyl CpG-binding protein 2 (MECP2) and affects the behavior of mice', *J Biol Chem*, 286: 42051-62.

Adcock, I. M., L. Tsaprouni, P. Bhavsar, and K. Ito. 2007. 'Epigenetic regulation of airway inflammation', *Curr Opin Immunol*, 19: 694-700.

Adeloye, D., S. Chua, C. Lee, C. Basquill, A. Papana, E. Theodoratou, H. Nair, D. Gasevic, D. Sridhar, H. Campbell, K. Y. Chan, A. Sheikh, I. Rudan, and Group Global Health Epidemiology Reference. 2015. 'Global and regional estimates of COPD prevalence: Systematic review and meta-analysis', *J Glob Health*, 5: 020415.

Alfonso, P. J., M. P. Crippa, J. J. Hayes, and M. Bustin. 1994. 'The footprint of chromosomal proteins HMG-14 and HMG-17 on chromatin subunits', *J Mol Biol*, 236: 189-98.

Allis, C. D., and T. Jenuwein. 2016. 'The molecular hallmarks of epigenetic control', *Nat Rev Genet*, 17: 487-500.

Annunziato, A. 2008. 'DNA packaging: nucleosomes and chromatin', *Nature Education*, 1: 26.

Anthonisen, N. R., M. A. Skeans, R. A. Wise, J. Manfreda, R. E. Kanner, J. E. Connett, and Group Lung Health Study Research. 2005. 'The effects of a smoking cessation intervention on 14.5-year mortality: a randomized clinical trial', *Ann Intern Med*, 142: 233-9.

Aoshiba, K., and A. Nagai. 2003. 'Oxidative stress, cell death, and other damage to alveolar epithelial cells induced by cigarette smoke', *Tob Induc Dis*, 1: 219-26.

Appleton, S., T. Jones, P. Poole, L. Pilotto, R. Adams, T. J. Lasserson, B. Smith, and J. Muhammad. 2006. 'Ipratropium bromide versus long-acting beta-2 agonists for stable chronic obstructive pulmonary disease', *Cochrane Database Syst Rev*: CD006101.

Barnes, P. J. 2008. 'Immunology of asthma and chronic obstructive pulmonary disease', *Nat Rev Immunol*, 8: 183-92.

Barnes, P. J. 2016. 'Inflammatory mechanisms in patients with chronic obstructive pulmonary disease', *J Allergy Clin Immunol*, 138: 16-27.

Barnes, Peter J., Peter G. J. Burney, Edwin K. Silverman, Bartolome R. Celli, Jørgen Vestbo, Jadwiga A. Wedzicha, and Emiel F. M. Wouters. 2015. 'Chronic obstructive pulmonary disease', *Nature Reviews Disease Primers*, 1: 15076.

Belmokhtar, C. A., J. Hillion, and E. Segal-Bendirdjian. 2001. 'Staurosporine induces apoptosis through both caspase-dependent and caspase-independent mechanisms', *Oncogene*, 20: 3354-62.

Berridge, Michael V, An S Tan, Kathy D McCoy, and Rui Wang. 1996. 'The biochemical and cellular basis of cell proliferation assays that use tetrazolium salts', *Biochemica*, 4: 14-19.

Bestall, J.C., EA Paul, R Garrod, R Garnham, PW Jones, and JA Wedzicha. 1999. 'Usefulness of the Medical Research Council (MRC) dyspnoea scale as a measure of disability in patients with chronic obstructive pulmonary disease', *Thorax*, 54: 581-86.

Bianchi, M. E., and A. Agresti. 2005. 'HMG proteins: dynamic players in gene regulation and differentiation', *Curr Opin Genet Dev*, 15: 496-506.

Birger, Y., F. Catez, T. Furusawa, J. H. Lim, M. Prymakowska-Bosak, K. L. West, Y. V. Postnikov, D. C. Haines, and M. Bustin. 2005. 'Increased tumorigenicity and sensitivity to ionizing radiation upon loss of chromosomal protein HMGN1', *Cancer Res*, 65: 6711-8.

Birger, Y., K. L. West, Y. V. Postnikov, J. H. Lim, T. Furusawa, J. P. Wagner, C. S. Laufer, K. H. Kraemer, and M. Bustin. 2003. 'Chromosomal protein HMGN1 enhances the rate of DNA repair in chromatin', *EMBO J*, 22: 1665-75.

Brusselle, G. G., and K. R. Bracke. 2015. 'Elucidating COPD pathogenesis by large-scale genetic analyses', *Lancet Respir Med*, 3: 737-9.

Burgel, P. R., P. Nesme-Meyer, P. Chanez, D. Caillaud, P. Carre, T. Perez, N. Roche, and Committee Initiatives Bronchopneumopathie Chronique Obstructive Scientific. 2009. 'Cough and sputum production are associated with frequent exacerbations and hospitalizations in COPD subjects', *Chest*, 135: 975-82.

Burney, P. 2017. 'Chronic respiratory disease - the acceptable epidemic?', *Clin Med (Lond)*, 17: 29-32.

Calverley, P. M., J. A. Anderson, B. Celli, G. T. Ferguson, C. Jenkins, P. W. Jones, J. C. Yates, J. Vestbo, and Torch investigators. 2007. 'Salmeterol and fluticasone propionate and survival in chronic obstructive pulmonary disease', *N Engl J Med*, 356: 775-89.

Castaldi, P. J., J. Dy, J. Ross, Y. Chang, G. R. Washko, D. Curran-Everett, A. Williams, D. A. Lynch, B. J. Make, J. D. Crapo, R. P. Bowler, E. A. Regan, J. E. Hokanson, G. L. Kinney, M. K. Han, X. Soler, J. W. Ramsdell, R. G. Barr, M. Foreman, E. van Beek, R. Casaburi, G. J. Criner, S. M. Lutz, S. I. Rennard, S. Santorico, F. C. Sciurba, D. L. DeMeo, C. P. Hersh, E. K. Silverman, and M. H. Cho. 2014. 'Cluster analysis in the COPDGene study identifies subtypes of smokers with distinct patterns of airway disease and emphysema', *Thorax*, 69: 415-22.

Catez, F., and R. Hock. 2010. 'Binding and interplay of HMG proteins on chromatin: lessons from live cell imaging', *Biochim Biophys Acta*, 1799: 15-27.

Cazzola, M., and M. Molimard. 2010. 'The scientific rationale for combining long-acting beta2-agonists and muscarinic antagonists in COPD', *Pulm Pharmacol Ther*, 23: 257-67.

Chen, P., X. L. Wang, Z. S. Ma, Z. Xu, B. Jia, J. Ren, Y. X. Hu, Q. H. Zhang, T. G. Ma, B. D. Yan, Q. Z. Yan, Y. L. Li, Z. Li, J. Y. Yu, R. Gao, N. Fan, B. Li, and J. L. Yang. 2012. 'Knockdown of HMGN5 expression by RNA interference induces cell cycle arrest in human lung cancer cells', *Asian Pac J Cancer Prev*, 13: 3223-8.

Cheng, L., J. Liu, B. Li, S. Liu, X. Li, and H. Tu. 2016. 'Cigarette Smoke-Induced Hypermethylation of the GCLC Gene Is Associated With COPD', *Chest*, 149: 474-82.

Cherukuri, S., R. Hock, T. Ueda, F. Catez, M. Rochman, and M. Bustin. 2008. 'Cell cycle-dependent binding of HMGN proteins to chromatin', *Mol Biol Cell*, 19: 1816-24.

Christofferson, D. E., and J. Yuan. 2010. 'Cyclophilin A release as a biomarker of necrotic cell death', *Cell Death Differ*, 17: 1942-3.

Conlon, T. M., G. John-Schuster, D. Heide, D. Pfister, M. Lehmann, Y. Hu, Z. Ertüz, M. A. Lopez, M. Ansari, M. Strunz, C. Mayr, I. Angelidis, C. Ciminieri, R. Costa, M. S. Kohlhepp, A. Guillot, G. Günes, A. Jeridi, M. C. Funk, G. Beroshvili, S. Prokosch, J. Hetzer, S. E. Verleden, H. Alsafadi,

M. Lindner, G. Burgstaller, L. Becker, M. Irmler, M. Dudek, J. Janzen, E. Goffin, R. Gosens, P. Knolle, B. Pirotte, T. Stoeger, J. Beckers, D. Wagner, I. Singh, F. J. Theis, M. H. de Angelis, T. O'Connor, F. Tacke, M. Boutros, E. Dejardin, O. Eickelberg, H. B. Schiller, M. Königshoff, M. Heikenwalder, and AÖ Yildirim. 2020. 'Inhibition of LTβR signalling activates WNT-induced regeneration in lung', *Nature*, 588: 151-56.

Cuvier, O., and B. Fierz. 2017. 'Dynamic chromatin technologies: from individual molecules to epigenomic regulation in cells', *Nat Rev Genet*, 18: 457-72.

de-Torres, J. P., D. O. Wilson, P. Sanchez-Salcedo, J. L. Weissfeld, J. Berto, A. Campo, A. B. Alcaide, M. García-Granero, B. R. Celli, and J. J. Zulueta. 2015. 'Lung cancer in patients with chronic obstructive pulmonary disease. Development and validation of the COPD Lung Cancer Screening Score', *Am J Respir Crit Care Med*, 191: 285-91.

de Torres, J. P., G. Bastarrika, J. P. Wisnivesky, A. B. Alcaide, A. Campo, L. M. Seijo, J. C. Pueyo, A. Villanueva, M. D. Lozano, U. Montes, L. Montuenga, and J. J. Zulueta. 2007. 'Assessing the relationship between lung cancer risk and emphysema detected on low-dose CT of the chest', *Chest*, 132: 1932-8.

Decramer, M. L., K. R. Chapman, R. Dahl, P. Frith, G. Devouassoux, C. Fritscher, R. Cameron, M. Shoaib, D. Lawrence, D. Young, D. McBryan, and Invigorate investigators. 2013. 'Once-daily indacaterol versus tiotropium for patients with severe chronic obstructive pulmonary disease (INVIGORATE): a randomised, blinded, parallel-group study', *Lancet Respir Med*, 1: 524-33.

Ebert, R. V., and M. J. Terracio. 1975. 'The bronchiolar epithelium in cigarette smokers. Observations with the scanning electron microscope', *Am Rev Respir Dis*, 111: 4-11.

Edgar, R. G., M. Patel, S. Bayliss, D. Crossley, E. Sapey, and A. M. Turner. 2017. 'Treatment of lung disease in alpha-1 antitrypsin deficiency: a systematic review', *Int J Chron Obstruct Pulmon Dis*, 12: 1295-308.

Eisner, M. D., N. Anthonisen, D. Coultas, N. Kuenzli, R. Perez-Padilla, D. Postma, I. Romieu, E. K. Silverman, J. R. Balmes, Environmental Committee on Nonsmoking Copd, and Assembly Occupational Health. 2010. 'An official American Thoracic Society public policy statement: Novel risk factors and the global burden of chronic obstructive pulmonary disease', *Am J Respir Crit Care Med*, 182: 693-718.

Fletcher, C., and R. Peto. 1977. 'The natural history of chronic airflow obstruction', *Br Med J*, 1: 1645-8.

Fletcher, C.M. 1960. 'Standardised questionnaire on respiratory symptoms: a statement prepared and approved by the MRC Committee on the Aetiology of Chronic Bronchitis (MRC breathlessness score)', *Bmj*, 2: 1665.

Gao, W., L. Li, Y. Wang, S. Zhang, I. M. Adcock, P. J. Barnes, M. Huang, and X. Yao. 2015. 'Bronchial epithelial cells: The key effector cells in the pathogenesis of chronic obstructive pulmonary disease?', *Respirology*, 20: 722-9.

Gershon, A. S., L. Warner, P. Cascagnette, J. C. Victor, and T. To. 2011. 'Lifetime risk of developing chronic obstructive pulmonary disease: a longitudinal population study', *Lancet*, 378: 991-6.

Hancock, D. B., M. Eijgelsheim, J. B. Wilk, S. A. Gharib, L. R. Loehr, K. D. Marciante, N. Franceschini, Y. M. van Durme, T. H. Chen, R. G. Barr, M. B. Schabath, D. J. Couper, G. G. Brusselle, B. M. Psaty, C. M. van Duijn, J. I. Rotter, A. G. Uitterlinden, A. Hofman, N. M. Punjabi, F. Rivadeneira,

A. C. Morrison, P. L. Enright, K. E. North, S. R. Heckbert, T. Lumley, B. H. Stricker, G. T. O'Connor, and S. J. London. 2010. 'Meta-analyses of genome-wide association studies identify multiple loci associated with pulmonary function', *Nat Genet*, 42: 45-52.

Hasegawa, M., Y. Nasuhara, Y. Onodera, H. Makita, K. Nagai, S. Fuke, Y. Ito, T. Betsuyaku, and M. Nishimura. 2006. 'Airflow limitation and airway dimensions in chronic obstructive pulmonary disease', *Am J Respir Crit Care Med*, 173: 1309-15.

Hashimoto, M., H. Tanaka, and S. Abe. 2005. 'Quantitative analysis of bronchial wall vascularity in the medium and small airways of patients with asthma and COPD', *Chest*, 127: 965-72.

Hergeth, S. P., and R. Schneider. 2015. 'The H1 linker histones: multifunctional proteins beyond the nucleosomal core particle', *EMBO Rep*, 16: 1439-53.

Hock, R., T. Furusawa, T. Ueda, and M. Bustin. 2007. 'HMG chromosomal proteins in development and disease', *Trends Cell Biol*, 17: 72-9.

Hock, R., U. Scheer, and M. Bustin. 1998. 'Chromosomal proteins HMG-14 and HMG-17 are released from mitotic chromosomes and imported into the nucleus by active transport', *J Cell Biol*, 143: 1427-36.

Hogg, J. C., F. S. Chu, W. C. Tan, D. D. Sin, S. A. Patel, P. D. Pare, F. J. Martinez, R. M. Rogers, B. J. Make, G. J. Criner, R. M. Cherniack, A. Sharafkhaneh, J. D. Luketich, H. O. Coxson, W. M. Elliott, and F. C. Sciurba. 2007. 'Survival after lung volume reduction in chronic obstructive pulmonary disease: insights from small airway pathology', *Am J Respir Crit Care Med*, 176: 454-9.

Hogg, J. C., J. E. McDonough, J. V. Gosselink, and S. Hayashi. 2009. 'What drives the peripheral lung-remodeling process in chronic obstructive pulmonary disease?', *Proc Am Thorac Soc*, 6: 668-72.

Hogg, J. C., and W. Timens. 2009. 'The pathology of chronic obstructive pulmonary disease', *Annu Rev Pathol*, 4: 435-59.

Hoshino, Y., T. Mio, S. Nagai, H. Miki, I. Ito, and T. Izumi. 2001. 'Cytotoxic effects of cigarette smoke extract on an alveolar type II cell-derived cell line', *Am J Physiol Lung Cell Mol Physiol*, 281: L509-16.

Hurst, J. R., J. Vestbo, A. Anzueto, N. Locantore, H. Mullerova, R. Tal-Singer, B. Miller, D. A. Lomas, A. Agusti, W. Macnee, P. Calverley, S. Rennard, E. F. Wouters, J. A. Wedzicha, and Copd Longitudinally to Identify Predictive Surrogate Endpoints Investigators Evaluation of. 2010. 'Susceptibility to exacerbation in chronic obstructive pulmonary disease', *N Engl J Med*, 363: 1128-38.

Ito, K., M. Ito, W. M. Elliott, B. Cosio, G. Caramori, O. M. Kon, A. Barczyk, S. Hayashi, I. M. Adcock, J. C. Hogg, and P. J. Barnes. 2005. 'Decreased histone deacetylase activity in chronic obstructive pulmonary disease', *N Engl J Med*, 352: 1967-76.

Ji, S. Q., L. Yao, X. Y. Zhang, X. S. Li, and L. Q. Zhou. 2012. 'Knockdown of the nucleosome binding protein 1 inhibits the growth and invasion of clear cell renal cell carcinoma cells in vitro and in vivo', *J Exp Clin Cancer Res*, 31: 22.

Jia, J., T. M. Conlon, R. S. Sarker, D. Tasdemir, N. F. Smirnova, B. Srivastava, S. E. Verleden, G. Gunes, X. Wu, C. Prehn, J. Gao, K. Heinzelmann, J. Lintelmann, M. Irmler, S. Pfeiffer, M. Schloter, R. Zimmermann, M. Hrabe de Angelis, J. Beckers, J. Adamski, H. Bayram, O. Eickelberg, and A. O.

Yildirim. 2018. 'Cholesterol metabolism promotes B-cell positioning during immune pathogenesis of chronic obstructive pulmonary disease', *EMBO Mol Med*, 10.

Jiang, N., L. Q. Zhou, and X. Y. Zhang. 2010. 'Downregulation of the nucleosome-binding protein 1 (NSBP1) gene can inhibit the in vitro and in vivo proliferation of prostate cancer cells', *Asian J Androl*, 12: 709-17.

Jimenez-Ruiz, C. A., S. Andreas, K. E. Lewis, P. Tonnesen, C. P. van Schayck, P. Hajek, S. Tonstad, B. Dautzenberg, M. Fletcher, S. Masefield, P. Powell, T. Hering, S. Nardini, T. Tonia, and C. Gratziou. 2015. 'Statement on smoking cessation in COPD and other pulmonary diseases and in smokers with comorbidities who find it difficult to quit', *Eur Respir J*, 46: 61-79.

John-Schuster, G., K. Hager, T. M. Conlon, M. Irmler, J. Beckers, O. Eickelberg, and AÖ Yildirim. 2014. 'Cigarette smoke-induced iBALT mediates macrophage activation in a B cell-dependent manner in COPD', *Am J Physiol Lung Cell Mol Physiol*, 307: L692-706.

Johnson, D. G., and C. L. Walker. 1999. 'Cyclins and cell cycle checkpoints', *Annu Rev Pharmacol Toxicol*, 39: 295-312.

Jones, P. W., M. Tabberer, and W. H. Chen. 2011. 'Creating scenarios of the impact of COPD and their relationship to COPD Assessment Test (CAT) scores', *BMC Pulm Med*, 11: 42.

Kato, H., H. van Ingen, B. R. Zhou, H. Feng, M. Bustin, L. E. Kay, and Y. Bai. 2011. 'Architecture of the high mobility group nucleosomal protein 2-nucleosome complex as revealed by methyl-based NMR', *Proc Natl Acad Sci U S A*, 108: 12283-8.

Kim, V., and G. J. Criner. 2013. 'Chronic bronchitis and chronic obstructive pulmonary disease', *Am J Respir Crit Care Med*, 187: 228-37.

Kim, V., M. K. Han, G. B. Vance, B. J. Make, J. D. Newell, J. E. Hokanson, C. P. Hersh, D. Stinson, E. K. Silverman, G. J. Criner, and C. OPDGene Investigators. 2011. 'The chronic bronchitic phenotype of COPD: an analysis of the COPDGene Study', *Chest*, 140: 626-33.

King, L. M., and C. A. Francomano. 2001. 'Characterization of a human gene encoding nucleosomal binding protein NSBP1', *Genomics*, 71: 163-73.

Kosmider, B., E. M. Messier, H. W. Chu, and R. J. Mason. 2011. 'Human alveolar epithelial cell injury induced by cigarette smoke', *PLoS One*, 6: e26059.

Krishan, A. 1975. 'Rapid flow cytofluorometric analysis of mammalian cell cycle by propidium iodide staining', *J Cell Biol*, 66: 188-93.

Kugler, J. E., T. Deng, and M. Bustin. 2012. 'The HMGN family of chromatin-binding proteins: dynamic modulators of epigenetic processes', *Biochim Biophys Acta*, 1819: 652-6.

Kugler, J. E., M. Horsch, D. Huang, T. Furusawa, M. Rochman, L. Garrett, L. Becker, A. Bohla, S. M. Holter, C. Prehn, B. Rathkolb, I. Racz, J. A. Aguilar-Pimentel, T. Adler, J. Adamski, J. Beckers, D. H. Busch, O. Eickelberg, T. Klopstock, M. Ollert, T. Stoger, E. Wolf, W. Wurst, A. O. Yildirim, A. Zimmer, V. Gailus-Durner, H. Fuchs, M. Hrabe de Angelis, B. Garfinkel, J. Orly, I. Ovcharenko, and M. Bustin. 2013. 'High mobility group N proteins modulate the fidelity of the cellular transcriptional profile in a tissue- and variant-specific manner', *J Biol Chem*, 288: 16690-703.

Lahousse, L., L. J. M. Seys, G. F. Joos, O. H. Franco, B. H. Stricker, and G. G. Brusselle. 2017. 'Epidemiology and impact of chronic bronchitis in chronic obstructive pulmonary disease', *Eur Respir J*, 50.

Lamprecht, B., M. A. McBurnie, W. M. Vollmer, G. Gudmundsson, T. Welte, E. Nizankowska-Mogilnicka, M. Studnicka, E. Bateman, J. M. Anto, P. Burney, D. M. Mannino, S. A. Buist, and Bold Collaborative Research Group. 2011. 'COPD in never smokers: results from the population-based burden of obstructive lung disease study', *Chest*, 139: 752-63.

Landis, S. H., H. Muellerova, D. M. Mannino, A. M. Menezes, M. K. Han, T. van der Molen, M. Ichinose, Z. Aisanov, Y. M. Oh, and K. J. Davis. 2014. 'Continuing to Confront COPD International Patient Survey: methods, COPD prevalence, and disease burden in 2012-2013', *Int J Chron Obstruct Pulmon Dis*, 9: 597-611.

Lange, P., B. Celli, A. Agusti, G. Boje Jensen, M. Divo, R. Faner, S. Guerra, J. L. Marott, F. D. Martinez, P. Martinez-Camblor, P. Meek, C. A. Owen, H. Petersen, V. Pinto-Plata, P. Schnohr, A. Sood, J. B. Soriano, Y. Tesfaigzi, and J. Vestbo. 2015. 'Lung-Function Trajectories Leading to Chronic Obstructive Pulmonary Disease', *N Engl J Med*, 373: 111-22.

Lange, S. S., D. L. Mitchell, and K. M. Vasquez. 2008. 'High mobility group protein B1 enhances DNA repair and chromatin modification after DNA damage', *Proc Natl Acad Sci U S A*, 105: 10320-5.

Lee, J. H., M. H. Cho, C. P. Hersh, M. L. McDonald, J. D. Crapo, P. S. Bakke, A. Gulsvik, A. P. Comellas, C. H. Wendt, D. A. Lomas, V. Kim, E. K. Silverman, Copdgene, and Eclipse Investigators. 2014. 'Genetic susceptibility for chronic bronchitis in chronic obstructive pulmonary disease', *Respir Res*, 15: 113.

Li, D., X. Du, A. Liu, and P. Li. 2016. 'Suppression of nucleosome-binding protein 1 by miR-326 impedes cell proliferation and invasion in non-small cell lung cancer cells', *Oncol Rep*, 35: 1117-24.

Li, D. Q., Y. F. Hou, J. Wu, Y. Chen, J. S. Lu, G. H. Di, Z. L. Ou, Z. Z. Shen, J. Ding, and Z. M. Shao. 2006. 'Gene expression profile analysis of an isogenic tumour metastasis model reveals a functional role for oncogene AF1Q in breast cancer metastasis', *Eur J Cancer*, 42: 3274-86.

Lim, J. H., F. Catez, Y. Birger, K. L. West, M. Prymakowska-Bosak, Y. V. Postnikov, and M. Bustin. 2004. 'Chromosomal protein HMGN1 modulates histone H3 phosphorylation', *Mol Cell*, 15: 573-84.

Lim, J. H., K. L. West, Y. Rubinstein, M. Bergel, Y. V. Postnikov, and M. Bustin. 2005. 'Chromosomal protein HMGN1 enhances the acetylation of lysine 14 in histone H3', *EMBO J*, 24: 3038-48.

Luger, K., M. L. Dechassa, and D. J. Tremethick. 2012. 'New insights into nucleosome and chromatin structure: an ordered state or a disordered affair?', *Nat Rev Mol Cell Biol*, 13: 436-47.

MacNee, W. 2001. 'Oxidants/antioxidants and chronic obstructive pulmonary disease: pathogenesis to therapy', *Novartis Found Symp*, 234: 169-85; discussion 85-8.

Mahler, D. A., E. Kerwin, T. Ayers, A. FowlerTaylor, S. Maitra, C. Thach, M. Lloyd, F. Patalano, and D. Banerji. 2015. 'FLIGHT1 and FLIGHT2: Efficacy and Safety of QVA149 (Indacaterol/Glycopyrrolate) versus Its Monocomponents and Placebo in Patients with Chronic Obstructive Pulmonary Disease', *Am J Respir Crit Care Med*, 192: 1068-79.

Malicet, C., M. Rochman, Y. Postnikov, and M. Bustin. 2011. 'Distinct properties of human HMGN5 reveal a rapidly evolving but functionally conserved nucleosome binding protein', *Mol Cell Biol*, 31: 2742-55.

Mannino, D. M., and A. S. Buist. 2007. 'Global burden of COPD: risk factors, prevalence, and future trends', *Lancet*, 370: 765-73.

Mannino, D. M., K. Higuchi, T. C. Yu, H. Zhou, Y. Li, H. Tian, and K. Suh. 2015. 'Economic Burden of COPD in the Presence of Comorbidities', *Chest*, 148: 138-50.

Martinez, C. H., Y. H. Chen, P. M. Westgate, L. X. Liu, S. Murray, J. L. Curtis, B. J. Make, E. A. Kazerooni, D. A. Lynch, N. Marchetti, G. R. Washko, F. J. Martinez, M. K. Han, and C. OPDGene Investigators. 2012. 'Relationship between quantitative CT metrics and health status and BODE in chronic obstructive pulmonary disease', *Thorax*, 67: 399-406.

Matsuoka, S., G. R. Washko, T. Yamashiro, R. S. Estepar, A. Diaz, E. K. Silverman, E. Hoffman, H. E. Fessler, G. J. Criner, N. Marchetti, S. M. Scharf, F. J. Martinez, J. J. Reilly, H. Hatabu, and Group National Emphysema Treatment Trial Research. 2010. 'Pulmonary hypertension and computed tomography measurement of small pulmonary vessels in severe emphysema', *Am J Respir Crit Care Med*, 181: 218-25.

McDonough, J. E., R. Yuan, M. Suzuki, N. Seyednejad, W. M. Elliott, P. G. Sanchez, A. C. Wright, W. B. Gefter, L. Litzky, H. O. Coxson, P. D. Pare, D. D. Sin, R. A. Pierce, J. C. Woods, A. M. McWilliams, J. R. Mayo, S. C. Lam, J. D. Cooper, and J. C. Hogg. 2011. 'Small-airway obstruction and emphysema in chronic obstructive pulmonary disease', *N Engl J Med*, 365: 1567-75.

Medical Research Council. 1965. 'Definition and classification of chronic bronchitis for clinical and epidemiological purposes. A report to the Medical Research Council by their Committee on the Aetiology of Chronic Bronchitis', *Lancet*, 1: 775-9.

Misteli, T., A. Gunjan, R. Hock, M. Bustin, and D. T. Brown. 2000. 'Dynamic binding of histone H1 to chromatin in living cells', *Nature*, 408: 877-81.

Monick, M. M., S. R. Beach, J. Plume, R. Sears, M. Gerrard, G. H. Brody, and R. A. Philibert. 2012. 'Coordinated changes in AHRR methylation in lymphoblasts and pulmonary macrophages from smokers', *Am J Med Genet B Neuropsychiatr Genet*, 159B: 141-51.

Mortality, G. B. D., and Collaborators Causes of Death. 2016. 'Global, regional, and national life expectancy, all-cause mortality, and cause-specific mortality for 249 causes of death, 1980-2015: a systematic analysis for the Global Burden of Disease Study 2015', *Lancet*, 388: 1459-544.

Nakagawa, T., S. Shimizu, T. Watanabe, O. Yamaguchi, K. Otsu, H. Yamagata, H. Inohara, T. Kubo, and Y. Tsujimoto. 2005. 'Cyclophilin D-dependent mitochondrial permeability transition regulates some necrotic but not apoptotic cell death', *Nature*, 434: 652-8.

Nakano, Y., S. Muro, H. Sakai, T. Hirai, K. Chin, M. Tsukino, K. Nishimura, H. Itoh, P. D. Pare, J. C. Hogg, and M. Mishima. 2000. 'Computed tomographic measurements of airway dimensions and emphysema in smokers. Correlation with lung function', *Am J Respir Crit Care Med*,162:1102-8.

Nardini, S., G. Camiciottoli, S. Locicero, R. Maselli, F. Pasqua, G. Passalacqua, R. Pela, A. Pesci, A. Sebastiani, and A. Vatrella. 2014. 'COPD: maximization of bronchodilation', *Multidiscip Respir Med*, 9: 50.

O'Donnell, D. E., T. Fluge, F. Gerken, A. Hamilton, K. Webb, B. Aguilaniu, B. Make, and H. Magnussen. 2004. 'Effects of tiotropium on lung hyperinflation, dyspnoea and exercise tolerance in COPD', *Eur Respir J*, 23: 832-40.

O'Donnell, D. E., F. Sciurba, B. Celli, D. A. Mahler, K. A. Webb, C. J. Kalberg, and K. Knobil. 2006. 'Effect of fluticasone propionate/salmeterol on lung hyperinflation and exercise endurance in COPD', *Chest*, 130: 647-56.

Oswald-Mammosser, M., E. Weitzenblum, E. Quoix, G. Moser, A. Chaouat, C. Charpentier, and R. Kessler. 1995. 'Prognostic factors in COPD patients receiving long-term oxygen therapy. Importance of pulmonary artery pressure', *Chest*, 107: 1193-8.

Pare, P. D., and P. G. Camp. 2012. 'Airway disease and emphysema on CT: not just phenotypes of lung pathology', *Thorax*, 67: 380-2.

Park, J. W., S. W. Ryter, and A. M. Choi. 2007. 'Functional significance of apoptosis in chronic obstructive pulmonary disease', *COPD*, 4: 347-53.

Pascoe, S., N. Locantore, M. T. Dransfield, N. C. Barnes, and I. D. Pavord. 2015. 'Blood eosinophil counts, exacerbations, and response to the addition of inhaled fluticasone furoate to vilanterol in patients with chronic obstructive pulmonary disease: a secondary analysis of data from two parallel randomised controlled trials', *Lancet Respir Med*, 3: 435-42.

Petrache, I., and K. Serban. 2016. 'Lost in Trans-IL-6 Signaling: Alveolar Type II Cell Death in Emphysema', *Am J Respir Crit Care Med*, 194: 1441-43.

Pillai, S. G., D. Ge, G. Zhu, X. Kong, K. V. Shianna, A. C. Need, S. Feng, C. P. Hersh, P. Bakke, A. Gulsvik, A. Ruppert, K. C. Lodrup Carlsen, A. Roses, W. Anderson, S. I. Rennard, D. A. Lomas, E. K. Silverman, D. B. Goldstein, and Icgn Investigators. 2009. 'A genome-wide association study in chronic obstructive pulmonary disease (COPD): identification of two major susceptibility loci', *PLoS Genet*, 5: e1000421.

Postnikov, Y., and M. Bustin. 2010. 'Regulation of chromatin structure and function by HMGN proteins', *Biochim Biophys Acta*, 1799: 62-8.

Prymakowska-Bosak, M., T. Misteli, J. E. Herrera, H. Shirakawa, Y. Birger, S. Garfield, and M. Bustin. 2001. 'Mitotic phosphorylation prevents the binding of HMGN proteins to chromatin', *Mol Cell Biol*, 21: 5169-78.

Qiu, W., A. Baccarelli, V. J. Carey, N. Boutaoui, H. Bacherman, B. Klanderman, S. Rennard, A. Agusti, W. Anderson, D. A. Lomas, and D. L. DeMeo. 2012. 'Variable DNA methylation is associated with chronic obstructive pulmonary disease and lung function', *Am J Respir Crit Care Med*, 185: 373-81.

Rabe, K. F., and H. Watz. 2017. 'Chronic obstructive pulmonary disease', *Lancet*, 389: 1931-40.

Raherison, C., and P-O Girodet. 2009. 'Epidemiology of COPD', *European Respiratory Review*, 18: 213-21.

Rajendrasozhan, S., S. R. Yang, V. L. Kinnula, and I. Rahman. 2008. 'SIRT1, an antiinflammatory and antiaging protein, is decreased in lungs of patients with chronic obstructive pulmonary disease', *Am J Respir Crit Care Med*, 177: 861-70.

Ram, F. S., P. W. Jones, A. A. Castro, J. A. De Brito, A. N. Atallah, Y. Lacasse, R. Mazzini, R. Goldstein, and S. Cendon. 2002. 'Oral theophylline for chronic obstructive pulmonary disease', *Cochrane Database Syst Rev*: CD003902.

Ramage, L., A. C. Jones, and C. J. Whelan. 2006. 'Induction of apoptosis with tobacco smoke and related products in A549 lung epithelial cells in vitro', *J Inflamm (Lond)*, 3: 3.

Rochester, C. L., I. Vogiatzis, A. E. Holland, S. C. Lareau, D. D. Marciniuk, M. A. Puhan, M. A. Spruit, S. Masefield, R. Casaburi, E. M. Clini, R. Crouch, J. Garcia-Aymerich, C. Garvey, R. S. Goldstein, K. Hill, M. Morgan, L. Nici, F. Pitta, A. L. Ries, S. J. Singh, T. Troosters, P. J. Wijkstra, B. P. Yawn, R. L. ZuWallack, and Ats Ers Task Force on Policy in Pulmonary Rehabilitation. 2015. 'An Official American Thoracic Society/European Respiratory Society Policy Statement: Enhancing Implementation, Use, and Delivery of Pulmonary Rehabilitation', *Am J Respir Crit Care Med*, 192: 1373-86.

Rochman, M., C. Malicet, and M. Bustin. 2010. 'HMGN5/NSBP1: a new member of the HMGN protein family that affects chromatin structure and function', *Biochim Biophys Acta*, 1799: 86-92.

Rochman, M., Y. Postnikov, S. Correll, C. Malicet, S. Wincovitch, T. S. Karpova, J. G. McNally, X. Wu, N. A. Bubunenko, S. Grigoryev, and M. Bustin. 2009. 'The interaction of NSBP1/HMGN5 with nucleosomes in euchromatin counteracts linker histone-mediated chromatin compaction and modulates transcription', *Mol Cell*, 35: 642-56.

Rochman, M., L. Taher, T. Kurahashi, S. Cherukuri, V. N. Uversky, D. Landsman, I. Ovcharenko, and M. Bustin. 2011. 'Effects of HMGN variants on the cellular transcription profile', *Nucleic Acids Res*, 39: 4076-87.

Rubin, L. L., K. L. Philpott, and S. F. Brooks. 1993. 'Apoptosis: the cell cycle and cell death', *Curr Biol*, 3: 391-4.

Sakao, S., N. F. Voelkel, and K. Tatsumi. 2014. 'The vascular bed in COPD: pulmonary hypertension and pulmonary vascular alterations', *Eur Respir Rev*, 23: 350-5.

Sakaue-Sawano, A., H. Kurokawa, T. Morimura, A. Hanyu, H. Hama, H. Osawa, S. Kashiwagi, K. Fukami, T. Miyata, H. Miyoshi, T. Imamura, M. Ogawa, H. Masai, and A. Miyawaki. 2008. 'Visualizing spatiotemporal dynamics of multicellular cell-cycle progression', *Cell*, 132: 487-98.

Salvi, S. S., and P. J. Barnes. 2009. 'Chronic obstructive pulmonary disease in non-smokers', *Lancet*, 374: 733-43.

Sarker, R. S., G. John-Schuster, A. Bohla, K. Mutze, G. Burgstaller, M. T. Bedford, M. Königshoff, O. Eickelberg, and AÖ Yildirim. 2015. 'Coactivator-Associated Arginine Methyltransferase-1 Function in Alveolar Epithelial Senescence and Elastase-Induced Emphysema Susceptibility', *Am J Respir Cell Mol Biol*, 53: 769-81.

Scanlon, P. D., J. E. Connett, L. A. Waller, M. D. Altose, W. C. Bailey, A. S. Buist, D. P. Tashkin, and Group Lung Health Study Research. 2000. 'Smoking cessation and lung function in mild-to-moderate chronic obstructive pulmonary disease. The Lung Health Study', *Am J Respir Crit Care Med*, 161: 381-90.

Schamberger, A. C., N. Mise, S. Meiners, and O. Eickelberg. 2014. 'Epigenetic mechanisms in COPD: implications for pathogenesis and drug discovery', *Expert Opin Drug Discov*, 9: 609-28.

Segura-Valdez, L., A. Pardo, M. Gaxiola, B. D. Uhal, C. Becerril, and M. Selman. 2000. 'Upregulation of gelatinases A and B, collagenases 1 and 2, and increased parenchymal cell death in COPD', *Chest*, 117: 684-94.

Sestini, P., E. Renzoni, S. Robinson, P. Poole, and F. S. Ram. 2002. 'Short-acting beta 2 agonists for stable chronic obstructive pulmonary disease', *Cochrane Database Syst Rev*: CD001495.

Shah, P. L., F. J. Herth, W. H. van Geffen, G. Deslee, and D. J. Slebos. 2017. 'Lung volume reduction for emphysema', *Lancet Respir Med*, 5: 147-56.

Shen, X., and M. A. Gorovsky. 1996. 'Linker histone H1 regulates specific gene expression but not global transcription in vivo', *Cell*, 86: 475-83.

Shi, Z., R. Tang, D. Wu, and X. Sun. 2016. 'Research advances in HMGN5 and cancer', *Tumour Biol*, 37: 1531-9.

Shirakawa, H., D. Landsman, Y. V. Postnikov, and M. Bustin. 2000. 'NBP-45, a novel nucleosomal binding protein with a tissue-specific and developmentally regulated expression', *J Biol Chem*, 275: 6368-74.

Shirakawa, H., M. Rochman, T. Furusawa, M. R. Kuehn, S. Horigome, K. Haketa, Y. Sugita, T. Inada, M. Komai, and M. Bustin. 2009. 'The nucleosomal binding protein NSBP1 is highly expressed in the placenta and modulates the expression of differentiation markers in placental Rcho-1 cells', *J Cell Biochem*, 106: 651-8.

Siddiqui, S. H., A. Guasconi, J. Vestbo, P. Jones, A. Agusti, P. Paggiaro, J. A. Wedzicha, and D. Singh. 2015. 'Blood Eosinophils: A Biomarker of Response to Extrafine Beclomethasone/Formoterol in Chronic Obstructive Pulmonary Disease', *Am J Respir Crit Care Med*, 192: 523-5.

Simmons, D. 2008. 'Epigenetic influence and disease', *Nature Education*, 1: 6.

Singh, D., G. T. Ferguson, J. Bolitschek, L. Gronke, C. Hallmann, N. Bennett, R. Abrahams, O. Schmidt, and L. Bjermer. 2015. 'Tiotropium + olodaterol shows clinically meaningful improvements in quality of life', *Respir Med*, 109: 1312-9.

Sirianni, F. E., F. S. Chu, and D. C. Walker. 2003. 'Human alveolar wall fibroblasts directly link epithelial type 2 cells to capillary endothelium', *Am J Respir Crit Care Med*, 168: 1532-7.

Snider, G. L., J. Kleinermann, W. M. Thurlbeck, and Z. H. Bengali. 1985. 'The definition of emphysema. Report of a National Heart, Lung, and Blood Institute, Division of Lung Diseases workshop', *Am Rev Respir Dis*, 132: 182-5.

Song, G., L. Q. Zhou, M. Weng, Q. He, Z. S. He, J. R. Hao, B. N. Pan, and Y. Q. Na. 2006. '[Expression of nucleosomal binding protein 1 in normal prostate benign prostate hyperplasia, and prostate cancer and significance thereof]', *Zhonghua Yi Xue Za Zhi*, 86: 1962-5.

Soriano, J. B., V. A. Kiri, N. B. Pride, and J. Vestbo. 2003. 'Inhaled corticosteroids with/without long-acting beta-agonists reduce the risk of rehospitalization and death in COPD patients', *Am J Respir Med*, 2: 67-74.

Soriano, J. B., D. D. Sin, X. Zhang, P. G. Camp, J. A. Anderson, N. R. Anthonisen, A. S. Buist, P. S. Burge, P. M. Calverley, J. E. Connett, S. Petersson, D. S. Postma, W. Szafranski, and J. Vestbo. 2007. 'A pooled analysis of FEV1 decline in COPD patients randomized to inhaled corticosteroids or placebo', *Chest*, 131: 682-89.

Spruit, M. A., S. J. Singh, C. Garvey, R. ZuWallack, L. Nici, C. Rochester, K. Hill, A. E. Holland, S. C. Lareau, W. D. Man, F. Pitta, L. Sewell, J. Raskin, J. Bourbeau, R. Crouch, F. M. Franssen, R. Casaburi, J. H. Vercoulen, I. Vogiatzis, R. Gosselink, E. M. Clini, T. W. Effing, F. Maltais, J. van der Palen, T. Troosters, D. J. Janssen, E. Collins, J. Garcia-Aymerich, D. Brooks, B. F. Fahy, M. A. Puhan, M. Hoogendoorn, R. Garrod, A. M. Schols, B. Carlin, R. Benzo, P. Meek, M. Morgan, M. P. Rutten-van Molken, A. L. Ries, B. Make, R. S. Goldstein, C. A. Dowson, J. L. Brozek, C.

F. Donner, E. F. Wouters, and Ats Ers Task Force on Pulmonary Rehabilitation. 2013. 'An official American Thoracic Society/European Respiratory Society statement: key concepts and advances in pulmonary rehabilitation', *Am J Respir Crit Care Med*, 188: e13-64.

Stead, L. F., P. Koilpillai, T. R. Fanshawe, and T. Lancaster. 2016. 'Combined pharmacotherapy and behavioural interventions for smoking cessation', *Cochrane Database Syst Rev*, 3: CD008286.

Stoller, J. K., R. J. Panos, S. Krachman, D. E. Doherty, B. Make, and Group Long-term Oxygen Treatment Trial Research. 2010. 'Oxygen therapy for patients with COPD: current evidence and the long-term oxygen treatment trial', *Chest*, 138: 179-87.

Suki, B., E. Bartolak-Suki, and P. R. M. Rocco. 2017. 'Elastase-Induced Lung Emphysema Models in Mice', *Methods Mol Biol*, 1639: 67-75.

Sundar, I. K., M. Z. Nevid, A. E. Friedman, and I. Rahman. 2014. 'Cigarette smoke induces distinct histone modifications in lung cells: implications for the pathogenesis of COPD and lung cancer', *J Proteome Res*, 13: 982-96.

Sundar, I. K., H. Yao, and I. Rahman. 2013. 'Oxidative stress and chromatin remodeling in chronic obstructive pulmonary disease and smoking-related diseases', *Antioxid Redox Signal*, 18: 1956-71.

Svanes, C., J. Sunyer, E. Plana, S. Dharmage, J. Heinrich, D. Jarvis, R. de Marco, D. Norback, C. Raherison, S. Villani, M. Wjst, K. Svanes, and J. M. Anto. 2010. 'Early life origins of chronic obstructive pulmonary disease', *Thorax*, 65: 14-20.

The Human Protein Atlas. 'RNA and Protein Expression of HMGN5', Accessed December 4, 2018. https://www.proteinatlas.org/ENSG00000198157-HMGN5/tissue.

Thomsen, M., B. G. Nordestgaard, J. Vestbo, and P. Lange. 2013. 'Characteristics and outcomes of chronic obstructive pulmonary disease in never smokers in Denmark: a prospective population study', *Lancet Respir Med*, 1: 543-50.

Trieschmann, L., P. J. Alfonso, M. P. Crippa, A. P. Wolffe, and M. Bustin. 1995. 'Incorporation of chromosomal proteins HMG-14/HMG-17 into nascent nucleosomes induces an extended chromatin conformation and enhances the utilization of active transcription complexes', *EMBO J*, 14: 1478-89.

Tsechkovski, M, V Boulyjenkov, and CC Heuck. 1997. 'a1-Antitrypsin deficiency: Memorandum from a WHO meeting', *Bull. World Health Organ*, 75: 397-415.

Tuder, R. M., and I. Petrache. 2012. 'Pathogenesis of chronic obstructive pulmonary disease', *J Clin Invest*, 122: 2749-55.

Tuder, R. M., T. Yoshida, W. Arap, R. Pasqualini, and I. Petrache. 2006. 'State of the art. Cellular and molecular mechanisms of alveolar destruction in emphysema: an evolutionary perspective', *Proc Am Thorac Soc*, 3: 503-10.

Ueda, T., F. Catez, G. Gerlitz, and M. Bustin. 2008. 'Delineation of the protein module that anchors HMGN proteins to nucleosomes in the chromatin of living cells', *Mol Cell Biol*, 28: 2872-83.

Ueda, T., T. Furusawa, T. Kurahashi, L. Tessarollo, and M. Bustin. 2009. 'The nucleosome binding protein HMGN3 modulates the transcription profile of pancreatic beta cells and affects insulin secretion', *Mol Cell Biol*, 29: 5264-76.

van der Molen, T., and M. Cazzola. 2012. 'Beyond lung function in COPD management: effectiveness of LABA/LAMA combination therapy on patient-centred outcomes', *Prim Care Respir J*, 21:101-8.

van der Toorn, M., D. J. Slebos, H. G. de Bruin, H. G. Leuvenink, S. J. Bakker, R. O. Gans, G. H. Koeter, A. J. van Oosterhout, and H. F. Kauffman. 2007. 'Cigarette smoke-induced blockade of the mitochondrial respiratory chain switches lung epithelial cell apoptosis into necrosis', *Am J Physiol Lung Cell Mol Physiol*, 292: L1211-8.

van Rijt, S. H., I. E. Keller, G. John, K. Kohse, A. O. Yildirim, O. Eickelberg, and S. Meiners. 2012. 'Acute cigarette smoke exposure impairs proteasome function in the lung', *Am J Physiol Lung Cell Mol Physiol*, 303: L814-23.

Vestbo, J., E. Prescott, and P. Lange. 1996. 'Association of chronic mucus hypersecretion with FEV1 decline and chronic obstructive pulmonary disease morbidity. Copenhagen City Heart Study Group', *Am J Respir Crit Care Med*, 153: 1530-5.

Vogelmeier, C. F., G. J. Criner, F. J. Martinez, A. Anzueto, P. J. Barnes, J. Bourbeau, B. R. Celli, R. Chen, M. Decramer, L. M. Fabbri, P. Frith, D. M. Halpin, M. V. Lopez Varela, M. Nishimura, N. Roche, R. Rodriguez-Roisin, D. D. Sin, D. Singh, R. Stockley, J. Vestbo, J. A. Wedzicha, and A. Agusti. 2017. 'Global Strategy for the Diagnosis, Management, and Prevention of Chronic Obstructive Lung Disease 2017 Report: GOLD Executive Summary', *Eur Respir J*, 49.

Vogelmeier, C., B. Hederer, T. Glaab, H. Schmidt, M. P. Rutten-van Molken, K. M. Beeh, K. F. Rabe, L. M. Fabbri, and Poet-Copd Investigators. 2011. 'Tiotropium versus salmeterol for the prevention of exacerbations of COPD', *N Engl J Med*, 364: 1093-103.

Vucic, E. A., R. Chari, K. L. Thu, I. M. Wilson, A. M. Cotton, J. Y. Kennett, M. Zhang, K. M. Lonergan, K. Steiling, C. J. Brown, A. McWilliams, K. Ohtani, M. E. Lenburg, D. D. Sin, A. Spira, C. E. Macaulay, S. Lam, and W. L. Lam. 2014. 'DNA methylation is globally disrupted and associated with expression changes in chronic obstructive pulmonary disease small airways', *Am J Respir Cell Mol Biol*, 50: 912-22.

Wahafu, W., Z. S. He, X. Y. Zhang, C. J. Zhang, K. Yao, H. Hao, G. Song, Q. He, X. S. Li, and L. Q. Zhou. 2011. 'The nucleosome binding protein NSBP1 is highly expressed in human bladder cancer and promotes the proliferation and invasion of bladder cancer cells', *Tumour Biol*, 32: 931-9.

Wain, L. V., N. Shrine, M. S. Artigas, A. M. Erzurumluoglu, B. Noyvert, L. Bossini-Castillo, M. Obeidat, A. P. Henry, M. A. Portelli, R. J. Hall, C. K. Billington, T. L. Rimington, A. G. Fenech, C. John, T. Blake, V. E. Jackson, R. J. Allen, B. P. Prins, Group Understanding Society Scientific, A. Campbell, D. J. Porteous, M. R. Jarvelin, M. Wielscher, A. L. James, J. Hui, N. J. Wareham, J. H. Zhao, J. F. Wilson, P. K. Joshi, B. Stubbe, R. Rawal, H. Schulz, M. Imboden, N. M. Probst-Hensch, S. Karrasch, C. Gieger, I. J. Deary, S. E. Harris, J. Marten, I. Rudan, S. Enroth, U. Gyllensten, S. M. Kerr, O. Polasek, M. Kahonen, I. Surakka, V. Vitart, C. Hayward, T. Lehtimaki, O. T. Raitakari, D. M. Evans, A. J. Henderson, C. E. Pennell, C. A. Wang, P. D. Sly, E. S. Wan, R. Busch, B. D. Hobbs, A. A. Litonjua, D. W. Sparrow, A. Gulsvik, P. S. Bakke, J. D. Crapo, T. H. Beaty, N. N. Hansel, R. A. Mathias, I. Ruczinski, K. C. Barnes, Y. Bosse, P. Joubert, M. van den Berge, C. A. Brandsma, P. D. Pare, D. D. Sin, D. C. Nickle, K. Hao, O. Gottesman, F. E. Dewey, S. E. Bruse, D. J. Carey, H. L. Kirchner, E. H. R. Collaboration Geisinger-Regeneron Discov, S. Jonsson, G. Thorleifsson, I. Jonsdottir, T. Gislason, K. Stefansson, C. Schurmann, G.

Nadkarni, E. P. Bottinger, R. J. Loos, R. G. Walters, Z. Chen, I. Y. Millwood, J. Vaucher, O. P. Kurmi, L. Li, A. L. Hansell, C. Brightling, E. Zeggini, M. H. Cho, E. K. Silverman, I. Sayers, G. Trynka, A. P. Morris, D. P. Strachan, I. P. Hall, and M. D. Tobin. 2017. 'Genome-wide association analyses for lung function and chronic obstructive pulmonary disease identify new loci and potential druggable targets', *Nat Genet*, 49: 416-25.

Watz, H., K. Tetzlaff, E. F. Wouters, A. Kirsten, H. Magnussen, R. Rodriguez-Roisin, C. Vogelmeier, L. M. Fabbri, P. Chanez, R. Dahl, B. Disse, H. Finnigan, and P. M. Calverley. 2016. 'Blood eosinophil count and exacerbations in severe chronic obstructive pulmonary disease after withdrawal of inhaled corticosteroids: a post-hoc analysis of the WISDOM trial', *Lancet Respir Med*, 4: 390-8.

Wedzicha, J. A., D. Banerji, K. R. Chapman, J. Vestbo, N. Roche, R. T. Ayers, C. Thach, R. Fogel, F. Patalano, C. F. Vogelmeier, and Flame Investigators. 2016. 'Indacaterol-Glycopyrronium versus Salmeterol-Fluticasone for COPD', *N Engl J Med*, 374: 2222-34.

Wedzicha, J. A., P. M. Calverley, T. A. Seemungal, G. Hagan, Z. Ansari, R. A. Stockley, and Inspire Investigators. 2008. 'The prevention of chronic obstructive pulmonary disease exacerbations by salmeterol/fluticasone propionate or tiotropium bromide', *Am J Respir Crit Care Med*, 177: 19-26.

Wedzicha, J. A., M. Decramer, J. H. Ficker, D. E. Niewoehner, T. Sandstrom, A. F. Taylor, P. D'Andrea, C. Arrasate, H. Chen, and D. Banerji. 2013. 'Analysis of chronic obstructive pulmonary disease exacerbations with the dual bronchodilator QVA149 compared with glycopyrronium and tiotropium (SPARK): a randomised, double-blind, parallel-group study', *Lancet Respir Med*, 1: 199-209.

Weinhold, B. 2006. 'Epigenetics: the science of change', *Environ Health Perspect*, 114: A160-7.

Weitzenblum, E., A. Sautegeau, M. Ehrhart, M. Mammosser, and A. Pelletier. 1985. 'Long-term oxygen therapy can reverse the progression of pulmonary hypertension in patients with chronic obstructive pulmonary disease', *Am Rev Respir Dis*, 131: 493-8.

Welte, T., C. Vogelmeier, and A. Papi. 2015. 'COPD: early diagnosis and treatment to slow disease progression', *Int J Clin Pract*, 69: 336-49.

Wickenden, J. A., M. C. Clarke, A. G. Rossi, I. Rahman, S. P. Faux, K. Donaldson, and W. MacNee. 2003. 'Cigarette smoke prevents apoptosis through inhibition of caspase activation and induces necrosis', *Am J Respir Cell Mol Biol*, 29: 562-70.

Wisdom, R., R. S. Johnson, and C. Moore. 1999. 'c-Jun regulates cell cycle progression and apoptosis by distinct mechanisms', *EMBO J*, 18: 188-97.

Wisniewski, J. R., A. Zougman, S. Kruger, and M. Mann. 2007. 'Mass spectrometric mapping of linker histone H1 variants reveals multiple acetylations, methylations, and phosphorylation as well as differences between cell culture and tissue', *Mol Cell Proteomics*, 6: 72-87.

Woodcock, C. L., A. I. Skoultchi, and Y. Fan. 2006. 'Role of linker histone in chromatin structure and function: H1 stoichiometry and nucleosome repeat length', *Chromosome Res*, 14: 17-25.

Wright, J. L., L. Lawson, P. D. Pare, R. O. Hooper, D. I. Peretz, J. M. Nelems, M. Schulzer, and J. C. Hogg. 1983. 'The structure and function of the pulmonary vasculature in mild chronic obstructive pulmonary disease. The effect of oxygen and exercise',*Am Rev Respir Dis*,128:702-7.

Ying, Y., and B. J. Padanilam. 2016. 'Regulation of necrotic cell death: p53, PARP1 and cyclophilin D-overlapping pathways of regulated necrosis?', *Cell Mol Life Sci*, 73: 2309-24.

Yoshida, T., and R. M. Tuder. 2007. 'Pathobiology of cigarette smoke-induced chronic obstructive pulmonary disease', *Physiol Rev*, 87: 1047-82.

Zeng, H., X. Kong, H. Peng, Y. Chen, S. Cai, H. Luo, and P. Chen. 2012. 'Apoptosis and Bcl-2 family proteins, taken to chronic obstructive pulmonary disease', *Eur Rev Med Pharmacol Sci*, 16: 711-27.

Zhang, S., I. Zhu, T. Deng, T. Furusawa, M. Rochman, M. S. Vacchio, R. Bosselut, A. Yamane, R. Casellas, D. Landsman, and M. Bustin. 2016. 'HMGN proteins modulate chromatin regulatory sites and gene expression during activation of naive B cells', *Nucleic Acids Res*, 44: 7144-58.

Zhang, X. Y., Z. Q. Guo, S. Q. Ji, M. Zhang, N. Jiang, X. S. Li, and L. Q. Zhou. 2012. 'Small interfering RNA targeting HMGN5 induces apoptosis via modulation of a mitochondrial pathway and Bcl-2 family proteins in prostate cancer cells', *Asian J Androl*, 14: 487-92.

Zhao, C. Z., X. C. Fang, D. Wang, F. D. Tang, and X. D. Wang. 2010. 'Involvement of type II pneumocytes in the pathogenesis of chronic obstructive pulmonary disease', *Respir Med*, 104: 1391-5.

Zhivotovsky, B., and S. Orrenius. 2010. 'Cell cycle and cell death in disease: past, present and future', *J Intern Med*, 268: 395-409.

Acknowledgments - Danksagung

Nun ist es mir ein Anliegen mich bei allen zu bedanken, die zu dieser Arbeit beigetragen haben.

Ich danke Dr. Ali Önder Yildirim, dass ich in seiner Arbeitsgruppe am CPC/ILBD tätig sein durfte, sowie für seine Unterstützung und die Betreuung meiner Forschungsarbeit. Seine wissenschaftliche Erfahrung und die regen Diskussionen mit ihm weiß ich sehr zu schätzen. Ich bedanke mich für die warme Aufnahme in seiner Forschungsgruppe und für die wissenschaftlichen und persönlichen Erfahrungen, die ich dadurch gemacht habe.

Ich danke Dr. Rim Sabrina Jahan Sarker für die Betreuung meiner Arbeit, für die wissenschaftlichen Anregungen und für die Bereitschaft als direkte Ansprechpartnerin zur Seite zu stehen.

Danke an Dr. Thomas Conlon für seinen ständigen Support, für seine Ideen und seine Hilfsbereitschaft bei jeglichen Fragen und Unklarheiten. Seine stetige Hilfsbereitschaft zeigt den Zusammenhalt und die gegenseitige Unterstützung, die ich in dieser Forschungsgruppe erfahren durfte.

Auch danke ich Prof. Dr. Oliver Eickelberg, ehemaliger Direktor des Comprehensive Pneumology Centers für die Möglichkeit an seinem Institut meine Doktorarbeit zu verwirklichen.

Ich danke Prof. Dr. Jürgen Behr, Direktor der Medizinischen Klinik und Poliklinik V am Klinikum der Universität München und Chefarzt der Asklepios Fachkliniken in Gauting für die Bereitschaft meine Arbeit als Doktorvater zu betreuen.

Ich danke Dr. Doreen Franke, Prof. Dr. Silke Meiners, PD Dr. Claudia Staab-Weijnitz und Dr. Darcy Wagner für die Organisation der Research School und der damit einhergehenden wissenschaftlichen Ausbildung und den zahlreichen Erfahrungen auf wissenschaftlicher und freundschaftlicher Ebene.

Des Weiteren, danke ich insbesondere allen in meiner Forschungsgruppe, die mir stets zur Seite standen und die Zeit zu einer so angenehmen und bereichernden gemacht haben. Danke an Christine, Carolina, Gizem und Zeynep.

Zu guter Letzt – und mir besonders wichtig – danke ich meinen Eltern. Ohne euch und eure ständige Unterstützung würde ich jetzt nicht hier sitzen und den letzten Satz meiner Doktorarbeit zu Papier bringen. Vielen Dank!